

Duquesne University

Duquesne Scholarship Collection


Electronic Theses and Dissertations

Fall 12-16-2022

SPECIATED ISOTOPE DILUTION MASS SPECTROMETRY IN COMBINATION WITH THOR'S HAMMER METASPIKE TECHNOLOGY FOR THE ASSESSMENT OF LOW-LEVEL BIOMARKERS FOR HUMAN HEALTH EVALUATION

Ashley Ebert

Follow this and additional works at: <https://dsc.duq.edu/etd>

 Part of the [Analytical Chemistry Commons](#), [Environmental Chemistry Commons](#), and the [Other Analytical, Diagnostic and Therapeutic Techniques and Equipment Commons](#)

Recommended Citation

Ebert, A. (2022). SPECIATED ISOTOPE DILUTION MASS SPECTROMETRY IN COMBINATION WITH THOR'S HAMMER METASPIKE TECHNOLOGY FOR THE ASSESSMENT OF LOW-LEVEL BIOMARKERS FOR HUMAN HEALTH EVALUATION (Doctoral dissertation, Duquesne University). Retrieved from <https://dsc.duq.edu/etd/2210>

This One-year Embargo is brought to you for free and open access by Duquesne Scholarship Collection. It has been accepted for inclusion in Electronic Theses and Dissertations by an authorized administrator of Duquesne Scholarship Collection. For more information, please contact beharyr@duq.edu.

SPECIATED ISOTOPE DILUTION MASS SPECTROMETRY IN COMBINATION WITH
THOR'S HAMMER METASPIKE TECHNOLOGY FOR THE ASSESSMENT OF LOW-
LEVEL BIOMARKERS FOR HUMAN HEALTH EVALUATION

A Dissertation

Submitted to the Bayer School of Natural and Environmental Sciences

Duquesne University

In partial fulfillment of the requirements for
the degree of Doctor of Philosophy

By

Ashley N. Ebert

December 2022

Copyright by

Ashley N. Ebert

2022

SPECIATED ISOTOPE DILUTION MASS SPECTROMETRY IN COMBINATION
WITH THOR'S HAMMER METASPIKE TECHNOLOGY FOR THE ASSESSMENT
OF LOW-LEVEL BIOMARKERS FOR HUMAN HEALTH EVALUATION

By

Ashley N. Ebert

Approved November 11, 2022

Dr. H. M. "Skip" Kingston
Professor of Chemistry
(Committee Chair)

Dr. Michael Van Stipdonk
Professor of Chemistry
(Committee Member)

Dr. Scott Faber
Developmental Pediatrician
(Committee Member - external)

Dr. Rita Mihailescu
(Committee Member)
Interim Chair, Department of Chemistry
and Biochemistry
Professor of Chemistry

Dr. Ellen Gawalt
Dean, Bayer School of Natural and
Environmental Sciences
Professor of Chemistry

ABSTRACT

SPECIATED ISOTOPE DILUTION MASS SPECTROMETRY IN COMBINATION WITH THOR'S HAMMER METASPIKE TECHNOLOGY FOR THE ASSESSMENT OF LOW-LEVEL BIOMARKERS FOR HUMAN HEALTH EVALUATION

By

Ashley N. Ebert

November 2022

Dissertation supervised by Professor H. M. "Skip" Kingston

Our research team has been focused on quantifying important biological analytes in human blood samples to delineate the biochemical processes underlying certain states of dysfunction and evaluate treatment efficacy. These efforts have been guided by laboratory measurements with the input of medical experts. Speciated isotope dilution mass spectrometry (SIDMS) explained in detail in EPA Method 6800 has been successfully applied in the quantification of an important biomarker analyte for immune function and detoxification processes: glutathione. Past research has proven the molecule a biomarker for autism spectrum disorder (ASD) in the form of the reduced/oxidized glutathione (GSH/GSSG) ratio, and literature has implicated this ratio a potential biomarker for various other disease states.

Previous researchers found the assessment of the GSH/GSSG ratio so challenging that literature disagreed on the ‘healthy’ ratio by over three orders of magnitude. The quantification continued to be a stumbling block for researchers until the Kingston research group published an accurate and precise methodology for whole blood extraction and SIDMS implementation in Analytical Chemistry. This dissertation work has centered around the development and optimization of a new extraction technique for the analysis of glutathione. Protocols have been minimized onto quantitative dried blood spot (Q-DBS) cards, enabling self-sampling and the potential for international assessment of patients. As discussed in Chapter 1, manual and fully automated extractions of DBS samples have been successfully validated according to guidance from the Federal Drug Administration (FDA) detailed in the “Bioanalytical Method Validation: Guidance for Industry” document. These newly developed methods have produced statistically similar data to that of validated methodology within the $\pm 15\%$ acceptance criteria. DBS cards boast various benefits to patient, analyst, and medical professional alike and the reported findings in Chapter 1 demonstrate that DBS cards are a potential replacement for phlebotomic blood draw sampling in a clinical setting.

The reduced/oxidized glutathione (GSH/GSSG) ratio can suffer broader uncertainty in the calculation due to the concentration of GSSG in blood being roughly ten times lower than that of GSH. To mitigate this issue, a novel instrumental signal boosting analytical technique termed ‘Thor’s Hammer’ or ‘Metaspiking’ has been developed to improve upon the IDMS and SIDMS capabilities of quantifying low-level analytes. Thor’s Hammer, discussed in Chapter 2, has enabled a full order of magnitude lower quantification capability beyond what the previous methodology has accomplished.

In applying Thor's Hammer, the accuracy and precision of GSSG quantification has improved greatly and the uncertainty in GSH/GSSG ratio determination has decreased.

Glutathione's role in detoxification of xenobiotic material from the body is an important aspect of a person's immunological health, though it can sometimes hinder medical efforts to treat certain diseases, such as cancer. In the field of oncology, several therapeutics are used for patients to rid their bodies of cancerous tissue and cells. One complication with a famous cancer drug, cisplatin, is its rapid expulsion from the body via glutathione Phase II detoxification. To track the elimination of cisplatin from a patient's system, a new method to evaluate glutathione-conjugated cisplatin in blood and urine has been developed. Two additional platinated drug compounds, carboplatin and oxaliplatin, have been synthesized and approved for clinical use in recent decades. These compounds were synthesized to avoid bodily detection and slow down elimination from the body. Future efforts can strive to further develop this method for quantitative purposes enabling the determination of blood and urine concentration of cisplatin, carboplatin, and oxaliplatin with IDMS and SIDMS mathematics to enable a better biochemical view of the drugs bodily pathways.

DEDICATION

I want to dedicate this dissertation to four individuals who have played a large role in my life. First, I want to dedicate this dissertation to my mother, father, and brother, Carol, Tony, and Adam Trouten. Throughout my entire life, my parents have taught me to strive for knowledge, learn about everything and anything that interests me, and work hard for the goals I wish to achieve. It is because of them that I have accomplished many amazing ambitions throughout my life. It is their love, support, guidance, and wisdom that has enabled me to make it to Duquesne and achieve the highest title in my academic career, Doctor of Philosophy in Chemistry. I love you to the moon and back, mom and dad. And to my brother, for the careful reminders that taking time from work and school are important too. You have always known how to crack a joke that would instantly put a smile on my face and for that and more I thank you. I love you little bro.

I would also like to dedicate this dissertation to my husband, Austin Ebert. When I doubted my abilities, skills, and intelligence, you reminded me why I have pushed to this point. Even when I felt like giving up, you reminded me that is not who I am. You have let me scream or cry when necessary, and never complained about the long nights in front of my computer practicing my talks for upcoming defenses. You have read, reviewed, and edited more chemistry related documents than you probably would have ever cared to look at. And for all of this, I thank you. Without you, I would not have made it through this program. I love you.

ACKNOWLEDGEMENT

I want to thank God, first and foremost, for giving me the opportunities in life that have led me to Duquesne. Without His guidance and strength, I would have never been able to accomplish the work described in this dissertation. I want to thank Dr. H. M. “Skip” Kingston for his time and guidance throughout my involvement at Duquesne. I would also like to thank Dr. Rita Mihailescu, Dr. Michael Van Stipdonk, and Dr. Scott Faber for serving as members of my committee and taking time out of their busy schedules to listen to my talks and offer direction in my work. It is their assistance and support that has enabled me to reach my goals. I would also like to thank Dr. Wetzel, who was not on my committee, but served as an integral part of my education regarding instrumental analysis and sample preparation techniques. Without her patience and training, I would not know half of what I do today. She has also helped mold me into the analyst and critical thinker I have become.

I would like to acknowledge the Kingston Research group, both past and present members: Dr. James Henderson, Dr. Weier Hao, Dr. Jeremiah Jamrom, Lauren Stubbert, and Caley Moore. The intelligence they have all passed onto me, the help they have given me with reading papers and listening to my practice talks, and the fun times we have shared are irreplaceable. Thank you. I wish to acknowledge the members of the maintenance team in the Bayer School of Natural and Environmental Sciences: Dan Bodnar, Lance Crosby, and Christopher Lawson. The support they have offered with repairs and upkeep has been a tremendous help. Finally, I would like to thank outside collaborators such as Matt Pamuku who has been integral in the search for funding and for his business insight and support, I am grateful. Dr. Rosalynn Fernandez has been a major personal collaborator of

mine and has not only enabled me to dip into research outside of my dissertation work but has been lovely to work and publish with.

TABLE OF CONTENTS

	Page
Abstract	iv
Dedication	vii
Acknowledgement	viii
List of Tables	xi
List of Figures	xv
List of Abbreviations	xx
Introduction: Glutathione Speciation in Immunological and Detoxification Processes	1
Chapter 1: Development of Manual and Fully Automated Dried Blood Spot (DBS) Card Desorption Techniques for SIDMS Quantification of Glutathione	17
Chapter 2: Metrology: Application of Thor's Hammer and Improvement to Speciated Isotope Dilution Mass Spectrometry (SIDMS) Quantification of Glutathione	52
Chapter 3: Glutathione and Cancer: Treatment Tracking for Platinating Agents in Chemotherapy	89
Concluding Remarks: Glutathione	132
Future Work	135

LIST OF TABLES

	Page
Table 1. 1. Valve positions and flow description for the DBS-A instrument.....	27
Table 1. 2. DBS-A method parameters for automated extraction of DBS sample spots..	27
Table 1. 3. MRM transitions for detection of glutathione species on the LC-MS/MS.....	31
Table 1. 4. Estimated LOD and LOQ concentrations for both analytes using different methodologies of extraction.....	35
Table 1. 5. Assessment of analytical accuracy regarding GS-NEM (GSH) and GSSG quantification following different extraction techniques, represented by %error from nominal concentration calculations.....	36
Table 1. 6. Assessment of analytical precision regarding GS-NEM (GSH) and GSSG quantification following different extraction techniques, represented by %CV calculations.	36
Table 1. 7. Statistical results for comparing GSH/GSSG ratio data achieved for DBS card manual extraction analysis following 48 hours in varying storage conditions.....	39
Table 1. 8. Statistical results for comparing GSH/GSSG ratio data achieved for DBS card manual extraction analysis following up to 6 months hours of storage in a sealed alumina bag.....	43
Table 2. 1. Instrumental MRM method for abundance determination of natural and isotopic GSSG content.....	60
Table 2. 2. Isotopic abundances of potential product ions for standard and Thor’s Hammer Metaspikes.....	61

Table 2. 3. Resulting precision assessment for quantification of 612GSSG using IDMS + TH spiking technique.....	63
Table 2. 4. Resulting accuracy assessment for quantification of 612GSSG using IDMS + TH spiking technique.....	64
Table 2. 5. Quantitative results for 306GS-NEM in an SIDMS+TH-A system.	66
Table 2. 6. Quantitative results for 612GSSG in an SIDMS+TH-A system.	66
Table 2. 7. Resulting quantification data for both target analyte species upon SIDMS and SIDMS+TH.....	67
Table 2. 8. Quantitative results of GS-NEM, GSSG, and ratio calculations with and without the application of Thor’s Hammer for neat sample analysis.	70
Table 2. 9. Quantitative results of GS-NEM, GSSG, and ratio calculations with and without the application of Thor’s Hammer for whole blood sample analysis.	70
Table 2. 10. Quantitative results of GS-NEM, GSSG, and ratio calculations with and without the application of Thor’s Hammer for DBS sample analysis.	70
Table 2. 11. Determined EPF for each spiking system for guidance on spiking levels....	73
Table 2. 12. Resulting data from SIDMS application of TH-A, TH-B, TH-C, and standard isotopic spike (N).....	74
Table 2. 13. External calibration standard of 612GSSG results.	75
Table 2. 14. Water blank analyses for the estimation of LOD and LOQ.	77
Table 2. 15. Resulting instrumental signal for the analysis of low level 612GSSG standards.	78
Table 2. 16. Product ion abundance for TH-G and TH-H.	79

Table 2. 17. Quantitative results for 612GSSG assessment via direct analysis utilizing the standard spiking technology.	80
Table 2. 18. Quantitative results for 612GSSG assessment via direct analysis utilizing the TH-G spiking technology.	81
Table 2. 19. Quantitative results for 612GSSG assessment via DBS manual extraction analysis utilizing the standard spiking technology.	81
Table 2. 20. Quantitative results for 612GSSG assessment via DBS manual extraction analysis utilizing the TH-G spiking technology.	82
Table 2. 21. Quantitative results for 612GSSG assessment via direct sample analysis utilizing the TH-H spiking technology.	82
Table 2. 22. Quantitative results for 306GS-NEM, 612GSSG, and GSH/GSSG ratio assessment via direct sample analysis utilizing the TH-H spiking technology in an SIDMS+TH system.....	84
Table 3. 1. Product ion scan results for the two primary precursor ions of cisplatin.	105
Table 3. 2. Proposed MRM detection method for all platinated drug compounds simultaneously.	106
Table 3. 3. LOD and LOQ for platinated drug compounds analyzed on the LC-QQQ-MS.	107
Table 3. 4. Fragmentation ions for each proposed structure of singly and doubly conjugated platinum with glutathione. (F=Figure, C=structure assignment number)	115
Table 3. 5. Extracted mass spectral data for the signal observed at 1.171 minutes.....	116
Table 3. 6. LOD and LOQ determinations for total platinum content from cisplatin and platinum metal analysis on the ICP-MS	122

Table 3. 7. Abundance determinations for the six platinum isotopes following ICP-MS analysis of cisplatin and ¹⁹⁵ Pt metal in solution.	122
Table 3. 8. Abundance determination for isotopically enriched ¹⁹⁴ Pt solution following ICP-MS analysis.	123
Table 3. 9. IDMS results of extracted biological samples.	125
Table 3. 10. Calibration curve results of extracted biological samples.	126

LIST OF FIGURES

	Page
Figure I 1. The molecular structure of natural reduced glutathione, GSH.	2
Figure I 2. The molecular structure of natural oxidized glutathione, GSSG.	3
Figure I 3. Reduction of a generic peroxide compound (ROOH) by two molecules of GSH yielding alcohol, water, and GSSG.	4
Figure I 4. Example of phase II detoxification of a persistent organic pollutant, benzene, through glutathione conjugation.	4
Figure I 5. Clinical results for the GSH/GSSG ratio calculation following SIDMS quantification of both glutathione species in ASD patient cohort as well as the age, sex, and geological location matched control. ^{14, 15}	6
Figure I 6. Example DBS card sample with three blood spots and one unspotted region. .	9
Figure 1. 1. Reported "healthy" values for the GSH/GSSG ratio estimated by researchers from 2001-2012. (1 = Cereser et al., 2 = Zitka et al., 3 = Michaellesen et al., 4 = Harwood et al) ^{3, 5, 6, 8}	18
Figure 1. 2. The molecular structure of reduced glutathione bound to N-ethylmaleimide (NEM).	21
Figure 1. 3. MRM chromatogram for 612GSSG species following manual extraction of DBS sample and LC-MS/MS analysis. RT for 2.294 minutes	29
Figure 1. 4. MRM chromatogram for 306GS-NEM species following manual extraction of DBS sample and LC-MS/MS analysis. RT at 4.741 minutes.	29
Figure 1. 5. MRM chromatogram for 612GSSG species following fully automated DBS-A extraction of DBS sample and LC-MS/MS analysis. RT for 3.523 minutes.	30

Figure 1. 6. MRM chromatogram for 306GS-NEM species following fully automated DBS-A extraction of DBS sample and LC-MS/MS analysis. RT for 3.625 minutes..... 30

Figure 1. 7. Graphical representation comparing the analytical result of the GSH/GSSG ratio calculations derived from quantification of both species following manual DBS extraction after varying storage conditions..... 38

Figure 1. 8. Graphical representation comparing the analytical result of the GSH/GSSG ratio calculations derived from quantification of both species following manual DBS extraction after varying timed stored in a clean-room setting prior to analysis..... 41

Figure 1. 9. Graphical representation comparing the analytical result of the GSH/GSSG ratio calculations derived from quantification of both glutathione species following manual DBS extraction after 6 months storage within a sealed alumina bag 42

Figure 1. 10. Closer examination of the comparison between GSH/GSSG ratios derived from whole blood extraction and card 1 manual extraction of Standard 4 whose student's t-test evaluation indicated significant difference. 44

Figure 1. 11. Closer examination of the comparison between GSH/GSSG ratios derived from direct analysis and card 2 manual extraction of Standard 3 whose student's t-test evaluation indicated significant difference. 44

Figure 1. 12. Closer examination of the comparison between GSH/GSSG ratios derived from whole blood extraction and card 2 manual extraction of Standard 3 whose student's t-test evaluation indicated significant difference. 45

Figure 1. 13. Closer examination of the comparison between GSH/GSSG ratios derived from card 1 manual extraction and card 2 manual extraction of Standard 3 whose student's t-test evaluation indicated significant difference. 45

Figure 1. 14. Graphical representation comparing the analytical result of the GSH/GSSG ratio calculations derived from quantification of both glutathione species following manual DBS extraction over the course of 1 year following open-air cleanroom storage.....	46
Figure 2. 1. Chromatographic results of analysis of a solution containing GSH and GSSG at the same concentration roughly 100 µg/g. The top chromatogram depicts the results following direct analysis of the sample and the bottom chromatogram depicts the results following direct analysis of the sample and the bottom chromatogram depicts the results following manual extraction of a DBS sample.	54
Figure 2. 2. Isotopic breakdown of natural and isotopically enriched solutions of 612GSSG and 616GSSG, respectively.	56
Figure 2. 3. Graphical demonstration of the artificial analytical signal boosting enabled by Metaspik technology.	57
Figure 2. 4. Reduction or change in error achieved by employing IDMS+TH.	65
Figure 2. 5. Calibration curve for 612GSSG following analysis on the LC-QqQ.....	76
Figure 3. 1. The molecular structure of cisplatin	89
Figure 3. 2. Biotransformation of cisplatin following entrance within the cellular membrane. ³	90
Figure 3. 3. DNA binding of cisplatin to guanine bases. ⁵	91
Figure 3. 4. The molecular structure of cisplatin conjugated to one molecule of reduced glutathione, GSH.....	91
Figure 3. 5. The molecular structure of carboplatin.....	92
Figure 3. 6. The molecular structure of oxaliplatin.	93
Figure 3. 7. Positive mode ESI scan result of carboplatin neat solution in water.	96

Figure 3. 8. Isotopic abundances for platinum's six isotopic species.	96
Figure 3. 9. Dimerized structure of two carboplatin molecules.	97
Figure 3. 10. Fragmentation pattern from 372 parent ion to the 355 m/z product ion.	97
Figure 3. 11. Aquated structure of carboplatin.	98
Figure 3. 12. Resulting product ion scan of carboplatin using the 372 m/z precursor ion and 25 kV collision energy.	98
Figure 3. 13. Resulting product ion scan of carboplatin using the 373 m/z precursor ion and 25 kV collision energy.	98
Figure 3. 14. Proposed fragmentation pattern for carboplatin molecule at a collision energy of 25 kV.	99
Figure 3. 15. Positive mode ESI scan result of oxaliplatin neat solution in water.	99
Figure 3. 16. Dimerized structure of two oxaliplatin molecules.	100
Figure 3. 17. Resulting product ion scan of oxaliplatin using the 398 m/z precursor ion and 25 kV collision energy.	100
Figure 3. 18. Resulting product ion scan of oxaliplatin using the 399 m/z precursor ion and 25 kV of collision energy.	101
Figure 3. 19. Fragmentation pattern of oxaliplatin to the formation of a Schiff base product ion.	101
Figure 3. 20. Positive mode ESI scan result of cisplatin neat solution in water.	102
Figure 3. 21. Aquation and subsequent oxidation of cisplatin in water solution.	103
Figure 3. 22. Extracted mass spectrum of the signal observed upon MS2 scan analysis of cisplatin SRM in water at 1.4 minutes.	104

Figure 3. 23. Extracted mass spectrum of the signal observed upon MS2 scan analysis of cisplatin SRM in water at 10.8 minutes.	104
Figure 3. 24. Fragmentation pattern of cisplatin.	106
Figure 3. 25. Chromatographic results of broad MS2 scan for incubated cisplatin+GSH sample on the LC-MS/MS.	108
Figure 3. 26. Mass spectrum extracted from the peak signal at 1.171 minutes.	109
Figure 3. 27. Mass spectrum extracted from the peak signal at 1.339 minutes.	109
Figure 3. 28. Mass spectrum extracted from the peak signal at 1.439 minutes.	109
Figure 3. 29. Mass spectrum extracted from the peak signal at 1.573 minutes.	110
Figure 3. 30. Mass spectrum extracted from the peak signal at 2.024 minutes.	110
Figure 3. 31. Mass spectrum extracted from the peak signal at 2.359 minutes.	110
Figure 3. 32. Potential fragmentation pattern of singly conjugated platinum to glutathione.	112
Figure 3. 33. Potential fragmentation pattern for doubly conjugated platinum with glutathione.	113
Figure 3. 34. Calibration curve for analysis of 195-Cisplatin standard solutions in water on the ICP-MS.	121
Figure 3. 35. Calibration curve for the analysis of 195Pt standard solutions in HNO ₃ on the ICP-MS.	121
Figure 3. 36. Graphical comparison of the quantification of cisplatin following microwave assisted acid digestion of biological matrices and ICP-MS analysis.	127

LIST OF ABBREVIATIONS

GSH – Reduced Glutathione

GSSG – Oxidized Glutathione

tGSH – Total Glutathione

ROS – Reactive Oxygen Species

ASD – Autism Spectrum Disorder

DBS – Dried Blood Spot

FDA – Food and Drug Administration

SIDMS – Speciated Isotope Dilution Mass Spectrometry

EPA – Environmental Protection Agency

DBS-A – Dried Blood Spot Autosampler

HPLC – High Performance Liquid Chromatography

MS/MS – Tandem Mass Spectrometry

QQQ – Triple Quadrupole Mass Spectrometer

ICP-MS – Inductively Coupled Plasma Mass Spectrometry

LOD – Limit of Detection

LOQ – Limit of Quantification

SRM – Standard Reference Material

Introduction: Glutathione Speciation in Immunological and Detoxification Processes

In recent decades, realization of the environment's interaction and impact on a person's biochemical status along with the resulting alteration of genetic components has prompted the advancement of epigenetics.¹⁻³ The environment is home to an abundance of problem-causing toxicants such as heavy metal pollution, reactive oxygen and nitrogen species, and persistent organic pollutants.^{1, 4} From the moment of conception, which is believed to be the most fragile and important stage of fetal development regarding exposure, human beings can be subjected to any number of harmful xenobiotic materials via the mother's blood.¹ This can hinder normal development, promote various disease states throughout life, and lead to a decreased life expectancy.⁴

Combatting xenobiotic and toxicant exposure can be difficult to manage, but medical professionals have been tirelessly seeking ways of identifying disease and dysfunction in its early stages to prevent the negative outcomes before excessive and irreparable damage has occurred. The most fundamental methodology for diagnosing, treating, and preventing disease onset is through biomarker measurements that reflect a person's biochemical status. This enables medical professionals to act soon, act carefully with hard data, and save lives.

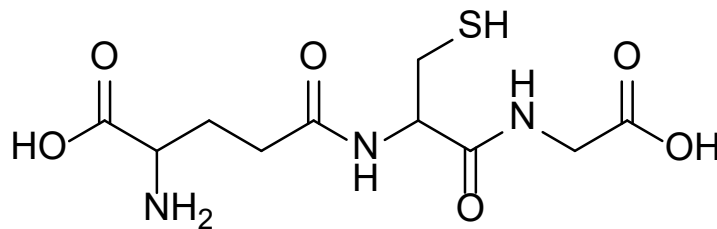
I. Biomarker Assessment in Personalized Medicine

As defined by the World Health Organization in partnership with the United Nations, a biomarker is "any substance, structure, or process that can be measured in the body or its products and influence or predict the incidence of outcome or disease."⁵ Biomarkers have a long history of use in the clinical realm for diagnostic evaluations and treatment tracking

to the point that their use is accepted almost without question.⁵ The ability to accurately, precisely, and reproducibly quantify a validated biomarker for a disease state enables sound, data-based decisions on the patient's status and treatment to be made by the medical professional, which eliminates guess work that may have previously been employed.

II. Speciated Glutathione and Its Biological Role

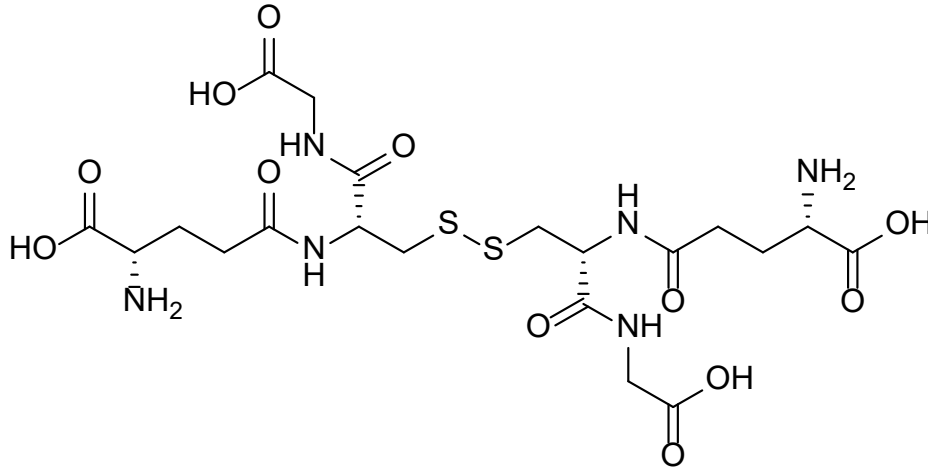
Of the biomarkers existent in clinical practice, glutathione is popular for diseases such as ASD, cancer, neurodegenerative disorders, and more.¹ Glutathione is the most abundant non-protein, amino-thiol in mammalian cells, ranging in concentration from 0.5 to 10 mM. Free glutathione in the cytosol of cells primarily exists in the reduced form, GSH, (**Figure I.1**) with a roughly 100-fold higher concentration than the oxidized form, GSSG, (**Figure I.2**).^{6, 7} However, within cell organelles, like the mitochondria, the concentration of GSSG can raise significantly due to normal biological processes such as cellular respiration.^{6, 8} A third specie of interest is protein-bound glutathione, GS-R, which binds to protein residues enabling the protein or enzyme to perform regular bodily reactions, such as that of glutathione transferase which works to conjugate GSH molecules to xenobiotic material like acrolein.⁹ The sum of GSH, GSSG, and GS-R is defined as the total glutathione (tGSH) concentration.



Molecular Weight: 307.32

Reduced Glutathione

Figure I 1. The molecular structure of natural reduced glutathione, GSH.



Molecular Weight: 612.63

Oxidized Glutathione

Figure I 2. The molecular structure of natural oxidized glutathione, GSSG.

Glutathione bears two important roles in the body: the reduction of reactive oxygen species (ROS) and the detoxification of xenobiotic material.⁹ Whether from pollution produced in the surrounding environment or the product of natural bodily processes such as cellular respiration, the reduction of ROS is crucial for preventing cellular membrane, lipid, and protein damage.^{4, 10} (Figure I.3) Unmanaged ROS, like the common OH radical, induce free radical chains causing lipid peroxidation.⁶ Not only does lipid peroxidation damage the cellular membrane disrupting cell integrity, but by-products of lipid peroxidation, like β -unsaturated aldehydes are toxic to the human body resulting in the deactivation of many functional proteins.⁶

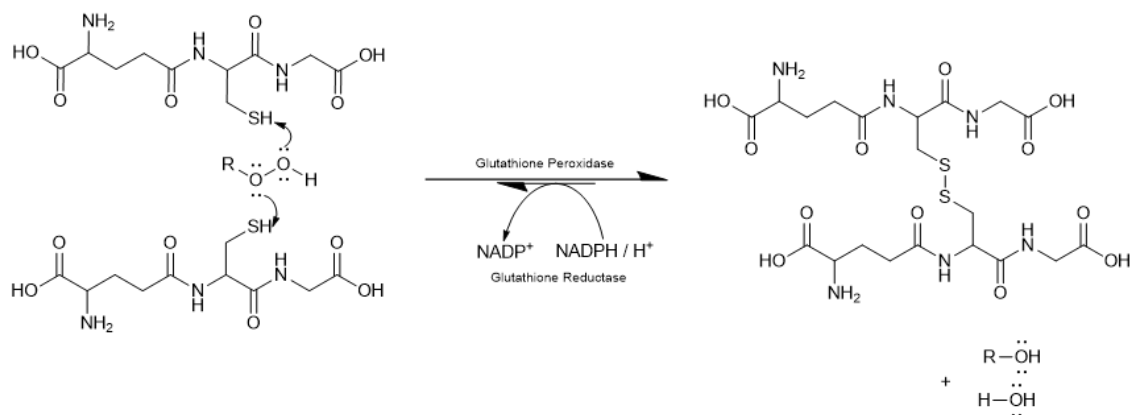


Figure I 3. Reduction of a generic peroxide compound (ROOH) by two molecules of GSH yielding alcohol, water, and GSSG.

Glutathione also works to protect the body from xenobiotic, or foreign to the body, materials such as heavy metals and persistent organic pollutants, like benzene. Glutathione will undergo phase I and phase II detoxification processes to defend against these foreign substances and eliminate them before excessive damage has incurred.^{6, 11} (Figure I.4)

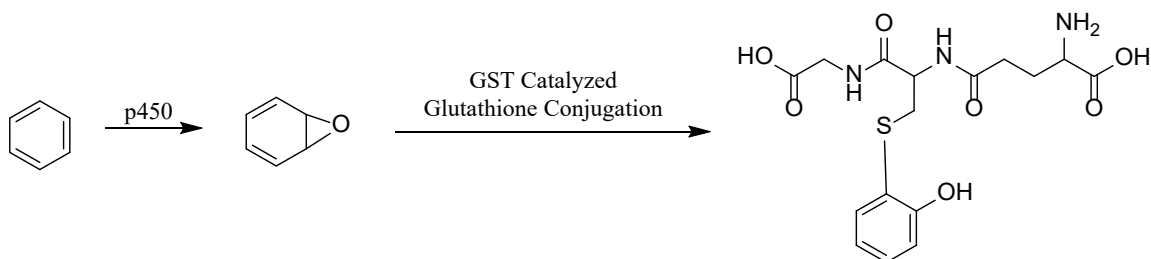


Figure I 4. Example of phase II detoxification of a persistent organic pollutant, benzene, through glutathione conjugation.

When cellular antioxidant and detoxification defenses are inadequate for maintaining appropriate levels of GSH, GSSG, and ROS and eliminating xenobiotic material, a state of dysfunction termed oxidative stress can be induced, which has been an underpinning of several disease states.⁴ A loss of balance between oxidative stress and antioxidant capacity will lead to an overproduction of ROS and reactive nitrogen species (RNS).^{1, 12} This state of distress has been noted as a major cause of neuroinflammation and impairment in the astrocyte-neuron crosstalk leading to ASD symptomology.^{1, 4}

From past research in the Kingston laboratory, as well as being reported by dozens of researchers in the biomarker field, glutathione, and its associated ratios, like GSH/GSSG and tGSH/GSSG, have been proven or implicated as strong and determinative biomarkers for ASD, cancer, Parkinson's, Alzheimer's, and more.¹³ In the lab's most recent work, published in 2019, a patient: control study evaluating healthy children and ASD patients was undertaken to assess the levels of glutathione in blood.¹⁴ ASD patients were matched to healthy control children based upon age, gender, geographical location, and socioeconomic status. Patients showed significantly different GSH/GSSG ratio calculations as compared to their matched control counterpart at the 95% confidence interval.^{14, 15} (**Figure I.5**) In general, the concentration of GSSG was significantly higher in ASD patients and the GSH/GSSG ratio was significantly lower. Some compensatory effects with heightened GSH concentrations due to heavy metal toxicity were noted as well.¹⁴

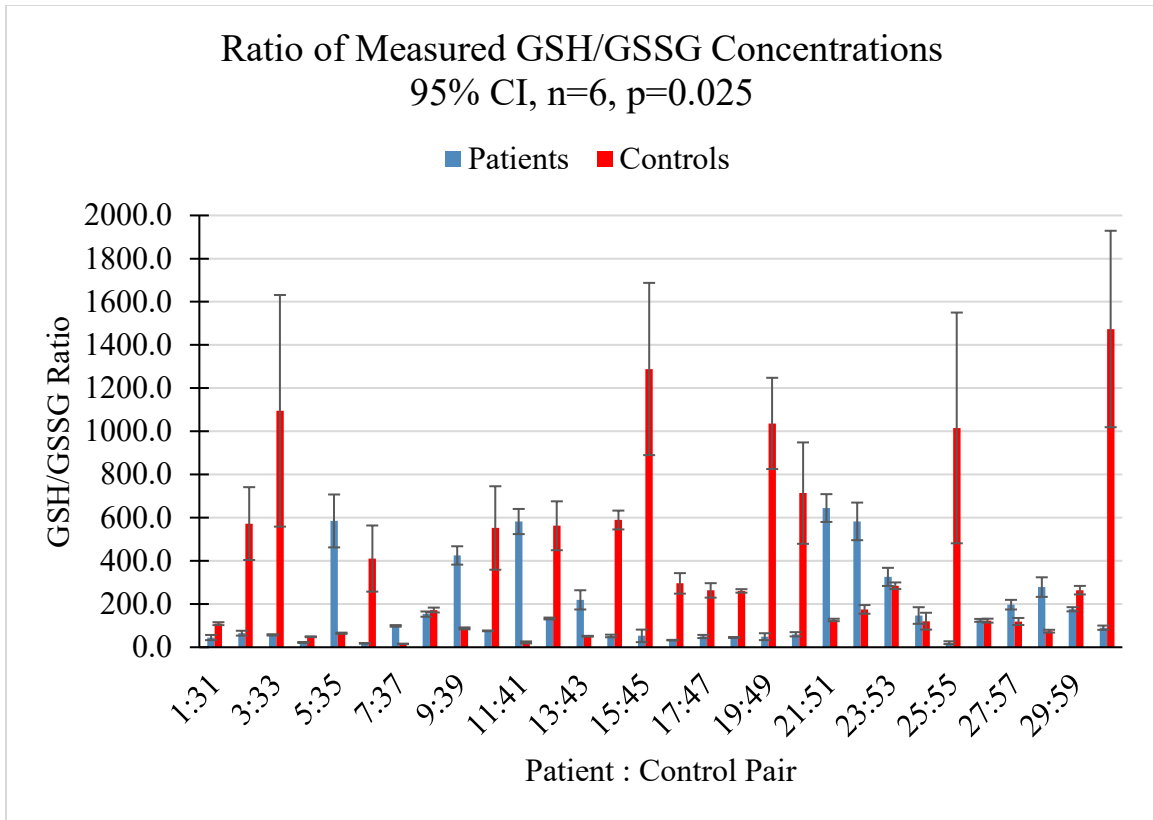


Figure I 5. Clinical results for the GSH/GSSG ratio calculation following SIDMS quantification of both glutathione species in ASD patient cohort as well as the age, sex, and geological location matched control.^{14, 15}

Oncological research has also turned towards glutathione as a biomarker of interest for evaluating patient disease status and treatment tracking.⁸ Multiple studies have confirmed the strong relationship between oxidative stress and the formation or progression of cancer.^{8, 13, 16} Specifically, ROS have great effect on normal cellular signaling pathways, leading to decreased regulation of apoptosis, as well as genomic and mitochondrial DNA damage resulting in mutations, both of which promote cancer formation.^{8, 13} Using glutathione as a biomarker of oxidative stress to assess cancer status and progression has proven clinically significant through various studies.^{16, 17}

Though typically beneficial, glutathione can also play a negative role in the field of oncology.¹⁶ Patients in later stages of disease progression who require chemotherapy often

utilize one of several platinated drug compounds currently approved for use by the FDA. Cisplatin, first synthesized in 1844 by M. Peyrone, and first recognized as a potential antitumor agent in 1965, was approved by the FDA for chemotherapy in 1978.^{18, 19} When transported into the cellular membrane, cisplatin becomes “aquated” replacing labile chlorine atoms with water ligands that can further oxidize to hydroxyl groups.²⁰

These bio-transformed species are believed to be the active form of cisplatin, which target DNA at the N7 position of purine bases.^{18, 21} Interaction with the DNA leads to the production of lesions and the additional hinderance of normal DNA repair systems by the platinated drugs induces apoptosis of the cancer cell.^{18, 21} However, before the active cisplatin species can attack the cancerous DNA, strong nucleophiles within the cell such as glutathione, cysteine, and metallothionein can bind to the platinated molecule and eliminate it from the body through phase II detoxification via the urine.^{19, 22} In fact, only ~1% of intracellular cisplatin is estimated to bind to nuclear DNA.²¹ Not only can GSH conjugate to platinated drug compounds to eliminate them from the body, but elevated levels of GSH as well as the enzyme that mediates conjugation reactions (glutathione-S-transferase) have been observed in patients with cisplatin chemoresistance.²¹ This promotes the hypothesis that measuring glutathione ratios in cancer patients, before, during, and after treatment may also be a useful assessment of body burden or treatment tracking.

The relationship between cisplatin and glutathione lays the ground for chemoresistance to cisplatin treatment and has led to the production of alternative derivatives of cisplatin such as carboplatin and oxaliplatin, both of which have recently been approved for clinical use in 1989 and 2002, respectively.^{16, 19, 21} The organic content surrounding the platinum

centers of these two derivatives hinders immunological detection permitting longer half-lives within the body and the potential for greater success with cancer elimination.

III. Past and Future Clinical Directions - Dried Blood Spot Technology

Clinical biomarker assessments are typically conducted on human samples obtained through venous blood draw, urine, saliva, or hair collection depending on the relevance of the biomarker concentration to sample retrieved. For assessment of glutathione concentrations in ASD patients, the best analytical sample of relevance is whole red blood cells, as demonstrated by our lab's previous work.^{14, 15} There are several drawbacks to the use of phlebotomic blood draw however, including but not limited to: heavy restrictions and safety considerations for obtaining, shipping, and handling blood samples, constraints on the amount of blood permitted to be taken from young children, and behavioral considerations regarding problematic disorders like ASD patients and mentally unstable individuals.^{23, 24}

Mitigation of the drawbacks surrounding blood draws has brought dried blood spot (DBS) analysis to the forefront of clinical research. DBS cards are small cellulose-based matrix devices used to collect spots of blood from a patient. DBS cards typically host four sampling regions able to contain roughly 10-30 μL of liquid volume each. **(Figure I.6)** Compared to the traditional withdrawal of up to 30 mL of blood following venipuncture, the use of DBS sampling greatly reduces the sample volume.

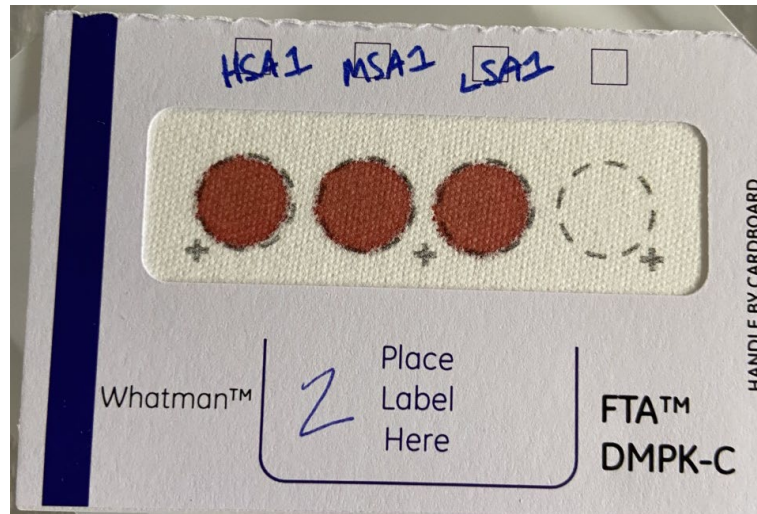


Figure I 6. Example DBS card sample with three blood spots and one unspotted region.

Preparation of the spots can be performed from the comfort of the patient's home with a minimally invasive and commonly used technique known as a finger stick to provoke a small volume of blood from the tip of a finger. This is then dripped onto the sampling region of the card and, once dried, is considered non-viable (no risk for pathogenic contamination or infection) and can be easily shipped without restriction through common mailing systems. DBS samples are also believed to increase the stability of certain analytes through interaction with the cellulose matrix of the card making long term storage simpler and lending way for potential biobanking of a patient's biological sample for retrospective studying.²⁵⁻²⁷ Of important clinical value is the frequency of which a patient's samples can be retrieved and utilized to assess biochemical status. If undergoing new forms of treatment, a patient's biochemical changes can be easily tracked through biomarker measurements on a more regular basis with less hassle and safer handling than a venipuncture draw by employing the DBS cards. Frequent assessments with ease of action enables a more personalized form of medicine instead of the one-size-fits-all or try-and-see techniques that are sometimes utilized in the medical realm.

As beneficial as this technique presents itself to be, DBS samples do not come without complication and issue. One of the most general concerns is the lack of validation with quantitative assessment owing to the traditional use of DBS cards for purely qualitative purposes.²⁸ Likewise, storage considerations may affect preservation of the analytical result, and long-term assessment of fragile or unstable compounds has not been thoroughly investigated. Cellulose is not typically amenable to humidity and high water-content in the air which can lead to mold formation or warping of the card material. Dampening of the cards may also hydrate the blood spots and result in unwanted spreading of the sample beyond its designated region. Temperature and light considerations may also affect card/analyte integrity, where ultra-violet light can often quicken the degradation of certain analytes, thus limiting the storage time frame.

Hematocrit, or the proportion of red blood cells within a total blood sample which affects blood viscosity and interaction with card matrix, has also been one of the most crucial hurdles currently preventing the transition from qualitative DBS to quantitative DBS.^{23, 28} Higher hematocrit levels often produce denser, smaller spots while low hematocrit levels result in disperse, larger spots.²⁹ This can ultimately affect the amount of blood/analyte within a respective punch used to assess the sample. Researchers have also proposed the inhomogeneous spreading of analyte concentration where some analytes may congregate in the center of the DBS while others spread to the outer edges, also resulting in uneven analyte presence in the analyzed punch.

Though the low volume sample collection from the patient is an attractive aspect of the DBS collection technique, it can disrupt the analytical assessment. Analytical samples derived from the body are dirty matrices requiring extraction and cleanup before

instrumental analysis to prevent damage to laboratory equipment. Even the most optimized extraction protocols often fail to be 100% efficient, resulting in some analyte loss. Couple low extraction efficiency with an already minimal sample volume to extract from and analysts begin seeing instrumental signals at or below limit of quantification. Sometimes analyte signal even falls below the limit of detection. Frequently, target biomarker analytes also exist in low-level concentrations within the body furthering the issue with instrumental detection and subsequent quantification.

Though troublesome as these issues may seem to other researchers, it is to this researcher's benefit that the technology of SIDMS and a new analytical advancement termed "Thor's Hammer" have for the first time addressed and mitigated the errors arising from these complications and enabled a quantitative method for glutathione and its conjugated forms from DBS sampling.

References

1. Bjorklund, G.; Meguid, N. A.; El-Bana, M. A.; Tinkov, A. A.; Saad, K.; Dadar, M.; Hemimi, M.; Skalny, A. V.; Hosnedlova, B.; Kizek, R.; Osredkar, J.; Urbina, M. A.; Fabjan, T.; El-Houfey, A. A.; Kaluzna-Czaplinska, J.; Gatarek, P.; Chirumbolo, S., Oxidative Stress in Autism Spectrum Disorder. *Mol Neurobiol* **2020**, *57* (5), 2314-2332.
2. Schaafsma, S. M.; Gagnidze, K.; Reyes, A.; Norstedt, N.; Mansson, K.; Francis, K.; Pfaff, D. W., Sex-specific gene-environment interactions underlying ASD-like behaviors. *Proc Natl Acad Sci U S A* **2017**, *114* (6), 1383-1388.
3. Ordovas, J. M.; Tai, E. S., Why study gene-environment interactions? *Curr Opin Lipidol* **2008**, *19* (2), 158-67.
4. Granot, E.; Kohen, R., Oxidative stress in childhood—in health and disease states. *Clinical Nutrition* **2004**, *23* (1), 3-11.
5. Strimbu, K.; Tavel, J. A., What are biomarkers? *Curr Opin HIV AIDS* **2010**, *5* (6), 463-6.
6. Forman, H. J.; Zhang, H.; Rinna, A., Glutathione: overview of its protective roles, measurement, and biosynthesis. *Mol Aspects Med* **2009**, *30* (1-2), 1-12.
7. Zitka, O.; Skalickova, S.; Gumulec, J.; Masarik, M.; Adam, V.; Hubalek, J.; Trnkova, L.; Kruseova, J.; Eckschlager, T.; Kizek, R., Redox status expressed as GSH:GSSG ratio as a marker for oxidative stress in paediatric tumour patients. *Oncol Lett* **2012**, *4* (6), 1247-1253.

8. Kennedy, L.; Sandhu, J. K.; Harper, M. E.; Cuperlovic-Culf, M., Role of Glutathione in Cancer: From Mechanisms to Therapies. *Biomolecules* **2020**, *10* (10).
9. Allocati, N.; Masulli, M.; Di Ilio, C.; Federici, L., Glutathione transferases: substrates, inhibitors and pro-drugs in cancer and neurodegenerative diseases. *Oncogenesis* **2018**, *7* (1), 8.
10. Dalle-Donne, I.; Rossi, R.; Colombo, R.; Giustarini, D.; Milzani, A., Biomarkers of oxidative damage in human disease. *Clin Chem* **2006**, *52* (4), 601-23.
11. Gunderson, M. P.; Nguyen, B. T.; Cervantes Reyes, J. C.; Holden, L. L.; French, J. M. T.; Smith, B. D.; Lineberger, C., Response of phase I and II detoxification enzymes, glutathione, metallothionein and acetylcholine esterase to mercury and dimethoate in signal crayfish (*Pacifastacus leniusculus*). *Chemosphere* **2018**, *208*, 749-756.
12. Yui, K.; Kawasaki, Y.; Yamada, H.; Ogawa, S., Oxidative Stress and Nitric Oxide in Autism Spectrum Disorder and Other Neuropsychiatric Disorders. *CNS Neurol Disord Drug Targets* **2016**, *15* (5), 587-96.
13. Klaunig, J. E., Oxidative Stress and Cancer. *Curr Pharm Des* **2018**, *24* (40), 4771-4778.
14. Faber, S.; Fahrenholz, T.; Wolle, M. M.; Kern, J. C., 2nd; Pamuku, M.; Miller, L.; Jamrom, J.; Skip Kingston, H. M., Chronic exposure to xenobiotic pollution leads to significantly higher total glutathione and lower reduced to oxidized glutathione ratio in red blood cells of children with autism. *Free Radic Biol Med* **2019**, *134*, 666-677.

15. Fahrenholz, T.; Wolle, M. M.; Kingston, H. M.; Faber, S.; Kern, J. C., 2nd; Pamuku, M.; Miller, L.; Chatragadda, H.; Kogelnik, A., Molecular speciated isotope dilution mass spectrometric methods for accurate, reproducible and direct quantification of reduced, oxidized and total glutathione in biological samples. *Anal Chem* **2015**, *87* (2), 1232-40.
16. Bansal, A.; Simon, M. C., Glutathione metabolism in cancer progression and treatment resistance. *J Cell Biol* **2018**, *217* (7), 2291-2298.
17. Li, H.; Ning, S.; Ghandi, M.; Kryukov, G. V.; Gopal, S.; Deik, A.; Souza, A.; Pierce, K.; Keskula, P.; Hernandez, D.; Ann, J.; Shkoza, D.; Apfel, V.; Zou, Y.; Vazquez, F.; Barretina, J.; Pagliarini, R. A.; Galli, G. G.; Root, D. E.; Hahn, W. C.; Tsherniak, A.; Giannakis, M.; Schreiber, S. L.; Clish, C. B.; Garraway, L. A.; Sellers, W. R., The landscape of cancer cell line metabolism. *Nat Med* **2019**, *25* (5), 850-860.
18. Dasari, S.; Tchounwou, P. B., Cisplatin in cancer therapy: molecular mechanisms of action. *Eur J Pharmacol* **2014**, *740*, 364-78.
19. Riddell, I. A., Cisplatin and Oxaliplatin: Our Current Understanding of Their Actions. *Met Ions Life Sci* **2018**, *18*.
20. Qi, L.; Luo, Q.; Zhang, Y.; Jia, F.; Zhao, Y.; Wang, F., Advances in Toxicological Research of the Anticancer Drug Cisplatin. *Chem Res Toxicol* **2019**, *32* (8), 1469-1486.

21. Galluzzi, L.; Senovilla, L.; Vitale, I.; Michels, J.; Martins, I.; Kepp, O.; Castedo, M.; Kroemer, G., Molecular mechanisms of cisplatin resistance. *Oncogene* **2012**, *31* (15), 1869-83.
22. Makovec, T., Cisplatin and beyond: molecular mechanisms of action and drug resistance development in cancer chemotherapy. *Radiol Oncol* **2019**, *53* (2), 148-158.
23. Henion, J.; Oliveira, R. V.; Chace, D. H., Microsample analyses via DBS: challenges and opportunities. *Bioanalysis* **2013**, *5* (20), 2547-65.
24. Lim, M. D., Dried Blood Spots for Global Health Diagnostics and Surveillance: Opportunities and Challenges. *Am J Trop Med Hyg* **2018**, *99* (2), 256-265.
25. Bastani, N. E.; Gundersen, T. E.; Blomhoff, R., Dried blood spot (DBS) sample collection for determination of the oxidative stress biomarker 8-epi-PGF(2alpha) in humans using liquid chromatography/tandem mass spectrometry. *Rapid Commun Mass Spectrom* **2012**, *26* (6), 645-52.
26. Ingels, A. S.; Lambert, W. E.; Stove, C. P., Determination of gamma-hydroxybutyric acid in dried blood spots using a simple GC-MS method with direct "on spot" derivatization. *Anal Bioanal Chem* **2010**, *398* (5), 2173-82.
27. Bowron, A.; Barton, A.; Scott, J.; Stansbie, D., Blood spot homocysteine: a feasibility and stability study. *Clin Chem* **2005**, *51* (1), 257-8.

28. Malsagova, K.; Kopylov, A.; Stepanov, A.; Butkova, T.; Izotov, A.; Kaysheva, A., Dried Blood Spot in Laboratory: Directions and Prospects. *Diagnostics (Basel)* **2020**, *10* (4).
29. Capiou, S.; Wilk, L. S.; De Kesel, P. M. M.; Aalders, M. C. G.; Stove, C. P., Correction for the Hematocrit Bias in Dried Blood Spot Analysis Using a Nondestructive, Single-Wavelength Reflectance-Based Hematocrit Prediction Method. *Anal Chem* **2018**, *90* (3), 1795-1804.

Chapter 1: Development of Manual and Fully Automated Dried Blood Spot (DBS) Card Desorption Techniques for SIDMS Quantification of Glutathione

The goal of this research is to take the previously validated methodology of retrieving a phlebotomic blood draw sample to quantify glutathione and minimize it to the DBS sampling technique with an acceptable level of accuracy and precision. Accomplishing this goal enables a simplified sample collection technique enabling more frequent biomarker assessments of patient condition for a personalized medical plan, thereby improving patient treatment and outcomes.

One of the biggest challenges with glutathione quantification is its unstable nature and likelihood for oxidation. During sample retrieval, processing, and analysis, GSH can autoxidize to its more stable dimer form, GSSG.¹⁻⁴ Previous researchers have struggled to accurately quantify GSH and GSSG concentrations due to this transformation between species, which often led to an underestimation of GSH concentration and overestimation of GSSG concentration within the analytical sample.^{3,5} This inaccuracy propagates further when ratios of GSH/GSSG are calculated causing the results of the biomarker analysis in relation to disease state to be improper. In fact, the literature argued over the correct way of determining the GSH/GSSG ratio by over three orders of magnitude prior to 2014.^{3,5-8} **(Figure 1.1)** The largest cause of this error is the use of calibration curve quantification which possesses no ability for the tracking and correcting of this conversion between species.

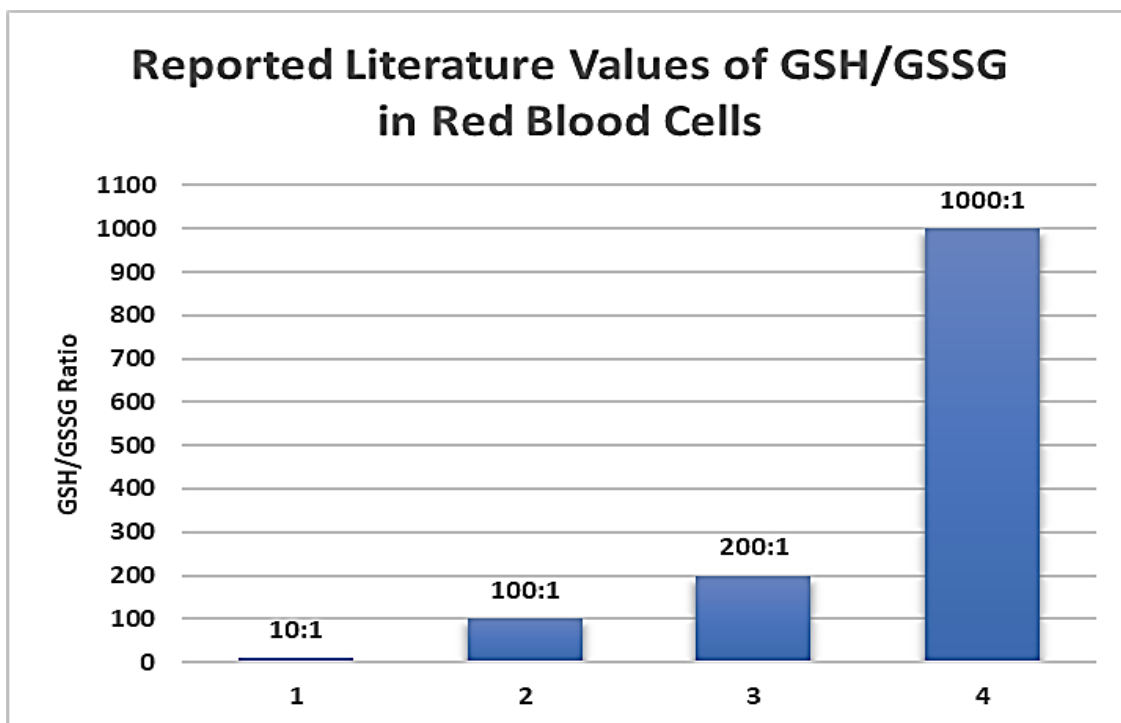


Figure 1. 1. Reported "healthy" values for the GSH/GSSG ratio estimated by researchers from 2001-2012. (1 = Cereser et al., 2 = Zitka et al., 3 = Michaelesen et al., 4 = Harwood et al)^{3, 5, 6, 8}

An additional complication in glutathione quantification was the misunderstanding of the biochemical nature of glutathione regarding a tGSH determination. Researchers often analyzed GSSG concentrations first and then fully reduced the biological sample with a reducing agent, like dithiothreitol (DTT), to obtain a tGSH measurement.^{3, 5} They would then subtract GSSG from tGSH to obtain a GSH concentration estimate rather than directly quantifying the individual species. This, however, does not account for the GS-R concentration, which would also be reduced following treatment with DTT. Again, this leads to over- and underestimation in GSH and GSSG concentrations, respectively.

In 2015, a previous researcher in the Kingston Laboratory, Dr. Timothy Farenholz, developed and validated an accurate, precise, and reproducible method for quantifying all species of glutathione by utilizing SIDMS, as described in EPA Method 6800.^{9, 10} SIDMS

(and IDMS for tGSH assessment) utilizes isotopically enriched, chemically indistinguishable forms of GSH and GSSG at known concentrations spiked into a natural sample upon collection which can later be differentiated via shifts in m/z using mass spectrometry. Isotopic materials used in sample collection and preparation enable the tracking of interconversion between species. Knowing the amount of oxidation incurred promotes the correction of respective concentrations to obtain the original concentrations of both species within the original obtained sample, something that researchers in the past were not able to accomplish.

SIDMS mathematics can be conducted in two forms: determinative or iterative. In the 2015 Analytical Chemistry Journal article by Fahrenholz et al, iterative mathematics were published.⁹ For this reported project, the determinative mathematics are employed. Determinative mathematics facilitate direct quantification of every participating species of interest, which is then deconvoluted to yield a single result. (Equations 1.1-1.7) Equation 1.1 and 1.2 demonstrate the initial estimation of ⁶¹²GSSG and ³⁰⁶GS-NEM concentrations, respectively. Equation 1.3 demonstrates the determination of ⁶¹⁵GSSG concentration, the important oxidation product. Equation 1.4 and 1.5 show the conversion of respective oxidation concentrations to amendable units of μmoles for deconvolution of original analyte concentrations. Equation 1.6 and 1.7 demonstrate the final steps for determining the original concentrations of both natural glutathione species.

Determinative SIDMS Mathematic Equations

$$C_x^{GSNEM} = \frac{C_s^{GSNEM} W_s^{GSNEM}}{W_x} \left(\frac{{}^{307}A_s - R_{307/304} {}^{304}A_s}{R_{307/304} {}^{304}A_x - {}^{307}A_x} \right)$$

Equation 1. 1

$$C_x^{GSSG} = \frac{C_s^{GSSG} W_s^{GSSG}}{W_x} \left(\frac{{}^{359}A_s - R_{359/355} {}^{355}A_s}{R_{359/355} {}^{355}A_x - {}^{359}A_x} \right)$$

Equation 1. 2

$$C_x^{615GSSG} = \frac{C_s^{616GSSG} W_s^{616GSSG}}{W_x} \left(\frac{{}^{359}A_s - R_{359/358} {}^{358}A_s}{R_{359/358} {}^{358}A_x - {}^{359}A_x} \right)$$

Equation 1. 3

$$\text{Concentration of GSH Oxidized } (\mu\text{g/g}) = \frac{1}{2} \left(\frac{\mu\text{mol } {}^{615}\text{GSSG}}{W_x} \right) \left(\frac{307.12 \mu\text{g}}{\mu\text{mol}} \right)$$

Equation 1. 4

Concentration of GSSG from Oxidation ($\mu\text{g/g}$)

$$= \frac{1}{4} \left(\frac{\mu\text{mol } {}^{615}\text{GSSG}}{W_x} \right) \left(\frac{612.63 \mu\text{g}}{\mu\text{mol}} \right)$$

Equation 1. 5

Original GSH Concentration = $C_x^{GSNEM} - \text{Oxidized GSH}$

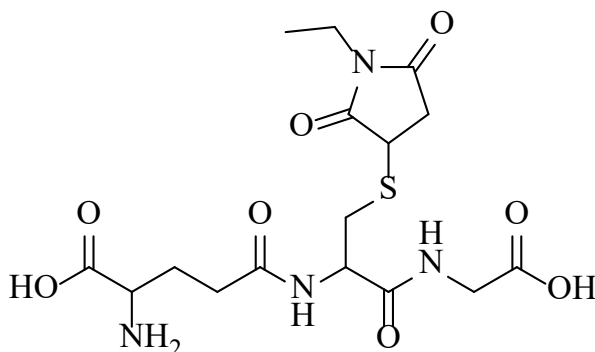
Equation 1. 6

Original GSSG Concentration = $C_x^{GSSG} - \text{GSSG from Oxidation}$

Equation 1. 7

This researcher found that preparing isotopically enriched ${}^{310}\text{GSH}$ in a solution of N-ethylmaleimide (NEM) in water immediately upon isotope retrieval binds the reactive thiol, producing the ${}^{309}\text{GS-NEM}$ species, and stabilizes the easily oxidized GSH molecule for increased shelf-life and stability. Derivatization with NEM is an irreversible binding working to prevent oxidation of sensitive compounds by blocking the reactive thiol group.

This binding takes about 20 minutes at room temperature to complete and demonstrates 99% efficiency. The concentration of $^{309}\text{GS-NEM}$ present within the spike solution is then certified via reverse-IDMS (RIDMS) utilizing natural standard reference materials for ^{307}GSH purchased at varying purities and from separate companies. These natural analytes are also immediately stabilized with NEM yielding the $^{306}\text{GS-NEM}$ compound. (**Figure 1.2**) Stabilization of the reactive thiol group negates the need for quantifying the ^{310}GSH - ^{310}GSH oxidation product of $^{618}\text{GSSG}$, previously undertaken in the work by Farenholz et al, as any unbound ^{310}GSH concentration is not utilized for future SIDMS calculations and $^{618}\text{GSSG}$ is clearly discerned from the target GSSG species, $^{612}\text{GSSG}$, with mass spectrometry analysis.



Molecular Weight: 432.45

Reduced Glutathione Bound to N-ethylmaleimide

Figure 1. 2. The molecular structure of reduced glutathione bound to N-ethylmaleimide (NEM).

During sample collection, preparation, and analysis target natural ^{307}GSH species can oxidize to the target natural $^{612}\text{GSSG}$ species if the ^{307}GSH is not bound to NEM quickly enough, demonstrating the need for correction to quantification of either species. Because NEM is introduced to the natural sample immediately, oxidation is minimal, typically less than 2%. To account for the minimal amount of oxidation taking place, the

concentration of hybrid oxidation product, $^{615}\text{GSSG}$, is quantified where one ^{307}GSH molecule and one ^{310}GSH molecule come together indicating the relative level of $^{612}\text{GSSG}$ produced before NEM binding can occur. (Equation 1.3) This concentration is used for correcting estimated $^{306}\text{GS-NEM}$ and $^{612}\text{GSSG}$ quantification (Equations 1.4-1.7) to yield the original concentration of either species present in the sample.

One of the key features of utilizing SIDMS or IDMS mathematics is the known weights of isotopic solution (W_s) and natural sample (W_x) combined for analytical sample preparation. Gravimetric analysis is far more precise a measure of the amount of sample utilized than volumetric, as it does not differ with changing temperature, pressure, or buoyancy of sample being weighed. When utilizing the DBS card sample collection, obtaining weight of sample applied to the card is complicated due to the very small sample size and the instantaneous drying of the sample upon introduction to the cellulose card matrix. Obtaining weights for specific blood spot application to a sample card is also not a feasible expectation of the method when put into practice. At-home kits will not provide or carry the expectation of the patient to weigh each individual application of blood, nor would this be considered a precise/accurate weight with lack of a precision balance. Therefore, either volumetric or weight estimation must be employed.

For method validation, isotopic and natural solutions were combined in the same microcentrifuge tube with the weight of both additions recorded, thorough mixing, and equilibration achieved PRIOR to sample spotting onto the card matrix. Once the extraction and analysis methods were validated, varying application techniques were employed to be a more feasible or favorable method for patients to employ at home. These included: (1) the shipment of a tube containing previously weighed isotopic solution to which a patient

would add four drops of blood from a finger stick so that isotopic solution and blood could be shaken to mix, permitted 10 minutes of time to equilibrate and then a supplied disposable micropipette would be used to spot a single drop of roughly 10 μ L to each of the sampling regions. (2) Isotopic solution was weighed in a microcentrifuge tube and 10 μ L volumes were spotted onto each of four sampling regions of the DBS card. This was given time to dry completely before a single drop of natural blood sample was spotted on top of isotope. (3) Microchannel fluidic devices from HemaXisTM calibrated at 10 μ L were used for applying both isotopic solution and natural blood sample to the sampling card. The main goal to testing various application techniques is finding the most feasible technique able to be employed by untrained patients yielding the best analytical result.

Materials and Methods

Reagents and Standards:

Negative synthetic blood was purchased from Immunalysis Corp (p/n:SB-0050). Naturally abundant reference standards for reduced glutathione (99%+ pure, p/n: 70-18-8) and oxidized glutathione (98%+ purity, p/n: 27025-41-8) standard reference materials were purchased from Sigma-Aldrich. A second naturally abundant reference standard for reduced glutathione (98%+ pure, p/n:70-18-8) was purchased from Alfa Aesar. Isotopically enriched reference standards of reduced glutathione (65-70% net peptide purity, glycine-13C2 and 15N, p/n: CNLM-6245-50) and oxidized glutathione (65-70% net peptide purity, glycines-13C2, p/n: CLM-8645-PK) were purchased from Cambridge Isotope Laboratories, Inc. (Cambridge, MA). Whatman DMPK-C dried blood spot cards of plain, non-treated cellulose matrix were purchased from Fisher Scientific (pure cellulose, p/n: 09-801-000). The mixed-mode strong anion exchange (MMAE) SPE cartridges were

purchased from SparkHolland. (Polymer Sax cartridges. 25 - 35um, p/n: 018804-022-00) Dithiothreitol (DTT) (98%+ purity, p/n: 3483-12-3) and N-ethylmaleimide (NEM) (98%+ purity, p/n: 128-53-0) reagents were purchased from Sigma-Aldrich. HPLC grade acetonitrile and methanol were purchased from Fisher Scientific. Formic acid (99%+ purity, p/n: 64-18-6) was purchased from Sigma-Aldrich. Doubly deionized water was generated by the Barnstead Nanopure in-lab water filtration and purification system from ThermoScientific. Trifluoroacetic acid was purchased from Fisher Scientific (99.7% purity, p/n: 76-05-1). Isopropanol was purchased from Acros (p/n: 67630). Methanol was purchased from Fisher Scientific. (HPLC Grade, p/n: 67561) Ammonium hydroxide was purchased from VWR. (28-30% w/w, p/n: 1336216) Ammonium bicarbonate was purchased from Fisher Scientific (21.43% w/w; p/n: 1066-33-7)

Equipment:

Online DBS desorption was achieved with the GERSTEL Dried-Blood Spot Autosampler (DBS-A, s/n: p0106) which possess a multipurpose autosampler (MPS) attached to the automated cartridge exchanger (ACE, s/n: 130017) and the high-pressure dispenser (HPD, s/n: 130021). The column used for glutathione analysis was a Phenomenex SynergiTM 4 μ m Hydro-RP 80 Å LC column C18, 150 x 4.6 mm (p/n: 5375-0097). The system used for LC-MS/MS analysis was the Agilent 1200 Series High Performance Liquid Chromatography (HPLC) system in tandem with the Agilent 6460 Triple Quadrupole Mass Spectrometer (s/n: US92170174, NSF MRI: 0821401) with an Agilent Jetstream electrospray ionization source (Model: G1958-65138; s/n: US91500324). All data was collected and processed using Agilent's MassHunter Acquisition and Qualitative Analysis programs (Version 10.0 SR1; Build: 10.0.142). Clear

airtight snap-cap 1.5 mL polypropylene microcentrifuge tubes were purchased from VWR (p/n: 20170-038). A VortexGenie2 from Scientific Industries, Savant SPD1010 SpeedVac Concentrator from Thermo Scientific, sonication bath from Branson, the XS105 DualRange analytical balance from Mettler Toledo, and a MiniSpin microcentrifuge from Eppendorf were used for various aspects of sample preparation.

Manual Extraction Method – Speciated Glutathione Analysis

After analytical samples had been spotted and dried onto Whatman DBS cards, each individual sampling region was manually punched from the card using a steel 8 mm punch. This card punch was then cut carefully into four small pieces with scissors using Teflon tipped tweezers to avoid touching the card matrix with gloved hands. These small pieces were placed into a respectively labeled microcentrifuge tube and 300 μ L of a 70:30 (v/v) water: acetonitrile desorption solution was added to the tube being sure all pieces of card matrix were fully covered by solvent. These samples were then vortexed for 30 seconds on the VortexGenie before being placed in a sonication bath at 60°C for 1 hour. Samples were then placed into a centrifuge at 4°C for 10 minutes to push card matrix to the base of the microcentrifuge tubes. Supernatant was transferred to a clean microcentrifuge tube and then placed on the Speedvac for 2 hours with 1.5 hours of heating at 50°C and maintenance of 5.1 bar pressure until samples were completely dried to a small pellet. Samples could then be stored in a 4°C refrigerator until ready for analysis or immediately reconstituted with 80 μ L of 18 Ω water with thorough agitation to dissolve the pellet. Samples were then centrifuged for 10 minutes at 4°C and supernatant was transferred to an LC-MS vial for instrumental analysis.

Manual Extraction Method – Total Glutathione Analysis

After analytical samples had been spotted and dried onto Whatman DBS cards, each individual sampling region was manually punched from the card using a steel 8 mm punch from Harris. This card punch was then cut carefully into four small pieces with scissors using Teflon tipped tweezers to avoid touching the card matrix with gloved hands. These small pieces were placed into a respectively labeled microcentrifuge tube and 300 μL of a 70:30 (v/v) 9,000 $\mu\text{g/g}$ DTT in water: acetonitrile desorption solution was added to the tube being sure all pieces of card matrix were fully covered by solvent. These samples were then vortexed for 30 seconds on the VortexGenie before being placed in a sonication bath at 60°C for 1 hour. Samples were then placed into a centrifuge at 4°C for 10 minutes to push card matrix to the base of the microcentrifuge tubes. Supernatant was transferred to a clean microcentrifuge tube and then placed on the Speedvac for 2 hours with 1.5 hours of heating at 50°C and maintenance of 5.1 bar pressure until samples were completely dried to a small pellet. Samples could then be stored in a 4°C refrigerator until ready for analysis or immediately reconstituted with 80 μL of 18 Ω water with thorough agitation to dissolve the pellet. Samples were then centrifuged for 10 minutes at 4°C and supernatant was transferred to an LC-MS vial for instrumental analysis.

Fully Automated Extraction Method of DBS Samples

Online Desorption Method

Instrument configuration for valve switching during extraction actions is demonstrated in **Table 1.1**. The HPD is connected to the desorption chamber of the MPS permitting flow of solvents A-F throughout the system. ISS2 valve is connected to the desorption chamber and plumbed to the right clamp valve. The right clamp valve is connected to the HPLC mobile phase pump as well as to the column.

Table 1. 1. Valve positions and flow description for the DBS-A instrument.

Mode of Action	Valve Position for ISS2	Valve Position for Right Clamp	Description of Flow
Load/Remove Cartridge	1-2	1-6	From HPD to desorption chamber to waste
Condition/Equilibrate/Wash Cartridge	1-2	1-6	From HPD to desorption chamber to waste
Inject Sample	1-6	1-2	From HPD to waste, LC lines through cartridge flow path

Using the ACE, the extraction cartridge of choice is selected from the position the rack and loaded into the right clamp. For MMAE extraction, the cartridge was conditioned with 1 mL of methanol and equilibrated for sample loading with 1 mL of 0.05059 M ammonium bicarbonate buffer in water. The sample spot was desorbed from the DBS card by flowing 1 mL ammonium bicarbonate buffer in water heated to 60 C. Sample elution from cartridge stationary phase was accomplished by flowing mobile phase solvent at 100% water with 0.1% formic acid at 1.0 mL/min. The cartridge was held in position with no movement for 7.0 minutes while the acquisition method was running. Upon 7.0 minutes, the cartridge was removed, and all clamps were rinsed before subsequent sample analysis was undertaken. A full display of sequential DBS-A online desorption and extraction method parameters can be found in **Table 1.2**.

Table 1. 2. DBS-A method parameters for automated extraction of DBS sample spots.

Mode of Action	Parameters
Condition Cartridge	HPLC Grade Methanol Volume: 1 mL Flow Aspirate: 3.0 mL/min Flow Dispense: 3.0 mL/min
Equilibrate Cartridge	HPLC Grade 0.05059 M Ammonium Bicarbonate Buffer

	Volume: 1 mL Flow Aspirate: 3.0 mL/min Flow Dispense: 3.0 mL/min
DBS Desorption	<u>Sample Mode & Recognition</u> Centered, Partial Spot Blood Spot Detection <u>Blood Spot Desorption</u> 0.05059 M Ammonium Bicarbonate Buffer Volume: 1 mL Flow Aspirate: 5 mL/min Flow Dispense: 1 mL/min Clamp Heating: 60 °C <u>Post Desorption Clamp Cleaning</u> 3:3:3:2 Acetonitrile: Methanol: Isopropanol: Water Volume: 1 mL
Wash Sample	5% Ammonium Hydroxide in Water Volume: 0.2 mL Flow Aspirate: 4 mL/min Flow Dispense: 0.4 mL/min
Inject Sample	Runtime set for 10.0 mins
Wait	“Do not move during wait time” 7.0 min duration
Total time for processing four sampling regions of a single card	~60 minutes

HPLC Method Parameters

For all manually extracted card samples, 7 μ L of the sample was injected onto the column with a 30 second pre- and post-injection needle wash with Mobile Phase B. Separation of glutathione species was accomplished using water with 0.1% formic acid as Mobile Phase A and acetonitrile with 0.1% formic acid as Mobile Phase B at a flow rate of 1.000 mL/min. (**Figure 1.3** and **1.4**) The binary gradient for manually extracted samples was designed to hold at 5% B for 2 minutes, increase to 70% B over the next two minutes, increase to 95% B over the next 1.5 minutes, hold at 95% B for 1.1 minutes, decrease to

5% B over the next 0.4 minutes, and equilibrate the column at 5% B for 3 minutes with a final stop time of 10 minutes.

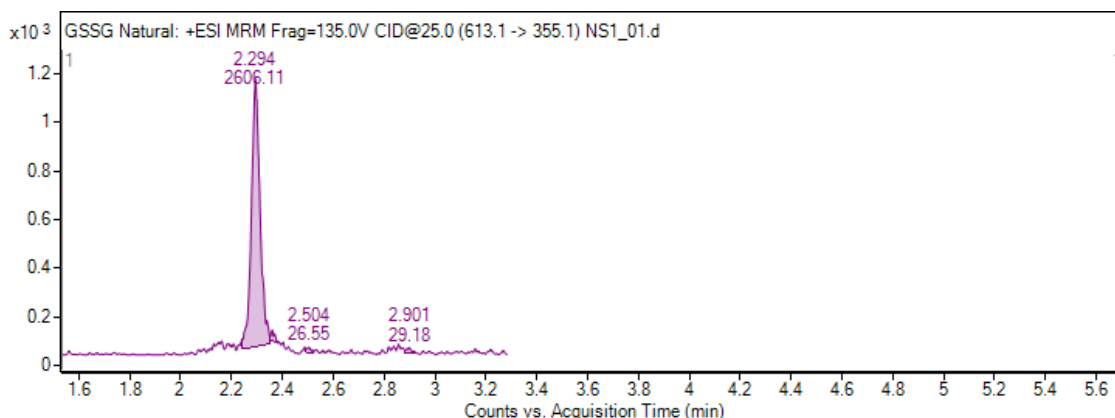


Figure 1. 3. MRM chromatogram for 612GSSG species following manual extraction of DBS sample and LC-MS/MS analysis. RT for 2.294 minutes

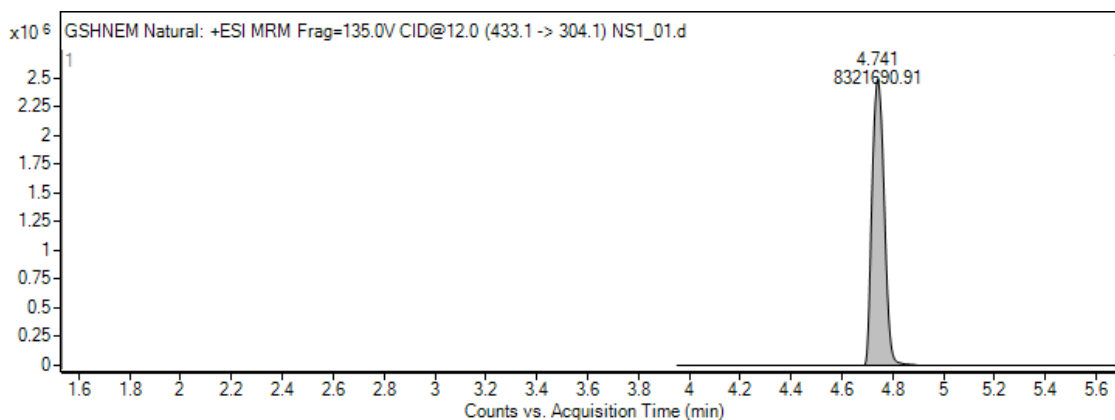


Figure 1. 4. MRM chromatogram for 306GS-NEM species following manual extraction of DBS sample and LC-MS/MS analysis. RT at 4.741 minutes.

The same solvent system employed for manually extracted sample analysis was utilized for the fully automated DBS-A system for separation of both analytes. (Figures 1.5 and 1.6) The binary gradient for online desorption samples was designed to hold at 0% B for 0.5 minutes, increase to 70% B over the next 3.5 minutes, increase to 95% B over the next 2 minutes, decrease to 0% B over the next 0.6 minutes, and equilibrate the column at 0% B for 3.4 minutes with a final stop time of 10 minutes.

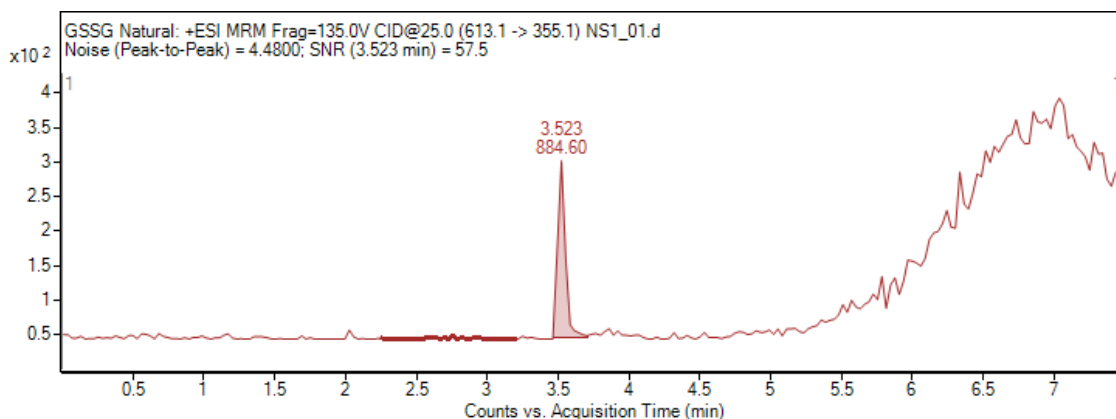


Figure 1. 5. MRM chromatogram for $^{612}\text{GSSG}$ species following fully automated DBS-A extraction of DBS sample and LC-MS/MS analysis. RT for 3.523 minutes.

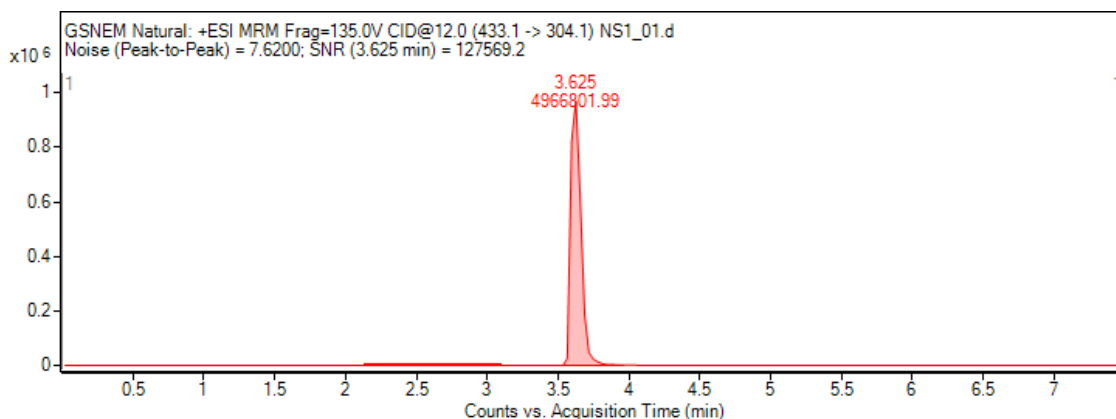


Figure 1. 6. MRM chromatogram for $^{306}\text{GS-NEM}$ species following fully automated DBS-A extraction of DBS sample and LC-MS/MS analysis. RT for 3.625 minutes.

The instrument was set up to run in multiple reaction monitoring (MRM) mode with instrument parameters as follows: gas temperature at 300 °C, gas flow at 8 L/min, nebulizer at 45 psi, sheath gas temperature at 250 °C, sheath gas flow at 11 L/min, capillary voltage set to 4000 V for both positive and negative, and nozzle voltage at 500 V for both positive and negative. The MRM transitions used for analyte detection are described in **Table 1.3** to track for all species of GSH and GSSG necessary for quantification, including: the natural species, $^{306}\text{GS-NEM}$ and $^{612}\text{GSSG}$, the isotopically enriched spikes, $^{309}\text{GS-}$

NEM and $^{616}\text{GSSG}$, and the oxidation products of $^{615}\text{GSSG}$ and $^{618}\text{GSSG}$ to correct for interconversion of species.

Table 1. 3. MRM transitions for detection of glutathione species on the LC-MS/MS.

<u>Compound</u>	<u>Precursor Ion</u>	<u>Product Ion</u>	<u>Fragmentor</u>	<u>Collision Energy</u>	<u>Cell Accelerator Voltage</u>
^{307}GSH	308.1	179.1	135	12	7
^{310}GSH	311.1	182.1	135	12	7
$^{306}\text{GS-NEM}$	433.1	304.1	135	12	7
$^{309}\text{GS-NEM}$	436.1	307.1	135	12	7
$^{616}\text{GSSG}$	617.1	359.1	135	25	7
$^{612}\text{GSSG}$	613.1	355.1	135	25	7
$^{615}\text{GSSG}$	616.1	358.1	135	25	7
$^{618}\text{GSSG}$	619.1	361.1	135	25	7

Method Validation

Using the Food and Drug Administration’s “*Bioanalytical Method Validation: Guidance for Industry*” document, the following aspects of both extraction methods were investigated for validation: quality control sample analysis, selectivity and specificity, sensitivity, accuracy, precision, recovery, and stability.¹¹ An additional layer of validation was completed by cross-validation with comparison to the previously validated and published methodology of whole blood extraction published by Farenholz et al.⁹ As stated in the validation guidelines, “In general, FDA’s guidance documents do not establish legally enforceable responsibilities. Instead, guidances describe the Agency’s current thinking on a topic and should be viewed only as recommendations, unless specific regulatory or statutory requirements are cited. The use of the word *should* in Agency guidances means that something is suggested or recommended, but not required.”¹¹ With this consideration in mind, particular aspects of the guidelines may not be applicable to the

current research such as that corresponding to calibration curve quantification considering SIDMS and IDMS mathematics are employed.

All standard reference materials (SRM) and certified reference materials (CRM) should be identical to the biological analyte of interest or as close as possible if an exact match cannot be purchased. SRM and CRM should have defined purity of analytical quality (+98% preferred) and researchers should provide certificates of analysis for each SRM or CRM. (appendix) Quality control (QC) samples are prepared using the SRM and CRM to assess accuracy and precision (A&P) of the assay as well as stability of the samples under varying conditions. QC samples should be prepared fresh for best assessment of A&P during method development and validation. To meet acceptance, >67% of QC analyses should be +/- 15% error of nominal concentration. Accuracy should be +/- 15% error from nominal concentration above LOQ and +/- 20% error below LOQ. Precision is demonstrated by the coefficient of variance (CV) see equation #. %CV should be +/- 15% to meet acceptance.

Selectivity demonstrates that the analyte of interest is being identified properly with limited or avoidance of interferences. Selectivity is demonstrated through blanks analysis of the appropriate matrix to determine signal presence mimicking that of the analyte. Specificity demonstrates the method's ability to differentiate analyte from matrix components or other analyte or non-target compounds within the sample. Analysts should minimize non-target interference as much as possible as well as determine the effects of the matrix on ion-suppression, ion enhancement, or extraction efficiency. Carryover between samples should be eliminated if possible or minimized so that blank signal does not exceed 20% of the limit of quantification. Acceptance is dictated by the lack of signal

present at the retention time of the analyte following blank analysis where the internal standard (IS) and natural analyte response should be less than 5% of average IS signal within QC analysis samples.

Sensitivity is defined by the LLOQ which can be assessed simultaneously with A&P as well as recovery. QC samples should be prepared in a biological relevant range to clinical sample expectation in the high, mid, and low concentration range to determine whether the method is applicable to biological samples. A minimum of three independent runs of QC samples should be conducted over several days. Recovery of analyte signal following extraction need not be 100% and should be assessed by comparing analytical results of extracted QC samples against blanks spiked with analyte SRM post-extraction. Analyte signal of QC prepared to be LOQ concentration observing signal five times greater than that of the zero calibrator (or blank) demonstrates sensitive analysis.

Stability should be assessed by submitting the sample to a variety of handling and storage conditions to determine the method's robustness. Considerations for storage include benchtop, autosampler, refrigeration, freezer, light-avoidance, air-avoidance, and other forms of temperature control. Handling conditions include length of time for sample shipment and long-term storage prior and post-extraction.

Partial and cross validation is accomplished by comparing quantification of QC samples between the new presently unvalidated method and a currently validated method. Cross validation is permissible when modifications are made to an already validated bioanalytical method. These changes include but are not limited to bioanalytical method transfers between laboratories, changes in analytical methodology (i.e. chromatography

method, detection system), changes in sample processing procedure, changes in sample volume, changes in instrument and/or software platform, and extensions of assay range.

Specific guidance surrounding DBS processing is offered emphasizing the need to assess storage and handling procedures, sample homogeneity, hematocrit impact, analyte stability over time pending storage, carryover, and reproducibility including incurred sample reanalysis (ISR). ISR involves reprocessing and analyzing the same sample several times ensuring that identical extraction and processing procedures are used each time. ISR should be conducted at least once.

Validation Results

Samples of negative synthetic blood were spotted onto DBS card matrix, permitted to dry, and underwent extraction/analysis through manual and fully automated methodologies to ensure no interference was observed at the retention times of the target analytes. For manually extracted cards, the average counts for intensity at retention time of 2.3 mins (GSSG) were 1409 +/- 55 counts and for 4.8 mins (GS-NEM) were 5369 +/- 1541 counts. For DBS-A extracted cards, the average counts for intensity at retention time of 3.462 mins (GSSG) were 156 +/- 47 counts and for 3.625 mins (GS-NEM) were 4516 +/- 3280 counts. This demonstrates the selectivity of the analysis for the intended analytes. Employment of HPLC to separate the analytes from matrix components and other analytes as well as the use of MRM transitions for analysis of glutathione permits satisfactory specificity.

Generation of calibration curves standards in negative synthetic blood were submitted to whole blood, manual, and fully automated extraction techniques. (**Table 1.4**) As expected, whole blood extraction which utilizes a larger sample volume yields a lower

LOD and LOQ for GS-NEM species. For GSSG, the DBSA extraction technique increases the sensitivity of the analysis permitting very low LOD and LOQ estimations.

Table 1. 4. Estimated LOD and LOQ concentrations for both analytes using different methodologies of extraction.

Methodology	³⁰⁶GS-NEM (µg/g)		⁶¹²GSSG (µg/g)	
	LOD	LOQ	LOD	LOQ
Whole Blood	34.17	103.6	1.904	5.770
DBS Manual	71.56	216.86	1.928	5.843
DBSA	105.21	318.82	0.541	1.640

All samples analyzed as part of this work are considered QC samples given the artificial production in comparable negative blood matrix before processing and analysis. Given the excellent and consistently high instrumental signal for the GS-NEM analyte along with the 100-fold higher physiological concentration compared to GSSG, issue with quantification of GS-NEM is rarely observed. The accuracy of natural GS-NEM concentration quantified by whole blood, manual, and DBS-A extraction protocols (detailed in the methods section) rarely exceeds 5% error from nominal concentration and, even with some deviation above 5% remain within the acceptable range of error. (**Table 1.5**)

Table 1. 5. Assessment of analytical accuracy regarding GS-NEM (GSH) and GSSG quantification following different extraction techniques, represented by %error from nominal concentration calculations.

Assessment of Analytical Accuracy													
Whole Blood Extraction Error							Manual Set 3 Extraction Error						
	GS-NEM			GSSG				GS-NEM			GSSG		
Sample	Theo	Calc	%Error	Theo	Calc	%Error	Sample	Theo	Calc	%Error	Theo	Calc	%Error
NS1	591.18	604.52	2.3%	2.02	3.05	51.2%	NS1	591.18	576.94	2.4%	2.02	2.32	14.9%
NS2	360.54	366.36	1.6%	11.45	10.44	8.8%	NS2	360.54	344.09	4.6%	11.45	10.06	12.1%
NS3	221.47	222.00	0.2%	29.21	26.58	9.0%	NS3	221.47	220.77	0.3%	29.21	26.63	8.9%
Manual Set 1 Extraction Error							DBSA1 Extraction Error						
	GS-NEM			GSSG				GS-NEM			GSSG		
Sample	Theo	Calc	%Error	Theo	Calc	%Error	Sample	Theo	Calc	%Error	Theo	Calc	%Error
NS1	591.18	577.43	2.3%	2.02	2.24	11.0%	NS1	591.18	566.62	4.2%	2.02	2.92	44.6%
NS2	360.54	343.90	4.6%	11.45	9.50	17.0%	NS2	360.54	339.25	5.9%	11.45	4.41	61.5%
NS3	221.47	220.56	0.4%	29.21	25.93	11.2%	NS3	221.47	198.98	10.2%	29.21	17.97	38.5%
Manual Set 2 Extraction Error							DBSA2 Extraction Error						
	GS-NEM			GSSG				GS-NEM			GSSG		
Sample	Theo	Calc	%Error	Theo	Calc	%Error	Sample	Theo	Calc	%Error	Theo	Calc	%Error
NS1	591.18	577.19	2.4%	2.02	2.17	7.5%	NS1	591.18	556.16	5.9%	2.02	1.16	42.4%
NS2	360.54	343.13	4.8%	11.45	9.70	15.2%	NS2	360.54	341.84	5.2%	11.45	10.71	6.4%
NS3	221.47	220.34	0.5%	29.21	25.93	11.2%	NS3	221.47	221.50	0.0%	29.21	10.01	65.7%

The precision of GS-NEM analysis is especially acceptable, where %CV does not often exceed 2% and consistently falls within the acceptable %CV range. (Table 1.6)

Table 1. 6. Assessment of analytical precision regarding GS-NEM (GSH) and GSSG quantification following different extraction techniques, represented by %CV calculations.

Assessment of Analytical Precision						
%CV for ³⁰⁶ GS-NEM Quantification						
Extraction Technique	Whole Blood	Manual 1	Manual 2	Manual 3	DBSA 1	DBSA 2
NS1	0.51%	0.14%	0.05%	0.02%	0.20%	2.06%
NS2	0.51%	0.21%	0.02%	0.27%	0.27%	0.28%
NS3	0.41%	0.12%	0.06%	0.16%	14.98%	0.16%
%CV for ⁶¹² GSSG Quantification						
Extraction Technique	Whole Blood	Manual 1	Manual 2	Manual 3	DBSA 1	DBSA 2
NS1	9.64%	6.51%	7.12%	2.72%	33.86%	60.98%
NS2	7.32%	3.11%	4.53%	2.43%	7.33%	52.65%
NS3	4.36%	2.19%	3.23%	0.76%	9.46%	40.04%

The recovery of GS-NEM from whole blood, manual, and DBSA extractions are between 40-50%, 20-35%, and 7-10%, respectively. Attained recoveries were expected based on the conditions surrounding each extraction technique, and despite the low %recovery, accurate and precise quantification of GS-NEM is maintained.

The lower concentration and difficulty producing adequate instrumental signal for the analyte, GSSG, contributes to the inaccuracy and imprecision seen with analyses. Likewise, the estimated LOQ for each extraction technique can demonstrate what concentration of the analyte is able to be quantified based on the described method. Whole blood and manual extraction techniques estimate an LOQ of ~6 µg/g for GSSG, explaining the higher indicated %error from nominal for sample concentrations below this value with the whole blood extraction technique. (**Table 1.6**) Manual extraction demonstrates acceptable accuracy above and below LOQ, an improvement beyond the method of whole blood extraction. DBS-A extraction rarely establishes accuracy for GSSG quantification, likely due to the very low recovery of analyte following online desorption. DBS-A extraction of GSSG will require further optimization and employment of a specialized, patent-pending analytical signal amplification technique to enable accurate quantification of this species. Precision via %CV of GSSG analysis falls within acceptable levels for both whole blood extraction and manual extraction techniques. The DBS-A extraction, however, does not meet satisfactory precision for concentrations of GSSG, due to the same issues affecting accuracy. (**Table 1.6**)

Given the validation of the manual extraction technique for analysis of both target species, DBS card samples were submitted to a range of storage conditions for different durations of time to determine the analytes' stabilities. Storage conditions included open-air clean-room benchtop, refrigeration at 4 °C, incubation at 37 °C, and sealed within an alumina bag for a duration of 48 hours. Upon manual extraction, quantification of both GS-NEM (GSH) and GSSG were accomplished (n=4). Data was then utilized to calculate the

important biomarker: GSH/GSSG ratio. Direct analysis was performed on a sample of clean QC standard analyzed without extraction.

The goal of the storage assessment was to observe what condition would yield agreement with the direct analysis result following 48 hours previously dictated storage condition. By plotting the calculated GSH/GSSG ratio with the uncertainty of the calculation represented by the error bars, we observe storage in a sealed alumina bag followed by manual extraction is the only technique in agreement with the direct analysis ratio at higher concentrations of both analytes. Interestingly, incubation at 37 °C performs best at mid-range concentrations while refrigeration at 4 °C performs best at lowest level concentrations when it comes to permitting agreement with the direct analysis result.

(Figure 1.7)

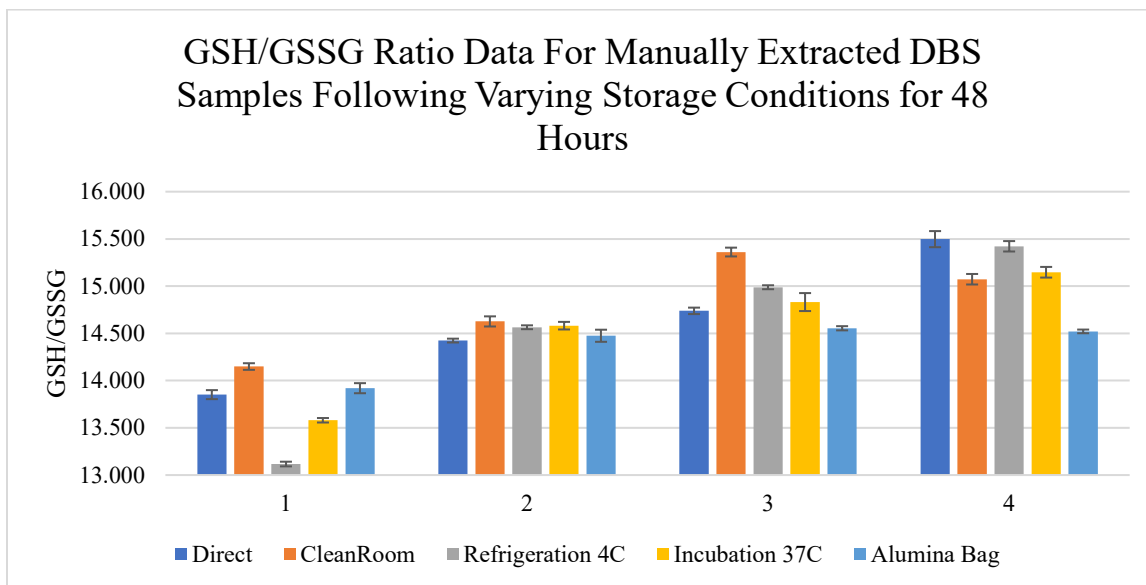


Figure 1. 7. Graphical representation comparing the analytical result of the GSH/GSSG ratio calculations derived from quantification of both species following manual DBS extraction after varying storage conditions.

Given the very narrow uncertainty demonstrated in the ratio calculation, additional statistical comparison of resulting data utilizing student's t-test was conducted.

It can be concluded data achieved are minimally different with p-values indicating no statistical difference in the analysis result ($p > 0.05$) between the direct ratio determination and any storage condition. (Table 1.7)

Table 1. 7. Statistical results for comparing GSH/GSSG ratio data achieved for DBS card manual extraction analysis following 48 hours in varying storage conditions

<i>Direct vs. Open-Air Cleanroom</i>							
Sample	Ratio	Uncertainty	Sample	Ratio	Uncertainty	%Diff	p-value
S1	13.851	0.030	Clean S1	14.149	0.022	2.12%	0.3567
S2	14.424	0.013	Clean S2	14.626	0.034	1.40%	0.4399
S3	14.738	0.021	Clean S3	15.361	0.029	4.14%	0.1576
S4	15.497	0.054	Clean S4	15.073	0.035	2.78%	0.151
<i>Direct vs. Refrigeration</i>							
Sample	Ratio	Uncertainty	Sample	Ratio	Uncertainty	%Diff	p-value
S1	13.851	0.030	Refrig S1	13.117	0.016	5.45%	0.0617
S2	14.424	0.013	Refrig S2	14.565	0.013	0.97%	0.1673
S3	14.738	0.021	Refrig S3	14.988	0.013	1.68%	0.3986
S4	15.497	0.054	Refrig S4	15.422	0.035	0.49%	0.8966
<i>Direct vs. Incubation</i>							
Sample	Ratio	Uncertainty	Sample	Ratio	Uncertainty	%Diff	p-value
S1	13.851	0.030	Incub S1	13.580	0.015	1.98%	0.4944
S2	14.424	0.013	Incub S2	14.581	0.025	1.09%	0.5844
S3	14.738	0.021	Incub S3	14.831	0.060	0.63%	0.78
S4	15.497	0.054	Incub S4	15.147	0.035	2.29%	0.3935
<i>Direct vs. Sealed in an Alumina Bag</i>							
Sample	Ratio	Uncertainty	Sample	Ratio	Uncertainty	%Diff	p-value
S1	13.851	0.030	Alumi S1	13.920	0.033	0.49%	0.8819
S2	14.424	0.013	Alumi S2	14.475	0.040	0.35%	0.8259
S3	14.738	0.021	Alumi S3	14.554	0.014	1.26%	0.267
S4	15.497	0.054	Alumi S4	14.521	0.012	6.51%	0.0764

The success of this initial examination indicates any of the presented storage conditions are permissible for a short time up to 48 hours, however, longer time periods may demonstrate different results considering potential issues arise with different storage conditions. Open air cleanroom storage permitted exposure to air, light, temperature fluctuations, and other potential contaminants from work being done within the laboratory. Given GSH and GSSG's sensitivity to light and temperature, potential degradation may occur. Likewise, lack of protection from outside lab work being performed in the laboratory could introduce contaminants, potentially diminishing GSH or GSSG concentrations. For

example, other research conducted in the laboratory involved mercury analysis, of which exposure to GSH could result in binding of the two analytes upon solvation. Storage within a refrigerator exposed cards to higher levels of humidity and dampness, both can potentially cause damage to the card matrix structure, affect dryness of the sample, and theoretically result in the spreading of DBS outside of the sampling regions leading to sample inhomogeneity. Incubation involves prolonged exposure to heat, potentially drying out the card matrix inducing structural damage. Likewise, GSH and GSSG are both less stable at higher temperatures potentially resulting in analyte degradation. Storing spotted cards within a sealed alumina bag with a desiccant pouch is the only present mechanism for shielding the samples from light, air, outside contamination, and water content, and wherever the bag is stored would dictate its temperature conditions.

Time-dependent assessments were completed to provide guidance on best storage duration. Time variations spanned from immediate analysis 2 hours after preparation and intervals within 1 year after sample preparation. The first experimentation centered on short-term storage length with four card sets prepared using the same samples to be analyzed weekly over the course of a month: card set 1 – immediate analysis once dry, card set 2 – one week after preparation, card set 3 – two weeks after preparation, card set 4 – three weeks after preparation. All cards were stored in the simplest storage technique of open-air clean room setting. Again, the quantification of GS-NEM (GSH) and GSSG were accomplished employing previously described mathematical equations to calculate the GSH/GSSG biomarker ratio ($n=3$). Eight standards with decreasing concentrations of both analyte species were analyzed from the DBS. Resulting data after four weeks' time from

card preparation to card extraction demonstrate the analytical results of GSH/GSSG agree with the original direct analysis results. (Figure 1.8)

Uncertainty in the ratio calculation does increase as the concentrations of analytes decrease, but as clearly observed in Figure 1.8, overlap of the uncertainty error bars with original direct analysis assessment is achieved even after four weeks of limited consideration storage.

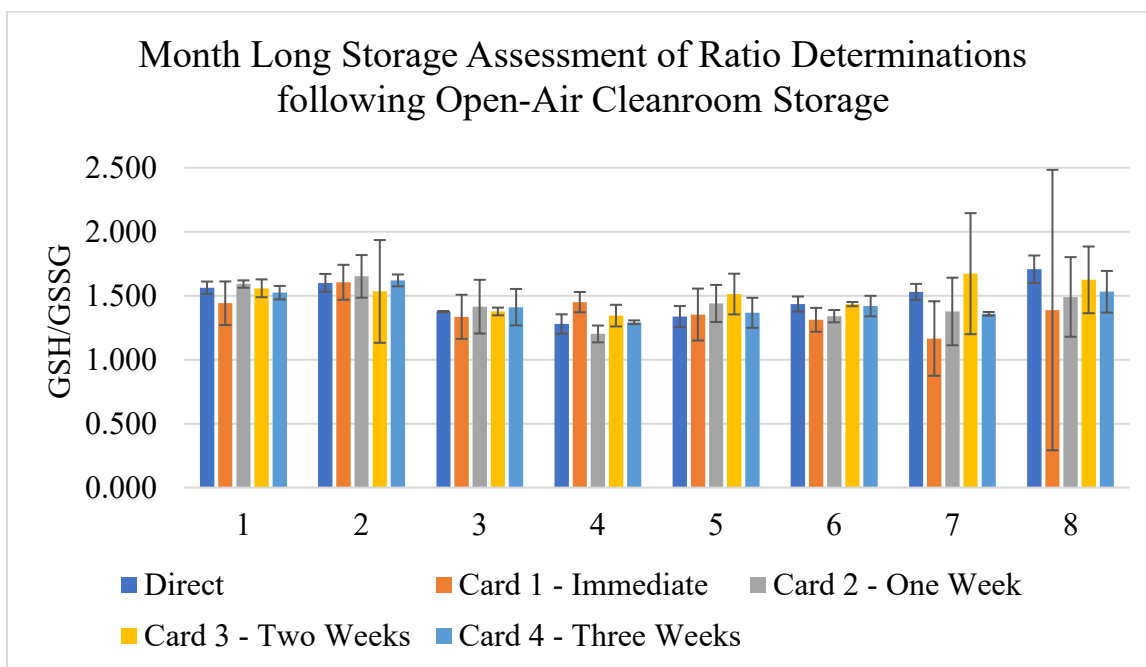


Figure 1. 8. Graphical representation comparing the analytical result of the GSH/GSSG ratio calculations derived from quantification of both species following manual DBS extraction after varying timed stored in a clean-room setting prior to analysis.

A long-term storage experiment involved two card sets: one manually extracted and analyzed immediately upon drying and one sealed in an alumina bag for 6 months. This data was also compared to analysis performed on the same set of samples through direct neat standard analysis as well as standard submitted to the whole blood extraction technique (n=3). (Figure 1.9)

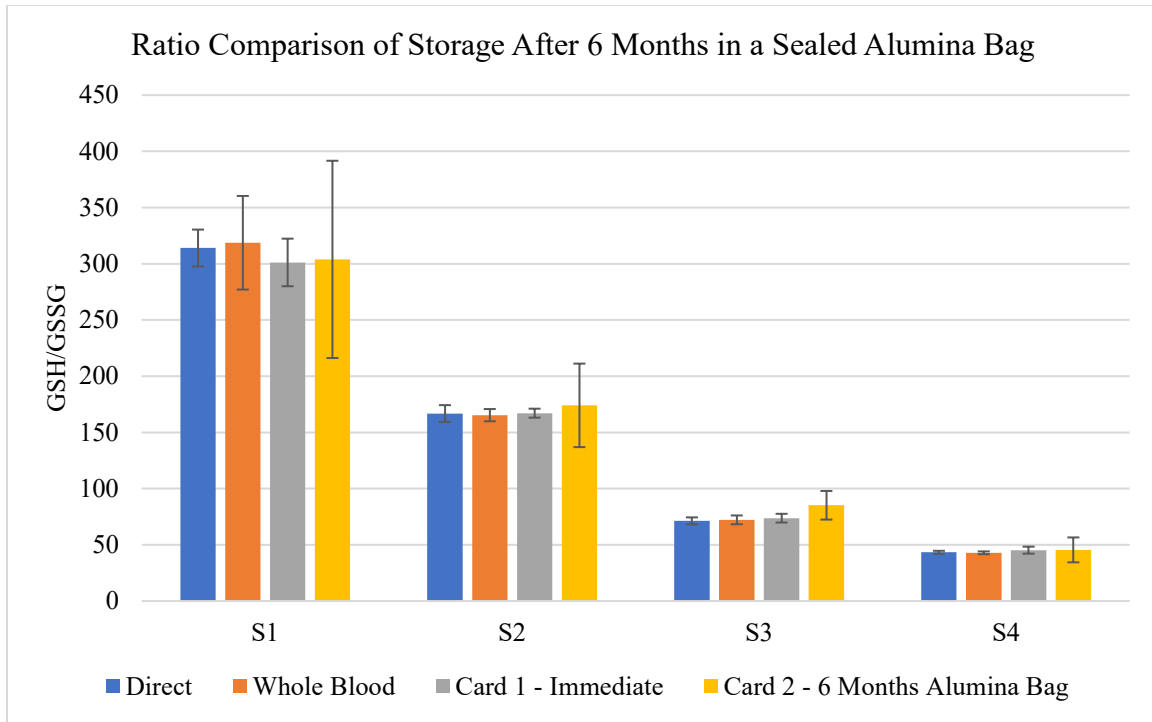


Figure 1. 9. Graphical representation comparing the analytical result of the GSH/GSSG ratio calculations derived from quantification of both glutathione species following manual DBS extraction after 6 months storage within a sealed alumina bag

Unlike the data presented in **Figure 1.8**, QC standards in this experiment were prepared to mimic physiological concentrations expected in a patient sample, where when GSH concentrations are high, GSSG concentrations are expected to be low and vice versa. Therefore, Standard 1 has the highest concentration of GSH and the lowest of GSSG. As observed in **Figure 1.9**, uncertainty in the calculation does increase with time, however, the analyst is still able to distinguish between each standard assessment from S1-S4. Through %difference calculations and student's t-test evaluation, we can observe the difference between analytical results of the GSH/GSSG ratio are minimal for most samples ($p\text{-value} > 0.05$) while some comparisons do indicate a significant difference ($p\text{-value} < 0.05$) indicated by red text within **Table 1.8**.

Table 1. 8. Statistical results for comparing GSH/GSSG ratio data achieved for DBS card manual extraction analysis following up to 6 months hours of storage in a sealed alumina bag.

<i>Direct vs. Card 1</i>							
Sample	Ratio	Uncertainty	Sample	Ratio	Uncertainty	%Diff	p-value
DS1	314.0255	16.38107	C1S1	301.174	21.168	4.18%	0.13761
DS2	166.7855	7.470384	C1S2	167.115	3.991	0.20%	0.87869
DS3	71.33444	3.083322	C1S3	73.721	3.879	3.29%	0.13301
DS4	43.37332	1.311997	C1S4	45.289	3.131	4.32%	0.09501
<i>Direct vs. Card 2</i>							
Sample	Ratio	Uncertainty	Sample	Ratio	Uncertainty	%Diff	p-value
DS1	314.0255	16.38107	C2S1	303.898	87.720	3.28%	0.64748
DS2	166.7855	7.470384	C2S2	174.060	37.137	4.27%	0.54517
DS3	71.33444	3.083322	C2S3	85.187	12.727	17.70%	0.02589
DS4	43.37332	1.311997	C2S4	45.515	11.075	4.82%	0.50818
<i>RBC vs. Card 1</i>							
Sample	Ratio	Uncertainty	Sample	Ratio	Uncertainty	%Diff	p-value
RS1	318.697	41.630	C1S1	301.174	21.168	5.65%	0.18882
RS2	165.342	5.444	C1S2	167.115	3.991	1.07%	0.47169
RS3	72.218	3.916	C1S3	73.721	3.879	2.06%	0.49008
RS4	42.922	1.246	C1S4	45.289	3.131	5.37%	0.03267
<i>RBC vs. Card 2</i>							
Sample	Ratio	Uncertainty	Sample	Ratio	Uncertainty	%Diff	p-value
RS1	318.697	41.630	C2S1	303.898	87.720	4.75%	0.52862
RS2	165.342	5.444	C2S2	174.060	37.137	5.14%	0.42829
RS3	72.218	3.916	C2S3	85.187	12.727	16.48%	0.07238
RS4	42.922	1.246	C2S4	45.515	11.075	5.86%	0.38879
<i>Card 1 vs. Card 2</i>							
Sample	Ratio	Uncertainty	Sample	Ratio	Uncertainty	%Diff	p-value
C1S1	301.174	21.168	C2S1	303.898	87.720	0.90%	0.92085
C1S2	167.115	3.991	C2S2	174.060	37.137	4.07%	0.53187
C1S3	73.721	3.879	C2S3	85.187	12.727	14.43%	0.04741
C1S4	45.289	3.131	C2S4	45.515	11.075	0.50%	0.9257

For samples whose statistical evaluation indicate significant difference, a closer plot of achieved ratio and associated uncertainty were generated, and despite the p-value indicating a significant difference between results, the uncertainties overlap at the 95% CI. (Figures 1.10-1.13)

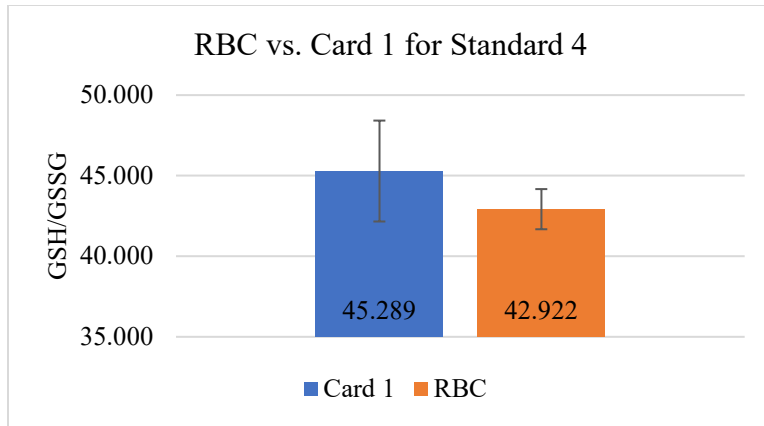


Figure 1. 10. Closer examination of the comparison between GSH/GSSG ratios derived from whole blood extraction and card 1 manual extraction of Standard 4 whose student's t-test evaluation indicated significant difference.

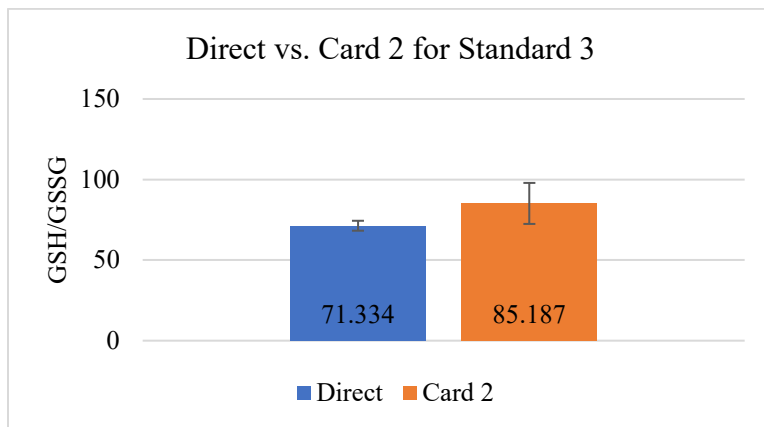


Figure 1. 11. Closer examination of the comparison between GSH/GSSG ratios derived from direct analysis and card 2 manual extraction of Standard 3 whose student's t-test evaluation indicated significant difference.

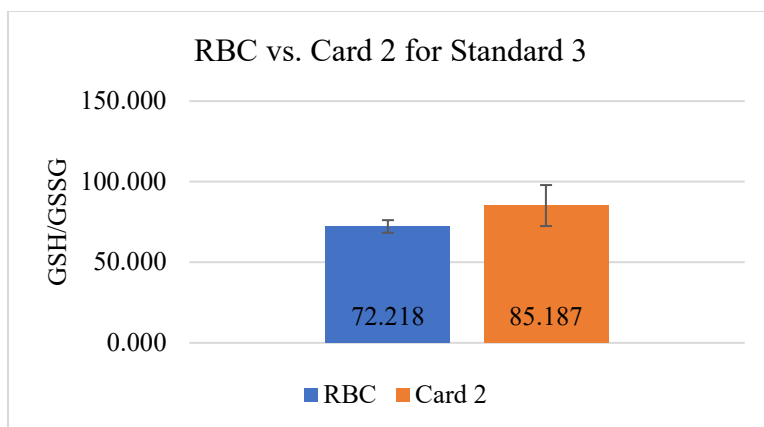


Figure 1. 12. Closer examination of the comparison between GSH/GSSG ratios derived from whole blood extraction and card 2 manual extraction of Standard 3 whose student's t-test evaluation indicated significant difference.

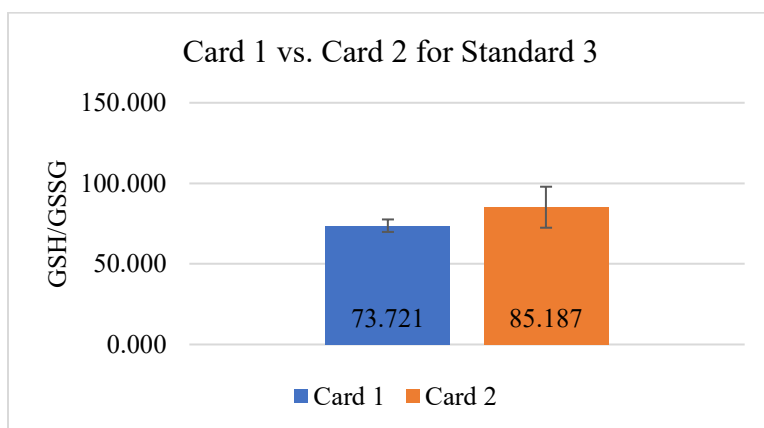


Figure 1. 13. Closer examination of the comparison between GSH/GSSG ratios derived from card 1 manual extraction and card 2 manual extraction of Standard 3 whose student's t-test evaluation indicated significant difference.

An unprotected long-term study was also conducted where four sets of cards were prepared and stored in open-air clean room storage: card set 1 - analyzed immediately upon drying, card set 2 - after three months, card set 3 - after six months, and card set 4 - after one full year from preparation. Manual extraction with analysis was utilized to quantify both analyte species (n=4). The DBS extracted results yielded a far narrower uncertainty than that presented in the ratio calculation following direct analysis, indicating an improved precision with DBS extraction techniques. (**Figure 1.14**) The uncertainty in ratio

calculations for direct analysis permits agreement to all card analyses up to 1 year from preparation at any level. A better comparison is to examine the agreement between card set 1 and subsequent card analyses. It is clear to see in **Figure 1.14**, ratio results from card analyses in samples 2-4 agree from immediate to a year of storage, whereas sample 1 seems to have some disagreement between card set 1 and card sets 2 and 3. Using a student's t-test examination comparing card set 1 to subsequent card analyses for sample 1 confirm that the data differ significantly with $p < 0.05$.

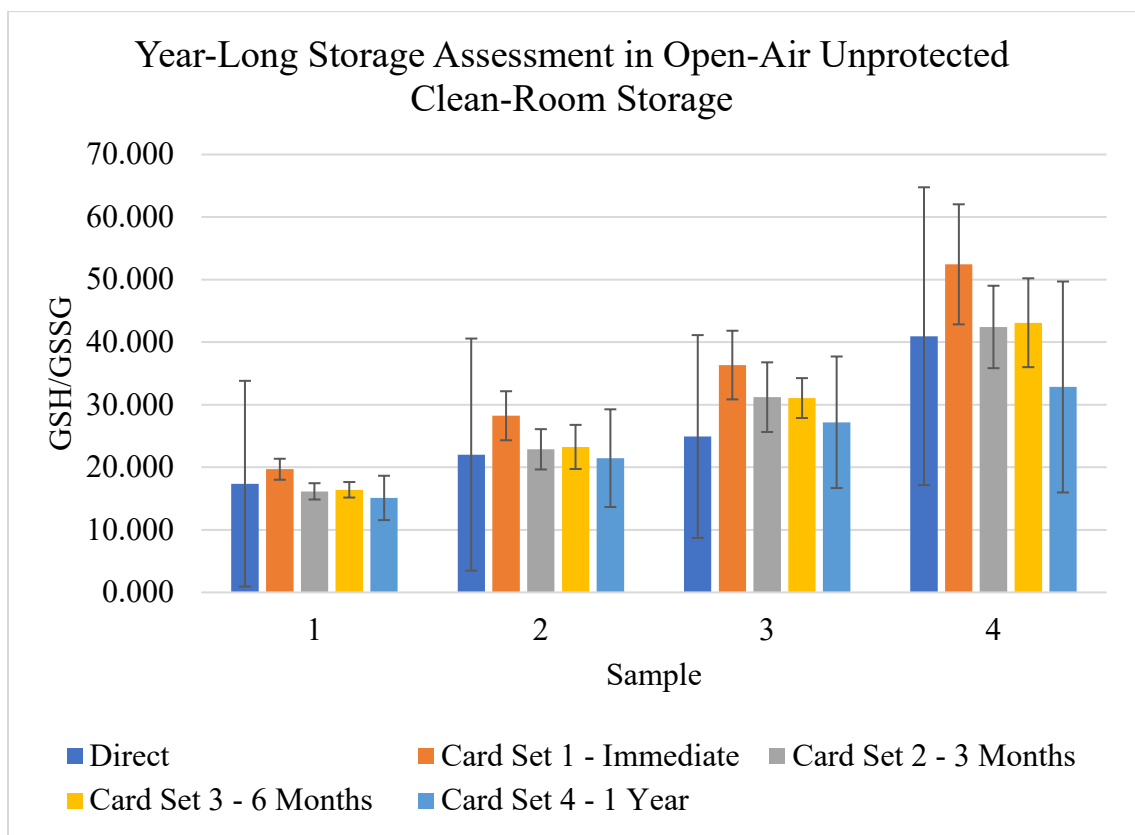


Figure 1. 14. Graphical representation comparing the analytical result of the GSH/GSSG ratio calculations derived from quantification of both glutathione species following manual DBS extraction over the course of 1 year following open-air cleanroom storage.

Conclusions

Previous work from our research laboratory has demonstrated the ability to quantify glutathione in whole blood samples accurately and precisely in its speciated form using

SIDMS.^{9, 12} Though more accurate than previous methods and highly beneficial, the protocol for obtaining a human sample via venous blood draw is invasive and stress-inducing for many people, especially those who struggle with ASD. Likewise, the venous blood draw must be done by a licensed phlebotomist at a clinic or hospital setting, which can be expensive, inconvenient, and, at times, not feasible because of restrictions on the blood volume and frequency of withdrawal permitted for children. The employment of DBS cards for sample collection has been an alluring technique to many researchers and medical professionals wishing to assess patients' conditions frequently and/or from a distance. However, DBS cards have traditionally been used in a purely qualitative format with little quantitative validation performed, until recent decades.

The present study demonstrates quantitative DBS (QDBS) sample collection can be utilized for speciated glutathione analysis, successfully meeting method validation parameters set forth by the FDA for a manual extraction technique. This optimized protocol vastly minimizes the previously used procedure, reducing cost of analysis as well as permitting at-home collection of small blood volumes via a minimally invasive finger stick. The stability work demonstrated in this research also promotes the robustness of the DBS collection technique, permitting storage of sensitive analyte samples in various conditions for lengths of time previously thought unattainable while preserving the analytical result. This study points to a future where DBS cards are a promising option for biobanking of a patient's sample for sample re-analysis, comparison studies, and retrospective assessments.¹³

With continued work to optimize the fully automated system of analysis, it will also be possible to streamline the extraction and analysis procedure. Future work should

aim to boost GSSG signal, better separate the GS-NEM and GSSG species following DBS-A extraction, and fully validate the partially validated method. Full validation of the automated system method will greatly reduce human error and create a high throughput workflow for use in the clinical realm with many patient samples.

References

1. Bukowski, M. R.; Picklo, M. J., Sr., Quantitation of Glutathione, Glutathione Disulphide, and Protein-Glutathione Mixed Disulphides by High-Performance Liquid Chromatography-Tandem Mass Spectrometry. *Methods Mol Biol* **2019**, *1967*, 197-210.
2. Camera, E.; Picardo, M., Analytical methods to investigate glutathione and related compounds in biological and pathological processes. *Journal of Chromatography B* **2002**, *781* (1-2), 181-206.
3. Cereser, C.; Guichard, J.; Draï, J.; Bannier, E.; Garcia, I.; Boget, S.; Parvaz, P.; Revol, A., Quantitation of reduced and total glutathione at the femtomole level by high-performance liquid chromatography with fluorescence detection: application to red blood cells and cultured fibroblasts. *Journal of Chromatography B: Biomedical Sciences and Applications* **2001**, *752* (1), 123-132.
4. Owen, J. B.; Butterfield, D. A., Measurement of oxidized/reduced glutathione ratio. *Methods Mol Biol* **2010**, *648*, 269-77.
5. Harwood, D. T.; Kettle, A. J.; Brennan, S.; Winterbourn, C. C., Simultaneous determination of reduced glutathione, glutathione disulphide and glutathione sulphonamide in cells and physiological fluids by isotope dilution liquid chromatography-tandem mass spectrometry. *J Chromatogr B Analyt Technol Biomed Life Sci* **2009**, *877* (28), 3393-9.
6. Michaelsen, J. T.; Dehnert, S.; Giustarini, D.; Beckmann, B.; Tsikas, D., HPLC analysis of human erythrocytic glutathione forms using OPA and N-acetyl-cysteine ethyl

ester: evidence for nitrite-induced GSH oxidation to GSSG. *J Chromatogr B Analyt Technol Biomed Life Sci* **2009**, 877 (28), 3405-17.

7. Pastore, A.; Federici, G.; Bertini, E.; Piemonte, F., Analysis of glutathione: implication in redox and detoxification. *Clinica Chimica Acta* **2003**, 333 (1), 19-39.

8. Zitka, O.; Skalickova, S.; Gumulec, J.; Masarik, M.; Adam, V.; Hubalek, J.; Trnkova, L.; Kruseova, J.; Eckschlager, T.; Kizek, R., Redox status expressed as GSH:GSSG ratio as a marker for oxidative stress in paediatric tumour patients. *Oncol Lett* **2012**, 4 (6), 1247-1253.

9. Fahrenholz, T.; Wolle, M. M.; Kingston, H. M.; Faber, S.; Kern, J. C., 2nd; Pamuku, M.; Miller, L.; Chatragadda, H.; Kogelnik, A., Molecular speciated isotope dilution mass spectrometric methods for accurate, reproducible and direct quantification of reduced, oxidized and total glutathione in biological samples. *Anal Chem* **2015**, 87 (2), 1232-40.

10. EPA Method 6800: Elemental and Molecular Speciated Isotope Dilution Mass Spectrometry. EPA, Ed. 2014; Vol. SW-846 Update V, pp 1-68.

11. Bioanalytical Method Validation: Guidance for Industry. U.S. Department of Health and Human Services, F. a. D. A., Center for Drug Evaluation and Research (CDER), Center for Veterinary Medicine (CVM), Ed. 2018; pp 1-41.

12. Faber, S.; Fahrenholz, T.; Wolle, M. M.; Kern, J. C., 2nd; Pamuku, M.; Miller, L.; Jamrom, J.; Skip Kingston, H. M., Chronic exposure to xenobiotic pollution leads to

significantly higher total glutathione and lower reduced to oxidized glutathione ratio in red blood cells of children with autism. *Free Radic Biol Med* **2019**, *134*, 666-677.

13. Bradburne, C.; Graham, D.; Kingston, H. M.; Brenner, R.; Pamuku, M.; Carruth, L., Overview of 'Omics Technologies for Military Occupational Health Surveillance and Medicine. *Mil Med* **2015**, *180* (10 Suppl), 34-48.

Chapter 2: Metrology: Application of Thor's Hammer and Improvement to Speciated Isotope Dilution Mass Spectrometry (SIDMS) Quantification of Glutathione

Biomarker measurements desired for biochemical assessment of a patient's condition are performed on various biological sample matrices, where certain target biomarkers can be found at varying concentrations in different matrices.¹ Therefore, it is important to understand the biochemical presence, relevance, and levels of your target biomarker within your designated matrix.^{2, 3} It is also essential to understand how the matrix assessed may affect your result.^{3, 4} Target analytes like glutathione have been quantified from samples such as whole blood, plasma, and saliva as part of the Kingston group's previous work.² However, saliva collection yielded far greater oxidation of the sensitive species, likely due to the abundance of oxygen in the mouth, and whole blood was determined to best represent the biochemical makeup of the patient's biomarker levels.²

Assessing analytes of interest requires extraction from the designated matrix, which is rarely 100% efficient.⁴ Lack of efficiency in pulling analytes from their matrix can lead to reduced signal from instrumental analysis, thereby hindering detection and ultimately quantification of the analyte.⁴ Many important biological compounds that permit an understanding of disease state or dysfunction exist at very low levels within the body, like that of GSSG, whose concentration is 10 times lower than that of GSH, its counterpart species.^{5, 6} Couple the low-level concentration present in the analytical sample with the lack of a fully efficient extraction procedures, and the greatest limitation to precise and accurate quantification of GSSG is displayed perfectly: researchers are attempting, and

struggling, to quantify important molecules in a reproducible manner at concentrations below that of the limit of quantification (LOQ) of their method/instrumentation.

Along with the low-level concentration of GSSG, the molecule (even in artificially generated higher concentrations) fails to produce comparable signal to that of its counterpart, GSH. Though at roughly the same concentration within an analytical sample, GSSG's instrumental signal is almost 200% lower than that of GSH bound to NEM. **(Figure 2.1)** This is likely due to the inefficiency of GSSG to ionize compared to the GS-NEM. This is further exacerbated by the extraction of the analyte from a DBS sample, which introduces an additional complication considering the very small sample sizes of only 10-30 μL when glutathione was previously analyzed in 200 μL of natural sample. The small sample size coupled with the poor extraction efficiency of the desorption methods currently employed (1-20% efficient) induces an even further reduced instrumental signal of GSSG from DBS extracted samples.

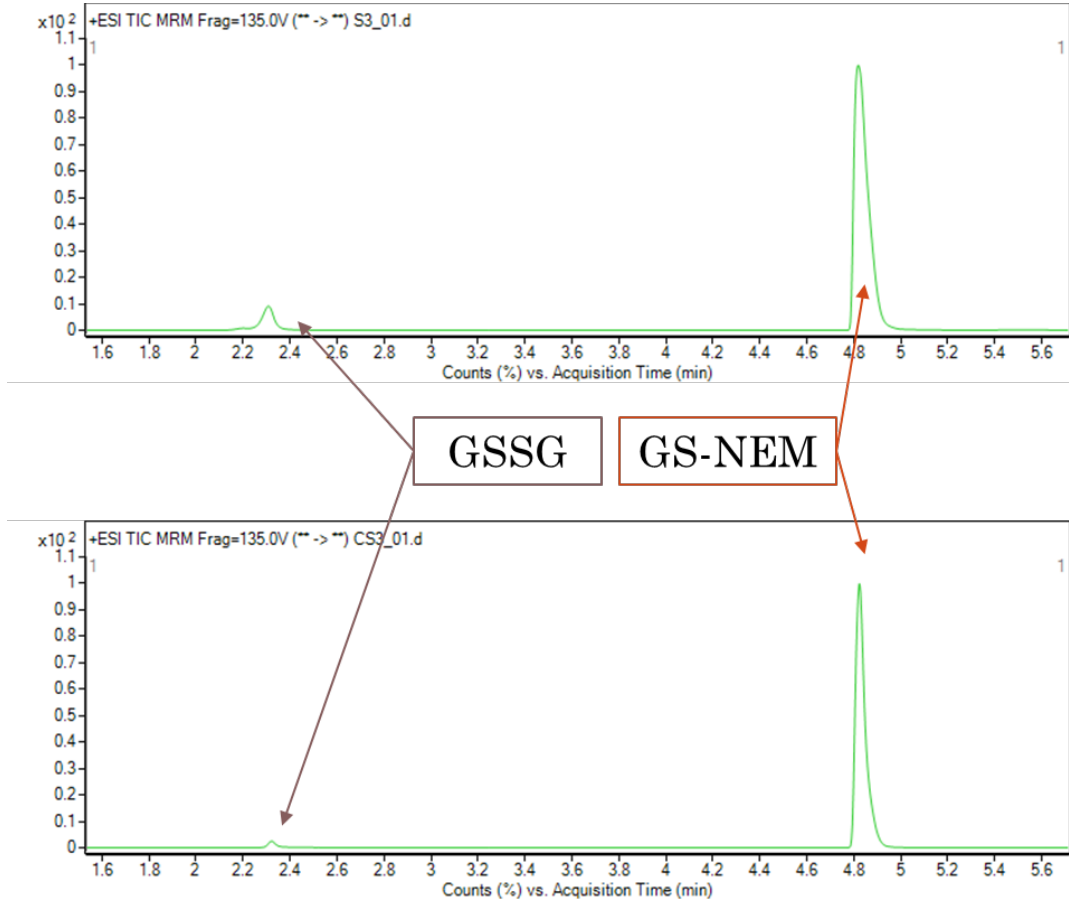


Figure 2. 1. Chromatographic results of analysis of a solution containing GSH and GSSG at the same concentration roughly 100 $\mu\text{g/g}$. The top chromatogram depicts the results following direct analysis of the sample and the bottom chromatogram depicts the results following direct analysis of the sample and the bottom chromatogram depicts the results following manual extraction of a DBS sample.

In **Figure 2.1**, S3 is indicative of neat sample direct analysis where the concentration of both GSSG and GSH are around 100 $\mu\text{g/g}$ and yet the signal differs greatly. The bottom chromatogram demonstrates the signal produced from CS3 which is the same sample spotted onto and extracted from DBS card matrix. Over 90% of the signal was lost. Low instrumental signal of a target analyte can result in complications with integration software failing to recognize the peak. This then requires the analyst to manually integrate peaks to

yield peak area estimations introducing error into the analysis because of human dependence.

Though current methodologies, including the previously published method by Farenholz et al, can quantify the analyte within the accepted +/-15 to 20% error dictated by the FDA for most samples, the uncertainty associated with GSSG quantification is typically much broader than that of GSH.² Likewise, the GSSG concentration and subsequent instrumental signal is sometimes too low to reliably detect which prevents quantification at all. Broad uncertainty with high degrees of imprecision in a specific measurement propagates the uncertainty in further calculations, like that of the GSH/GSSG ratio. The more uncertain this ratio calculation is, the less helpful it may be to a medical professional who is attempting to diagnose or base a patient's treatment progress on the biomarker measurement. To mitigate this issue, accurate and precise measurements of both GSH and GSSG concentrations need to be made to ensure a narrower uncertainty interval associated with the GSH/GSSG calculation.

Thor's Hammer is the answer to this problem. Thor's Hammer is a novel isotopic spiking technique utilized to improve upon the already rather robust analytical technique of SIDMS and IDMS.^{7, 8} Isotopically enriched spikes are mixed with a proportion of naturally occurring isotope to yield what is referred to as the "Metaspikes™." (Metaspikes is a trademark of Applied Isotope Technologies in Sunnyvale, California.) The present metaspikes are thoroughly analyzed to determine the new isotopic abundances of the solution. In a traditional solution of ⁶¹²GSSG, the carbon content is typically 99% C-12 abundant and ~1% C-13 abundant whereas in the solution of ⁶¹⁶GSSG, C-13 isotopic abundance is enriched yielding a 99% C-13 and ~1% C-12 isotopic breakdown. (**Figure 2.2**) The

Metaspikes displays altered abundances increasing the %abundance of C-12 while consequently reducing the %abundance of C-13. Abundances of the Metaspikes solution are experimentally determined and replaced within the traditional SIDMS and IDMS equations.

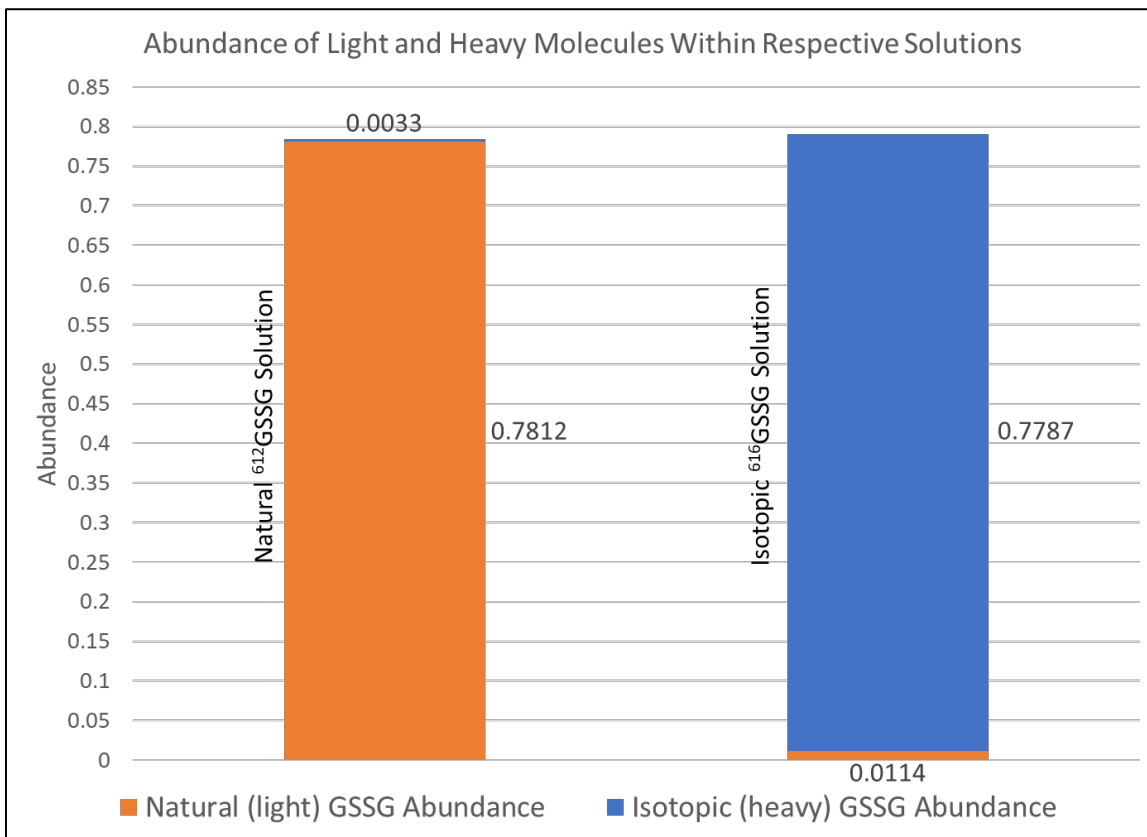


Figure 2. 2. Isotopic breakdown of natural and isotopically enriched solutions of ⁶¹²GSSG and ⁶¹⁶GSSG, respectively.

The increase in C-12 content within the Metaspikes, with a known concentration and experimentally determined abundance, helps to boost the analytical signal of the presently low-level ⁶¹²GSSG above that of the LOQ making it possible to quantify this species more accurately and precisely. (Figure 2.3) With increased precision in GSSG quantification through use of Thor's Hammer + SIDMS, the uncertainty in the calculation of GSH/GSSG

ratio is expected to decrease in comparison to the traditional spiking system utilized with SIDMS.

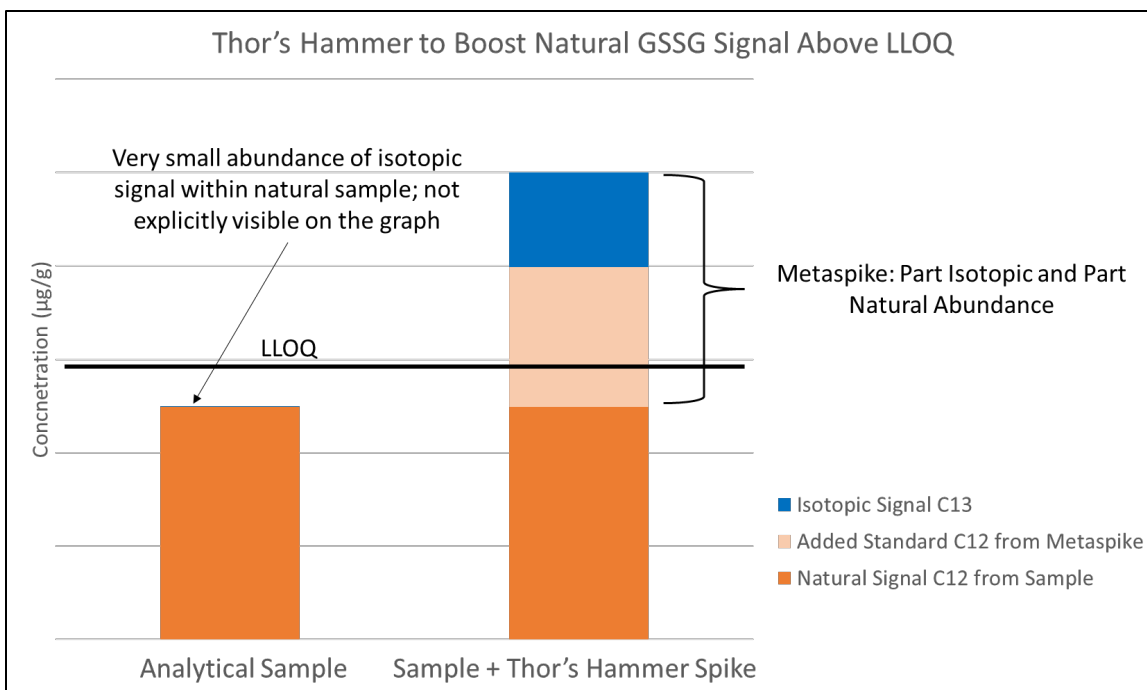


Figure 2. 3. Graphical demonstration of the artificial analytical signal boosting enabled by Metaspikes technology.

Thor's Hammer application in an IDMS setting shows steep decreases in the percent error of the quantification. Presently, this researcher has enabled quantification of GSSG concentrations from an IDMS standpoint almost 2 orders of magnitude lower than that of what was previously feasible while simultaneously decreasing the associated error.

Reagents and Standards:

Negative synthetic blood was purchased from Immalysis Corp (p/n: SB-0050). Naturally abundant reference standards for reduced glutathione (99%+ pure, p/n: 70-18-8) and oxidized glutathione (98%+ purity, p/n: 27025-41-8) standard reference materials were purchased from Sigma-Aldrich. A second naturally abundant reference standard for reduced glutathione (98%+ pure, p/n:70-18-8) was purchased from Alfa Aesar. Isotopically enriched reference standards of reduced glutathione (65-70% net peptide purity, glycine-

¹³C₂ and ¹⁵N, p/n: CNLM-6245-50) and oxidized glutathione (65-70% net peptide purity, glycines-¹³C₂, p/n: CLM-8645-PK) were purchased from Cambridge Isotope Laboratories, Inc. (Cambridge, MA). Whatman DMPK-C dried blood spot cards of plain, non-treated cellulose matrix were purchased from Fisher Scientific (pure cellulose, p/n: 09-801-000). The mixed-mode strong anion exchange (MMAE) SPE cartridges were purchased from SparkHolland. (Polymer Sax cartridges. 25 - 35µm, p/n: 018804-022-00) N-ethylmaleimide (NEM) (98%+ purity, p/n: 128-53-0) reagent was purchased from Sigma-Aldrich. HPLC grade acetonitrile and methanol was purchased from Fisher Scientific. Formic acid (99%+ purity, p/n: 64-18-6) was purchased from Sigma-Aldrich. Doubly deionized water was generated by the Barnstead Nanopure in-lab water filtration and purification system from ThermoScientific. Trifluoroacetic acid was purchased from Fisher Scientific (99.7% purity, p/n: 76-05-1). Isopropanol was purchased from Acros (p/n: 67630). Methanol was purchased from Fisher Scientific. (HPLC Grade, p/n: 67561) Ammonium hydroxide was purchased from VWR. (28-30% w/w, p/n: 1336216) Ammonium bicarbonate was purchased from Fisher Scientific (21.43% w/w; p/n: 1066-33-7)

Equipment:

The column used for glutathione analysis was a Phenomenex SynergiTM 4 µm Hydro-RP 80 Å LC column C18, 150 x 4.6 mm (p/n: 5375-0097). The system used for LC-MS/MS analysis was the Agilent 1200 Series High Performance Liquid Chromatography (HPLC) system in tandem with the Agilent 6460 Triple Quadrupole Mass Spectrometer (s/n: US92170174, NSF MRI: 0821401) with an Agilent Jetstream electrospray ionization source (Model: G1958-65138; s/n: US91500324). All data was collected and processed

using Agilent's MassHunter Acquisition and Qualitative Analysis programs (Version 10.0 SR1; Build: 10.0.142). Clear airtight snap-cap 1.5 mL polypropylene microcentrifuge tubes were purchased from VWR (p/n: 20170-038). A VortexGenie2 from Scientific Industries, Savant SPD1010 SpeedVac Concentrator from Thermo Scientific, sonication bath from Branson, the XS105 DualRange analytical balance from Mettler Toledo, and a MiniSpin microcentrifuge from Eppendorf were used for various aspects of sample preparation.

Thor's Hammer Spike Development

Traditional $^{616}\text{GSSG}$ isotope is purchased with C-13 enrichment on 2 carbon atoms of either glycine portion in the dimer structure. This ultimately leads to a molecular weight of 616 g/mol, approximately 4 mass units higher than our natural GSSG compound at 612 g/mol. Isotopic standard is purchased in its solid state and dissolved in water to form the isotopic solution used to spike an analytical sample. A mathematical equivalent to IDMS referred to as reverse-IDMS (RIDMS) is used to verify the concentration of this isotopically enriched standard. Several solutions of natural standard, $^{612}\text{GSSG}$, are generated in water at various concentrations consistent with that expected in the isotopic solution. RIDMS involves swapping the role of isotope and natural where the isotopic solution now becomes your analytical "sample" and your various natural solution become your "spike." Standard reference materials of natural analyte must be of high purity and preferably derived from multiple companies to ensure any bias in the material is accounted for. The isotopic solution is utilized for the preparation of the Thor's Hammer Metaspikes once its concentration of $^{616}\text{GSSG}$ has been certified.

The initial phase of Thor's Hammer spike development took a trial-and-error approach, with little certainty of what exact amount of added natural signal would best

improve the quantitative data. Solutions of ⁶¹⁶GSSG and ⁶¹²GSSG at known concentrations of 268.30 µg/g and 274.34 µg/g, respectively, were mixed in volume/volume ratios of isotope/natural. Six Thor's Hammer spikes were prepared at 90/10, 80/20, 70/30, 60/40, 50/50, and 30/70 v/v isotopic/natural, labeled D, E, A, F, B, and C respectively. An aliquot of these neat solutions is then transferred to an LC-MS vial and analyzed directly using the method described in **Table 2.1**.

Table 2. 1. Instrumental MRM method for abundance determination of natural and isotopic GSSG content.

Parameter	Setting
Gas Temp	300 °C
Gas Flow	8 L/min
Nebulizer Pressure	45 psi
Sheath Gas Temp	250 °C
Sheath Gas Flow	11 L/min
Capillary Voltage	4000 V (+ and -)
Nozzle Voltage	500 V (+ and -)
MRM Transitions	
Precursor Ion (m/z) – 613.1	Product Ions (m/z) – 355.1, 356.1, 357.1, 358.1, 359.1, 360.1, 361.1, 362.1, 363.1, 364.1
Precursor Ion (m/z) – 617.1	Product Ions (m/z) – 355.1, 356.1, 357.1, 358.1, 359.1, 360.1, 361.1, 362.1, 363.1, 364.1

The method described in **Table 2.1** is designed to track a range of fragmentation patterns of the isotopic and natural species of oxidized glutathione. The data obtained from the analysis is used to determine the abundance of the two important product ions, 355 and 359, within the Thor's Hammer Spike which are necessary to know for both IDMS and SIDMS applications. Because the isotopically enriched and natural species of GSSG are not 100% pure, there can be signal from different isotopic compositions of the GSSG compound, which result in slightly different $[M+H]^+$ ions for the precursor and product

ions. Counts for each respective MRM transition tracked are obtained and summed together for a total counts assessment of each replicate of the standard. The counts of individual MRM transitions are then divided by the total counts value to yield a relative abundance to that of all likely fragmentation patterns a particular molecule may undergo during instrumental analysis. (**Equation 2.1**)

$$\text{Abundance of Product Ion } X = \frac{\text{Peak Area of Product Ion } X}{\sum \text{Peak Area of All Product Ions}}$$

Equation 2. 1. Calculation for the determination of abundance for a generic product ion 'X'.

When done properly, all calculated abundance values for each product ion should add up to 1. In accordance with the goal volumetric ratios of isotope to natural, the abundances of the 355 and 359 (natural and isotope, respectively) determined for each TH spike A-F align well. (**Table 2.2**)

Table 2. 2. Isotopic abundances of potential product ions for standard and Thor's Hammer Metaspikes.

m/z Product Ion	Abundance of Product Ion in Spike (As)						
	Standard	TH-A	TH-B	TH-C	TH-D	TH-E	TH-F
355.1	0.000114	0.287851	0.488406	0.687265	0.102008	0.196031	0.396859
356.1	0.000219	0.000064	0.000112	0.000152	0.000020	0.000043	0.000093
357.1	0.001813	0.000585	0.000924	0.001263	0.000212	0.000397	0.000736
358.1	0.008811	0.005864	0.004492	0.003338	0.006364	0.005760	0.004604
359.1	0.988993	0.704502	0.504214	0.305445	0.891000	0.797027	0.596302
360.1	0.000027	0.000028	0.000014	0.000014	0.000034	0.000031	0.000024
361.1	0.000003	0.000002	0.000001	0.000003	0.000004	0.000003	0.000002
362.1	0.000003	0.000003	0.000002	0.000000	0.000004	0.000003	0.000002
363.1	0.000001	0.000000	0.000001	0.000002	0.000000	0.000001	0.000001
364.1	0.0000132	0.0000070	0.000007	0.000005	0.000011	0.000007	0.000006

Results

IDMS Application of Thor's Hammer Metaspiking Technology

IDMS analysis is the simpler quantitative method given its focus on a single analyte which does not convert between species. Given its greater stability, GSSG is unlikely to revert to GSH. For this reason, IDMS application of TH spiking technology was assessed first. Four neat standard solutions, S1, S2, S3, and S4, of $^{612}\text{GSSG}$ were generated at 48.819, 24.362, 6.151, and 3.091 $\mu\text{g/g}$, respectively. An aliquot of each natural standard was spiked with each system at equal volumetric amounts being sure to record the weight of each addition. Samples were equilibrated and analyzed on the LC-MS/MS system (n=6) to identify which spiking system yielded the most accurate and precise results for IDMS quantification of $^{612}\text{GSSG}$.

The precision meets acceptance for all spiking systems when assessing S1-S3, however, S4 does not perform to standard for all spiking systems. (**Table 2.3**) Standard isotope, TH-A, TH-D, and TH-E spikes performed best in terms of precision at the S4 level. In comparing overall improvement in precision over the standard spiking technique, an obvious winner is not observed for the IDMS application.

Table 2. 3. Resulting precision assessment for quantification of $^{612}\text{GSSG}$ using IDMS + TH spiking technique.

Thor's Hammer Spiking Precision - IDMS			
Sample	Average Concentration $^{612}\text{GSSG}$ (ug/g)	Uncertainty	%CV
NS1	47.18	0.17	0.4%
NS2	22.85	0.16	0.7%
NS4	5.51	0.071	1.3%
NS5	2.56	0.044	1.7%
AS1	48.58	0.28	0.6%
AS2	23.82	0.62	2.6%
AS4	5.54	0.56	10%
AS5	2.98	0.35	12%
BS1	48.83	0.77	1.6%
BS2	24.06	0.63	2.6%
BS4	5.64	1.06	19%
BS5	2.74	0.55	20%
CS1	49.28	0.50	1.0%
CS2	24.76	1.51	6.1%
CS4	5.69	0.65	12%
CS5	2.30	0.62	27%
DS1	49.99	0.30	0.6%
DS2	24.77	0.12	0.5%
DS4	6.28	0.40	6.3%
DS5	3.08	0.070	2.3%
ES1	49.014	0.35	0.7%
ES2	24.034	0.36	1.5%
ES4	6.046	0.27	4.4%
ES5	3.189	0.41	13%
FS1	47.958	0.51	1.1%
FS2	23.425	0.45	1.9%
FS4	5.588	0.44	7.9%
FS5	2.301	0.57	24%

Accuracy is also an important factor in quantification, where all spiking systems meet acceptable error levels across all four standard analyses except TH-C and TH-F for S4. (Table 2.4) Several TH spiking systems reduced the error as compared to the standard isotopic spike, with reduction in error ranging from as little as 4% to as much as 98% reduction in error. (Figure 2.4)

Table 2. 4. Resulting accuracy assessment for quantification of ⁶¹²GSSG using IDMS + TH spiking technique.

Thor's Hammer Spiking Accuracy - IDMS			
Sample	Theoretical Concentration ⁶¹² GSSG (ug/g)	IDMS Calculated Concentration ⁶¹² GSSG (ug/g)	%Error
NS1	48.82	47.18	3.4%
NS2	24.36	22.85	6.2%
NS3	6.15	5.51	10%
NS4	3.09	2.56	17%
AS1	48.82	48.58	0.5%
AS2	24.36	23.82	2.2%
AS3	6.15	5.54	10%
AS4	3.09	2.98	3.6%
BS1	48.82	48.83	0.0%
BS2	24.36	24.06	1.3%
BS3	6.15	5.64	8.2%
BS4	3.09	2.74	11%
CS1	48.82	49.28	1.0%
CS2	24.36	24.76	1.6%
CS3	6.15	5.69	7.6%
CS4	3.09	2.30	26%
DS1	48.82	49.99	2.4%
DS2	24.36	24.77	1.7%
DS3	6.15	6.28	2.2%
DS4	3.09	3.08	0.3%
ES1	48.82	49.01	0.4%
ES2	24.36	24.03	1.3%
ES3	6.15	6.05	1.7%
ES4	3.09	3.19	3.2%
FS1	48.82	47.96	1.8%
FS2	24.36	23.42	3.8%
FS3	6.15	5.59	9.2%
FS4	3.09	2.30	26%

Results of the IDMS application provided the first indication certain TH spikes may suit better at different concentration levels. As an example, at higher concentrations of GSSG (S1), TH-B and TH-E performed the best in terms of reducing the associated error from nominal concentration. Whereas at very low concentrations of GSSG (S4), TH-D performed the best. (Figure 2.4) Overall, the average associated error was lowest using

TH-D (1.6%) and TH-E (1.7%). The highest average associated error was observed with TH-F (10.1%) with TH-C a close second (8.9%).

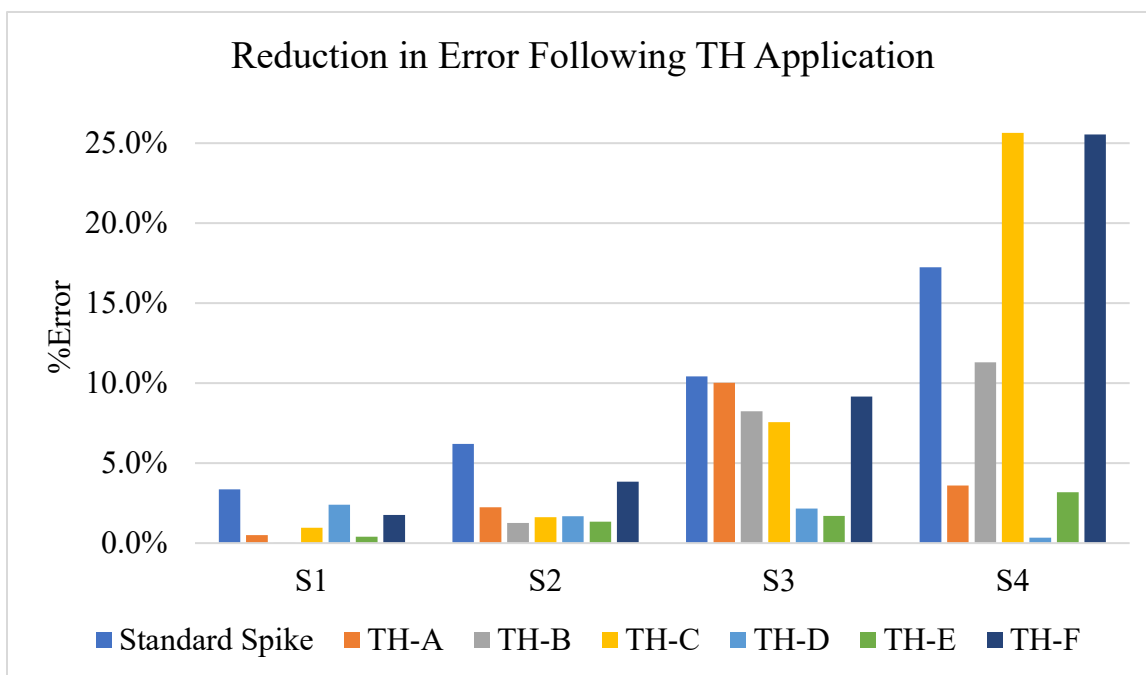


Figure 2. 4.Reduction or change in error achieved by employing IDMS+TH.

SIDMS Application of Thor’s Hammer Metaspiking Technology

The more complex of the quantitative systems, SIDMS involves the interchange between species where GSH can autoxidize to GSSG during sample collection, preparation, and analysis which complicates the mathematical assessment. After IDMS testing, select TH spikes were applied to an SIDMS system.

With SIDMS quantification, it was important to change the abundance values of the 355 and 359 product ions (As^{355} and As^{359}) reflecting the spike system utilized. But inputting an adjusted isotopic concentration for Cs^{616} reflective of the diluted concentration upon addition of the natural solution to the isotopic solution was crucial for accurate quantification as well. In the IDMS system, the spiked sample involves only the weight of natural sample being analyzed and the weight of TH spike. The resulting abundances after

instrumental analysis will therefore account for the difference in isotopic concentration. However, SIDMS situations include a second spike for the $^{309}\text{GS-NEM}$ species, which further dilutes the GSSG isotope concentration and can skew the resulting quantitation if not accounted for.

When applied in the SIDMS system, TH-A performed beautifully to decrease the error from nominal. Little to no change is observed with GS-NEM quantification which is likely due to the fact the spiking system has not been altered for that species. (**Table 2.5**) Extraordinary reduction in associated error for $^{612}\text{GSSG}$ quantification is observed when applying SIDMS+TH. Error ranges from 23-42% with the standard isotopic spiking technique while introduction of TH spiking diminishes this error to less than 5% across all concentration levels. (**Table 2.6**) The results of this study indicate TH greatly improves the accuracy of analysis regarding determination of the GSSG concentrations beyond what the SIDMS technology can do alone.

Table 2. 5. Quantitative results for $^{306}\text{GS-NEM}$ in an SIDMS+TH-A system.

$^{306}\text{GS-NEM Conc (}\mu\text{g/g)}$					
Standard	Theoretical	Standard Analysis	%Error	TH Analysis	%Error
S1	517.70	584.36	13%	591.57	14%
S2	308.96	349.70	13%	351.69	14%
S3	184.40	207.48	13%	201.46	9.3%
S4	110.12	121.13	10%	120.27	9.2%

Table 2. 6. Quantitative results for $^{612}\text{GSSG}$ in an SIDMS+TH-A system.

$^{612}\text{GSSG Conc (}\mu\text{g/g)}$					
Standard	Theoretical	Standard Analysis	%Error	TH Analysis	%Error
S1	29.78	42.19	42%	30.29	1.7%
S2	17.77	24.25	36%	17.93	0.9%
S3	10.61	14.08	33%	10.58	0.2%
S4	6.33	7.82	23%	6.10	3.6%

In a separate experiment, the standard spike, TH-A, and TH-B were all applied to an SIDMS system on a range of standards (S1-S4) with decreasing concentrations of both analytes. (**Table 2.7**)

Table 2. 7. Resulting quantification data for both target analyte species upon SIDMS and SIDMS+TH.

Sample	GS-NEM Concentration (ug/g)			GSSG Concentration (ug/g)		
	Theoretical	Calculated	%Error	Theoretical	Calculated	%Error
N1	799.34	865.18	8.2%	30.44	49.79	64%
N2	583.76	626.49	7.3%	14.65	28.44	94%
N3	446.25	492.46	10%	7.98	19.76	148%
N4	333.73	336.20	0.7%	3.24	8.21	153%
A1	799.34	875.81	9.6%	30.44	29.60	2.8%
A2	583.76	613.66	5.1%	14.65	14.62	0.2%
A3	446.25	460.95	3.3%	7.98	5.36	33%
A4	333.73	339.49	1.7%	3.24	1.07	67%
B1	799.34	850.85	6.4%	30.44	24.29	20%
B2	583.76	622.17	6.6%	14.65	13.38	8.7%
B3	446.25	470.68	5.5%	7.98	8.65	8.4%
B4	333.73	341.93	2.5%	3.24	3.18	1.8%

As shown in **Table 2.7**, the standard spiking method fails to meet acceptable accuracy for the quantification of GSSG, with errors ranging from 64-153%. However, with the application of TH-A, we boost the signal of the higher analyte levels (S1 and S2) enough to achieve exceptionally acceptable quantification with error decreased to less than 3%. The error for S3 and S4 when applying TH-A does decrease significantly but not within the acceptance criteria. These two standards are quantified accurately through the application of TH-B which decreases the error within acceptance below 10%. The data results of this experiment demonstrate that different Thor’s Hammer spiking systems could be more beneficial at different levels of analyte concentration within the sample.

It should be noted as well that previous analysis using TH-A spiking in an SIDMS system (**Table 2.5 and 2.6**) was able to maintain accuracy in the lower-level standards.

Part of the reason for the success in its first assessment while performing poorly in the second assessment (**Table 2.7**) could be related to the levels of GSH present. In the first assessment, GS-NEM concentrations of the lower standard samples were around 100-200 $\mu\text{g/g}$ while the lower-level standards in the second assessment were prepared at concentrations 300-450 $\mu\text{g/g}$. If not all GSH was bound to NEM to stabilize the compound, oxidation can occur between two GSH molecules generating additional GSSG levels. The SIDMS mathematics can help to correct for this oxidation, but if the oxidation to GSSG of unknown concentration overwhelms the very low concentration from the original sample we are attempting to quantify, increased error can be observed. With higher concentrations of GS-NEM in the second SIDMS application of TH-A, more consistent with physiological levels expected in a patient sample, the potential for oxidation is greater. This lends the necessity for boosted “known” natural signal spiked into the sample to better differentiate oxidation product from target GSSG, hence why TH-B performs better at our lower-level concentrations.

The highest priority in improving the quantification of GSSG at low level concentrations is to enable a more precise calculation of the important GSH/GSSG ratio. When calculating the ratio, you must divide the calculated GSH concentration by the GSSG concentration and then handle the associated uncertainties appropriately. The propagation of error equation for division is shown in **Equation 2.2** where the generic “Uncertainty ^A” corresponds to the standard deviation determined for GSH quantitation and “Uncertainty ^B” corresponds to the standard deviation determined for GSSG quantitation. Value ^A is then representative of the average GSH concentration while Value ^B is the average GSSG concentration.

$$\text{Propagation of Error} = \sqrt{\left(\frac{\text{Uncertainty}^A}{\text{Value}^A}\right)^2 + \left(\frac{\text{Uncertainty}^B}{\text{Value}^B}\right)^2}$$

Equation 2. 2. Propagation of error calculation for multiplication or division mathematical functions.

When the uncertainty in either of the concentrations is very high, this will propagate into the GSH/GSSG ratio calculation therefore increasing the uncertainty in the ratio determination. Utilizing a separate spiking system, TH-D, for SIDMS application, we can observe the improvement of quantification and subsequent calculations.

Table 2. 8. Quantitative results of GS-NEM, GSSG, and ratio calculations with and without the application of Thor's Hammer for neat sample analysis.

Error Analysis for Direct Samples															
Sample	GS-NEM Concentration (µg/g)					GSSG Concentration (µg/g)					GSH/GSSG Ratio				
	Theo	Calc	SD	%Error	%CV	Theo	Calc	SD	%Error	%CV	Theo	GSH/GSSG	Uncertainty	%Error	%CV
NS1	651.36	738.92	13.07	13%	1.8%	2.79	0.99	0.048	65%	4.8%	233.17	749.42	0.052	221%	0.007%
NS2	575.64	643.89	1.10	12%	0.2%	5.39	3.14	0.063	42%	2.0%	106.84	205.22	0.020	92%	0.01%
NS3	418.82	461.95	3.60	10%	0.8%	9.90	7.26	0.11	27%	1.5%	42.29	63.63	0.017	51%	0.03%
NS4	388.43	430.75	0.89	11%	0.2%	15.03	12.24	0.15	19%	1.2%	25.85	35.18	0.013	36%	0.04%
DS1	651.36	723.99	1.66	11%	0.2%	2.79	2.18	0.11	22%	5.1%	233.17	332.45	0.051	43%	0.02%
DS2	575.64	641.06	2.42	11%	0.4%	5.39	4.70	0.14	13%	3.0%	106.84	136.40	0.031	28%	0.02%
DS3	418.82	461.59	1.23	10%	0.3%	9.90	8.97	0.31	9.4%	3.4%	42.29	51.46	0.034	22%	0.07%
DS4	388.43	427.41	1.99	10%	0.5%	15.03	14.09	0.16	6.2%	1.1%	25.85	30.33	0.012	17%	0.04%

Table 2. 9. Quantitative results of GS-NEM, GSSG, and ratio calculations with and without the application of Thor's Hammer for whole blood sample analysis.

Error Analysis for Whole Blood Samples															
Sample	GS-NEM Concentration (µg/g)					GSSG Concentration (µg/g)					GSH/GSSG Ratio				
	Theo	Calc	SD	%Error	%CV	Theo	Calc	SD	%Error	%CV	Theo	GSH/GSSG	Uncertainty	%Error	%CV
NS1	651.36	741.23	16.51	14%	2.2%	2.79	0.91	0.13	68%	14%	233.17	817.44	0.14	251%	0.02%
NS2	575.64	643.90	2.56	12%	0.4%	5.39	3.22	0.089	40%	2.8%	106.84	199.71	0.028	87%	0.01%
NS3	418.82	466.17	7.99	11%	1.7%	9.90	7.18	0.078	28%	1.1%	42.29	64.95	0.020	54%	0.03%
NS4	388.43	429.11	3.55	11%	0.8%	15.03	12.37	0.11	18%	0.9%	25.85	34.69	0.012	34%	0.03%
DS1	651.36	727.87	2.87	12%	0.4%	2.79	2.04	0.038	27%	1.9%	233.17	357.07	0.019	53%	0.005%
DS2	575.64	640.34	2.01	11%	0.3%	5.39	4.53	0.091	16%	2.0%	106.84	141.42	0.020	32%	0.01%
DS3	418.82	460.38	0.93	9.9%	0.2%	9.90	9.02	0.10	9.0%	1.1%	42.29	51.07	0.012	21%	0.02%
DS4	388.43	427.35	0.97	10%	0.2%	15.03	14.39	0.19	4.2%	1.3%	25.85	29.70	0.013	15%	0.05%

Table 2. 10. Quantitative results of GS-NEM, GSSG, and ratio calculations with and without the application of Thor's Hammer for DBS sample analysis.

Error Analysis for DBS Samples															
Sample	GS-NEM Concentration (µg/g)					GSSG Concentration (µg/g)					GSH/GSSG Ratio				
	Theo	Calc	SD	%Error	%CV	Theo	Calc	SD	%Error	%CV	Theo	GSH/GSSG	Uncertainty	%Error	%CV
NS1	651.36	729.05	2.18	12%	0.3%	2.79	1.05	0.25	63%	24%	233.17	697.60	0.2353	199%	0.03%
NS2	575.64	642.20	1.51	12%	0.2%	5.39	3.07	0.13	43%	3.9%	106.84	209.41	0.0389	96%	0.02%
NS3	418.82	461.68	0.26	10%	0.1%	9.90	6.93	0.17	30%	2.5%	42.29	66.59	0.0246	56%	0.04%
NS4	388.43	431.03	0.52	11%	0.1%	15.03	11.70	0.16	22%	1.4%	25.85	36.85	0.0140	43%	0.04%
DS1	651.36	725.63	0.68	11%	0.1%	2.79	1.13	0.53	60%	47%	233.17	644.89	0.4678	177%	0.07%
DS2	575.64	639.69	0.56	11%	0.1%	5.39	3.94	0.17	27%	4.4%	106.84	162.22	0.0440	53%	0.03%
DS3	418.82	461.31	0.43	10%	0.1%	9.90	7.89	0.18	20%	2.3%	42.29	58.45	0.0225	38%	0.04%
DS4	388.43	429.27	0.64	11%	0.1%	15.03	14.05	0.51	6.5%	3.6%	25.85	30.55	0.0360	18%	0.1%

The data presented in **Tables 2.8-2.10** demonstrate the analysis of a set of standards submitted to different methodologies of extraction through the employment of standard spiking+SIDMS as well as TH-D+SIDMS. Standards were not prepared in a blood matrix, but rather prepared in water. This negates the need for extraction in order to perform instrumental analysis. However, to mimic extraction conditions, the water standard can be sent through the respective processes to observe changes with the quantification based upon extraction conditions.

First looking to the direct analysis, not only are both analyte species quantified with improved accuracy following application of TH-D, but the standard deviation (SD) associated with the quantification is narrower. Given the increased accuracy, the subsequent GSH/GSSG ratio calculation following TH-D application is more accurate than the standard spiking technique. For either spiking system the uncertainty is very narrow with %CV well below 1%. (**Table 2.8**; where N indicates the standard spiking technique, D indicates the TH spiking technique, and the concentration of GSSG increases from S1 to S4)

TH becomes most important when referring to methodology of sample collection, extraction, and analysis with small sample size and low efficiency of extraction. The whole blood extraction method is an example and with the standard spiking technique, the error from nominal of the GSSG analyte, ranging from 17-68%, does not meet acceptance at any of the levels above or below LOQ. (**Table 2.9**) However, when TH-D is used, the error is significantly decreased across all concentration levels, ranging between 4-27%. S1 and S2 following whole blood extraction methodology fall outside of our acceptance criteria, S3 and S4 at the higher concentration levels are now meeting acceptance. This situation is

likely impacted by the same trend we observed with TH-A and TH-B, where some Metaspikes may perform better at different levels, and given TH-D is only composed of 10% natural GSSG and 90% isotopic GSSG presence, it is possible the natural signal boost implemented in the Metaspike is not great enough for these low-level concentrations. Accuracy is not the only matter improved following the extraction, with exceptional decrease in the %CV for individual analyte quantification as well as the ratio calculation.

As reported in Chapter 1, the manual card extraction technique has an even lower extraction efficiency compared to that of the whole blood extraction technique. Though TH-D improves the accuracy of GSSG quantification following DBS manual extraction, only S4, the highest concentration standard, is brought within the acceptable range of error. (**Table 2.10**) The %CV does not improve and both spiking systems demonstrate inaccurate ratio calculations. With the lowest determined extraction efficiency, DBS manual extraction will require more of a natural signal boost to aid the quantification of GSSG following this extraction method.

Error Propagation Factor and Instrumental LOD: Guidance for Spiking and Metaspike Preparation

Of importance when developing and working with isotopic spiking techniques is something referred to as the Error Propagation Factor (EPF) which directs an analysts understanding regarding the proportion of spike to natural needed within the final sample for optimal quantification.^{9, 10} Each spike demonstrates a different abundance breakdown of product ions, refer to **Table 2.2**. An example EPF calculation is demonstrated in **Equation 2.3**.

$$EPF = \sqrt{\frac{\text{Major Spike Abundance}}{\text{Minor Spike Abundance}} \cdot \frac{\text{Minor Sample Abundance}}{\text{Major Sample Abundance}}}$$

$$= \sqrt{\frac{0.9889931}{0.0001148} \cdot \frac{0.00001448}{0.99584}} = 0.3539$$

Equation 2. 3. Example EPF determination for the standard isotopic spiking technique where: 'Major Spike Abundance' refers to the abundance of the ⁶¹⁶GSSG product ion 359, 'Minor Spike Abundance' refers to the abundance of the ⁶¹⁶GSSG product ion 355, 'Major Sample Abundance' refers to the abundance of the ⁶¹²GSSG product ion 355, and 'Minor Sample Abundance' refers to the abundance of the ⁶¹²GSSG product ion 359.

Using the inverse calculation of 1/EPF for the above determined EPF of 0.3539, the factor becomes 2.826. Based on this calculation, there should be ~2.8 times the spike concentration of ⁶¹⁶GSSG compared to the natural concentration of ⁶¹²GSSG within the final analyzed sample for optimal quantification of the natural species. This would mean for a typical patient sample containing between 2-15 µg/g ⁶¹²GSSG, the spike concentration should be between 6-30 µg/g when using the standard spiking methodology. However, the EPF changes based on the experimentally determined abundances values for each spiking system. (Table 2.11)

Table 2. 11. Determined EPF for each spiking system for guidance on spiking levels.

Spiking System	Nat/Iso (v:v)	EPF	1/EPF
Standard (N)	0/100	0.35	2.8
TH-A	30/70	0.0060	167.8
TH-B	50/50	0.0039	258.4
TH-C	70/30	0.0025	393.4
TH-D	10/90	0.011	88.5
TH-E	20/80	0.0078	130.0
TH-F	40/60	0.0047	214.1

Experimentally we can see the impact of this EPF on the quantification. In an experiment, five standard samples were prepared at decreasing concentrations of $^{612}\text{GSSG}$: (1) 27.19 $\mu\text{g/g}$, (2) 16.42 $\mu\text{g/g}$, (3) 9.85 $\mu\text{g/g}$, (4) 5.93 $\mu\text{g/g}$, (5) 3.54 $\mu\text{g/g}$. Spiking systems N, TH-A, TH-B, and TH-C were all used to quantify the natural GSSG concentration in each sample. Using the known concentrations of isotope and natural GSSG species derived from both the analytical sample and the spike utilized, as well as the amount of each used for sample preparation, the final concentration seen by the instrument of each could be determined. This data was then utilized to calculate the proportion of natural/isotopic and compared to the associated percent error following quantification of the sample. (**Table 2.12**)

Table 2. 12. Resulting data from SIDMS application of TH-A, TH-B, TH-C, and standard isotopic spike (N).

Combo	Nat	Iso	Nat/Iso	Assoc. Err	%CV
N 1	10.20	67.08	0.15	3.1%	0.8%
N 2	6.18	67.08	0.092	0.9%	2.1%
N 3	3.69	67.08	0.055	7.1%	1.4%
N 4	2.22	67.08	0.033	10%	2.1%
N 5	1.33	67.08	0.020	16%	2.1%
A 1	30.65	46.86	0.65	18%	3.0%
A 2	26.61	46.86	0.57	17%	5.5%
A 3	24.15	46.86	0.52	13%	6.1%
A 4	22.68	46.86	0.48	11%	8.7%
A 5	21.78	46.86	0.46	5.2%	18%
B 1	44.28	33.38	1.33	40%	3.4%
B 2	40.25	33.38	1.21	38%	4.2%
B 3	37.78	33.38	1.13	33%	9.0%
B 4	36.31	33.38	1.09	19%	11%
B 5	35.42	33.38	1.06	9.0%	5.5%
C 1	57.86	19.97	2.90	67%	2.9%
C 2	53.82	19.97	2.69	64%	3.2%
C 3	51.35	19.97	2.57	60%	6.3%
C 4	49.88	19.97	2.50	49%	11%
C 5	48.99	19.97	2.45	36%	8.7%

TH-A has a calculated EPF at 0.0060 which is very small compared to the standard spiking technique at 0.35. This necessitates a ~167 times greater presence of isotope as compared to natural, which is likely why as we decrease in concentration of natural, the percent error gets smaller. A similar trend can be observed for TH-B and TH-C, however, the isotopic presence is never great enough compared to the natural presence in order to reduce the error within an acceptable range. The precision of the quantification is also important and interestingly we observed the opposite trend with TH-A where precision is greatest when the natural to isotopic presence is closer to 1:1 and gets worse as the isotopic presence begins to outweigh the natural presence. Similar trends can be observed with TH-B and TH-C.

Aside from EPF calculations for guidance of spiking levels, one must also consider the instrumental capabilities. Each instrument possesses different detection capabilities in general based on instrument age, detector ability, ionization efficiency of the target analyte, efficiency of the extraction procedure used, etc.³ One way to assess this is through the preparation of several calibration standards at increasingly lower concentrations of your target analyte using serial dilution, preferably to levels well below expected concentrations from a patient sample. These standard solutions are then analyzed with the instrument of choice using the method intended for analytical sample analysis and the peak area or intensity of the signal is plotted against the concentration to yield an external calibration curve. An experiment of this nature was undertaken. (**Table 2.13** and **Figure 2.5**)

Table 2. 13. External calibration standard of 612GSSG results.

Standard	Conc ⁶¹²GSSG (ug/g)	Average Counts 612
Blank	0	58
S_1	23.85	544832

S_2	11.93	281792
S_3	6.01	139511
S_4	3.02	61418
S_5	1.51	24961
S_6	0.76	10678
S_7	0.38	3818
S_8	0.19	1741
S_9	0.097	730
S_10	0.048	309

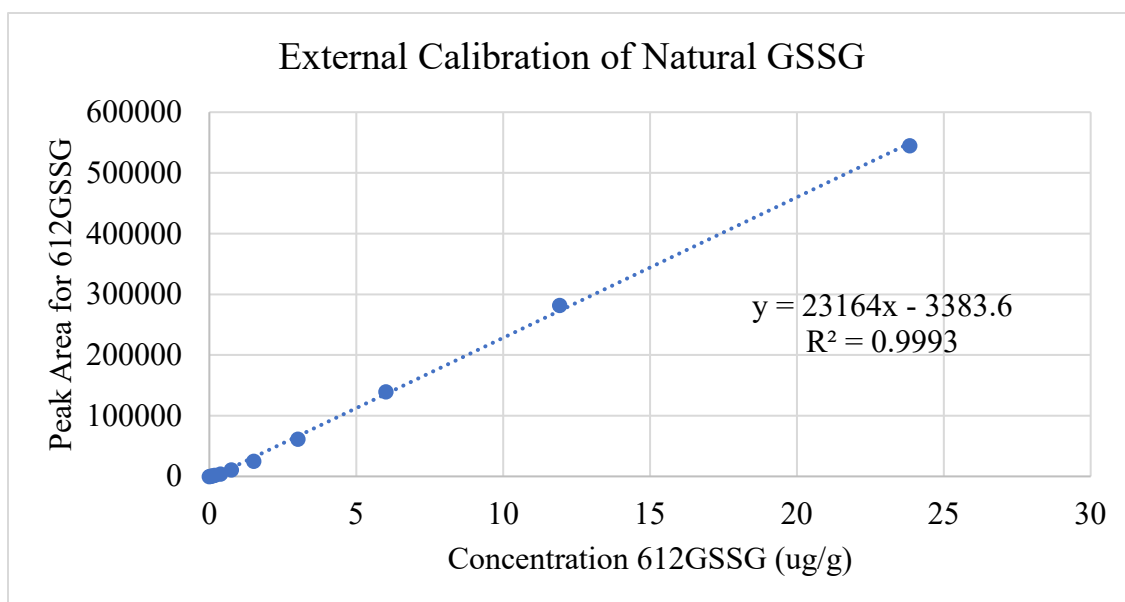


Figure 2. 5. Calibration curve for 612GSSG following analysis on the LC-QqQ.

Utilizing the linest function in Excel, the standard uncertainty in the slope can be determined. This enables the calculation of LOD and LOQ via **Equation 2.4** and **Equation 2.5** which, for ⁶¹²GSSG, were determined to be 0.70 ug/g and 2.12 ug/g, respectively. This is one way to provide guidance of the instrument's capability, instrumental detection limit according to guidance set forth by the International Union of Pure and Applied Chemistry.¹¹

$$LOD = \left(\frac{3.3 * \text{standard uncertainty in slope}}{\text{slope}} \right)$$

Equation 2. 4. Calculation of LOD using data derived from the external calibration curve.

$$LOD = \left(\frac{10 * \text{standard uncertainty in slope}}{\text{slope}} \right)$$

Equation 2. 5. Calculation of LOQ using data derived from the external calibration curve.

An additional recommendation of LOD and LOQ assessments suggested by IUPAC involves the assessment of a suitable blank in several replicate analyses employing chromatography and instrumentation to be used for analytical sample analysis.^{3, 11} Alongside the blank sample, a sample containing low level concentration of the target analyte should also be assessed to determine the comparable signal of the analyte in a true sample versus a true blank.¹¹ This provides guidance regarding the lowest level of analyte that can be distinguished from instrumental noise based upon the specific instrument of choice.³ For the glutathione analysis, the final samples are contained in water, so a water blank was analyzed twenty times to detect for the signal of 355 m/z, the most abundant product ion of GSSG. (Table 2.14)

Table 2. 14. Water blank analyses for the estimation of LOD and LOQ.

Replicate	Counts 613.1 → 355.1	Replicate	Counts 613.1 → 355.1	Result (counts)	
Blank 01	2	Blank 11	34.6	Average Signal	5.92
Blank 02	1.5	Blank 12	1.5	Standard Deviation	8.43
Blank 03	1.7	Blank 13	1.4	LOD	27.81
Blank 04	2.4	Blank 14	9.9	LOD (-)	21.89
Blank 05	2	Blank 15	1.4	LOD (+)	33.73
Blank 06	2.5	Blank 16	20.6		
Blank 07	2.8	Blank 17	10.2		
Blank 08	1.5	Blank 18	1.4		
Blank 09	2.8	Blank 19	16		
Blank 10	1.5	Blank 20	2.5		

The average signal of 355 in the blank water sample where the GSSG analyte is expected to elute (~2.3 mins) was determined to be 5.92 +/- 8.43 counts. The calculated standard deviation is then multiplied by 3.3 and added or subtracted from the average signal counts to estimate the LOD signal of analyte at low (-) and high (+) ends to denote presence of analyte. These values are calculated to be 21.89 and 33.73 counts, respectively. Therefore, to confidently distinguish between true analyte signal and baseline instrument noise, the counts of an integrated peak at 2.3 minutes must be greater than 34 counts for the detection of GSSG.

Using the information derived from the determinations of LOD based on the calibration technique, five standards of ⁶¹²GSSG in water were prepared at concentrations at and below 0.70 µg/g: (1) 0.759, (2) 0.381, (3) 0.192, (4) 0.096, and (5) 0.048 µg/g. Samples were analyzed in duplicate tracking for the 355-product ion representing natural GSSG. (Table 2.15)

Table 2. 15. Resulting instrumental signal for the analysis of low level ⁶¹²GSSG standards.

Sample	Counts of 355	Signal-to-noise
Std 1 01	11402	2221
Std 1 02	9953	1998
Std 2 01	4110	556
Std 2 02	3525	465
Std 3 01	1841	432
Std 3 02	1640	268
Std 4 01	746	182
Std 4 02	714	127
Std 5 01	346	41
Std 5 02	271	59

Using the higher end of the water blank result (33.73 counts), we can see even at extraordinarily low levels of GSSG (0.048 µg/g), the counts of the analytical sample are

well above the counts necessary to denote positive detection of analyte presence and discernment from instrumental noise.

Extraction of the sample reduces the efficiency of how much analyte is present within the analytical sample the instrument is analyzing. To account for the loss of analyte, standards can be prepared in a comparable matrix to analytical samples and processed with respective extraction protocols. This was done for the extraction methods in Chapter 1, which represents the method detection limit. Please refer to **Table 1.4**, in Chapter 1, for those determined values.

Using the information regarding LOD and LOQ, a more guided and targeted approach to preparing a Thor’s Hammer Metaspikes was undertaken. TH-G and TH-H were prepared in such a way that, following extraction, enough natural GSSG would be present in the final sample the instrument detects to be above the LOQ. (**Table 2.16**) The ratio of natural concentration to isotopic concentration and associated errors from experimental data was also utilized to guide the preparation where TH-G targeted the 1:1 ratio while TH-H targeted the 0.1:1 ratio. Both new Metaspikes were prepared with concentrations that following extraction would also be well above what is needed for positive detection of analyte presence and discernment from instrumental noise.

Table 2. 16. Product ion abundance for TH-G and TH-H.

m/z Product Ion	Product Ion Abundance (As)	
	TH-G	TH-H
355.1	0.416900	0.079201
356.1	0.000020	0.000019
357.1	0.000212	0.000200
358.1	0.006364	0.006483
359.1	0.576596	0.913670
360.1	0.000034	0.000057
361.1	0.000004	0.000004
362.1	0.000004	0.000001
363.1	0.000001	0.000001
364.1	0.000011	0.000013

In an IDMS system, TH-G was applied to the analysis of eight samples at decreasing concentrations of ⁶¹²GSSG: (1) 30.293, (2) 18.004, (3) 10.706, (4) 6.388, (5) 3.804, (6) 2.265, (7) 1.351, and (8) 0.807 µg/g. Not only were the neat solutions analyzed directly upon isotopic spiking, but samples were also spotted onto DBS cards and processed with the manual extraction technique described in Chapter 1. Where TH-G helped to improve the accuracy of S5 and S7, the other samples were not improved and in fact, error was worse for the TH-G technique than the standard spiking technique. (**Tables 2.17 and 2.18**) In a similar fashion, the precision of the standard spiking technique outperforms the TH-G spiking technique. (**Tables 2.17 and 2.18**)

Table 2. 17. Quantitative results for 612GSSG assessment via direct analysis utilizing the standard spiking technology.

Summarized IDMS Results for Direct - Standard						
Sample	Theoretical ⁶¹² GSSG Concentration (ug/g)	Calculated ⁶¹² GSSG \Concentration (ug/g)	SD	95% CI	%Error	%CV
SS1	30.293	28.021	0.073	0.180	7.5%	0.3%
SS2	18.004	17.167	0.164	0.407	4.7%	1.0%
SS3	10.706	9.526	0.045	0.112	11.0%	0.5%
SS4	6.388	5.785	0.036	0.090	9.4%	0.6%
SS5	3.804	3.263	0.064	0.159	14.2%	2.0%
SS6	2.265	1.841	0.041	0.102	18.7%	2.2%
SS7	1.351	1.084	0.005	0.012	19.8%	0.4%
SS8	0.807	0.616	0.029	0.072	23.6%	4.7%

Table 2. 18. Quantitative results for 612GSSG assessment via direct analysis utilizing the TH-G spiking technology.

Summarized IDMS Results for Direct - TH-G						
Sample	Theoretical ⁶¹² GSSG Concentration (ug/g)	Calculated ⁶¹² GSSG Concentration (ug/g)	SD	95% CI	%Error	%CV
GS1	30.293	35.047	0.554	1.377	15.7%	1.6%
GS2	18.004	20.550	0.455	1.131	14.1%	2.2%
GS3	10.706	12.202	0.198	0.493	14.0%	1.6%
GS4	6.388	7.182	0.135	0.336	12.4%	1.9%
GS5	3.804	3.923	0.446	1.107	3.1%	11.4%
GS6	2.265	2.692	0.105	0.260	18.9%	3.9%
GS7	1.351	1.462	0.084	0.209	8.2%	5.7%
GS8	0.807	1.075	0.225	0.559	33.1%	20.9%

Moving to the samples analyzed after extracting from the card, we do see an improvement in the quantification of S3-S5 over what the standard spiking technique is able to accomplish. (Tables 2.19 and 2.20) Again, precision maintained acceptable levels across all concentration ranges when utilizing the standard spiking technique but was increased for TH-G spiking while also falling out of acceptance for S7 and S8. Given the apparent lack of success with TH-G in an IDMS system, it was not utilized for SIDMS applications.

Table 2. 19. Quantitative results for 612GSSG assessment via DBS manual extraction analysis utilizing the standard spiking technology.

Summarized IDMS Results for Card - Standard						
Sample	Theoretical ⁶¹² GSSG Concentration (ug/g)	Calculated ⁶¹² GSSG Concentration (ug/g)	SD	95% CI	%Error	%CV
SS1	30.293	26.336	0.133	0.331	13.1%	0.5%
SS2	18.004	15.997	0.167	0.414	11.1%	1.0%
SS3	10.706	9.071	0.128	0.317	15.3%	1.4%
SS4	6.388	5.490	0.068	0.170	14.1%	1.2%
SS5	3.804	3.059	0.004	0.009	19.6%	0.1%
SS6	2.265	1.840	0.053	0.132	18.8%	2.9%
SS7	1.351	1.083	0.020	0.050	19.8%	1.9%
SS8	0.807	0.646	0.014	0.035	19.9%	2.2%

Table 2. 20. Quantitative results for 612GSSG assessment via DBS manual extraction analysis utilizing the TH-G spiking technology.

Summarized IDMS Results for Card - TH-G						
Sample	Theoretical ⁶¹² GSSG Concentration (ug/g)	Calculated ⁶¹² GSSG Concentration (ug/g)	SD	95% CI	%Error	%CV
GS1	30.293	35.184	0.710	1.763	16.1%	2.0%
GS2	18.004	20.363	0.666	1.654	13.1%	3.3%
GS3	10.706	11.999	0.287	0.714	12.1%	2.4%
GS4	6.388	6.632	0.209	0.519	3.8%	3.2%
GS5	3.804	3.597	0.301	0.747	5.5%	8.4%
GS6	2.265	1.744	0.214	0.533	23.0%	12.3%
GS7	1.351	0.988	0.219	0.544	26.9%	22.2%
GS8	0.807	0.479	0.483	1.199	40.7%	100.8%

In an IDMS system, TH-H was applied to the analysis of six samples at decreasing concentrations of ⁶¹²GSSG: (1) 23.846, (2) 11.930, (3) 6.012, (4) 3.015, (5) 1.513, and (6) 0.759 µg/g. (Table 2.21) The standard spiking technique meets acceptable precision across all levels of GSSG, but the error falls outside of acceptance from S3-S6. When applying the TH-H spike, the error is decreased significantly for S1-S4 bringing S3 into the acceptable range beyond what the standard spike can manage. At the very low levels of GSSG, neither spike meets acceptable error.

Table 2. 21. Quantitative results for 612GSSG assessment via direct sample analysis utilizing the TH-H spiking technology.

Summarized IDMS Results - TH-H							
Sample	Concentration of ⁶¹² GSSG (ug/g)						
	Theoretical	Average	SD	95% CI	99% CI	%Error	%CV
N 1	23.846	20.690	0.198	0.315	0.578	13.2%	1.0%
N 2	11.930	10.140	0.051	0.082	0.150	15.0%	0.5%
N 3	6.012	4.887	0.079	0.125	0.230	18.7%	1.6%
N 4	3.015	2.420	0.017	0.027	0.049	19.7%	0.7%
N 5	1.513	1.153	0.007	0.011	0.021	23.8%	0.6%
N 6	0.759	0.563	0.003	0.005	0.010	25.9%	0.6%
H 1	23.846	22.075	0.436	0.694	1.274	7.4%	2.0%
H 2	11.930	10.845	0.047	0.074	0.136	9.1%	0.4%
H 3	6.012	5.339	0.030	0.048	0.089	11.2%	0.6%
H 4	3.015	2.522	0.240	0.382	0.701	16.4%	9.5%
H 5	1.513	1.053	0.045	0.072	0.132	30.4%	4.3%
H 6	0.759	0.415	0.129	0.205	0.377	45.4%	31.1%

TH-H was then applied to an SIDMS system where four synthetic blood samples were prepared at increasing concentrations of $^{612}\text{GSSG}$: (1) 0.878, (2) 5.00, (3) 11.94, and (4) 19.63 $\mu\text{g/g}$ while the $^{306}\text{GS-NEM}$ concentration decreased: (1) 893.83, (2) 688.55, (3) 499.92, and (4) 295.04 $\mu\text{g/g}$. The quantification of GS-NEM demonstrated acceptable accuracy and precision regardless of spike system. At very low levels of GSSG, like S1, the precision was worse for the TH-H data than the standard spiking method and the accuracy was well outside the range of acceptance though the TH-H showed minor improvement. TH-H improved the accuracy of GSSG quantification for S3 and S4 beyond what the standard spike accomplished, demonstrating acceptable accuracy and precision. (**Table 2.22**) The imprecision noted with the GSH/GSSG ratio calculation was extraordinarily low, below 1 %CV for all levels, with no significant improvement in uncertainty for the TH-H spiking system beyond what can be accomplished with the standard spiking technique. However, the accuracy of the ratio calculation following TH-H employment was improved for S3 and S4, decreasing the error slightly from what was determined using the standard spiking technique

Table 2. 22. Quantitative results for $^{306}\text{GS-NEM}$, $^{612}\text{GSSG}$, and GSH/GSSG ratio assessment via direct sample analysis utilizing the TH-H spiking technology in an SIDMS+TH system.

Summarized SIDMS Results																	
Sample	$^{306}\text{GS-NEM}$ Concentration (ug/g)						$^{612}\text{GSSG}$ Concentration (ug/g)						GSH/GSSG Ratio				
	Theo	Calc	SD	95%CI	%Error	%CV	Theo	Calc	SD	95%CI	%Error	%CV	Theo	Calc	Uncertainty	%Error	%CV
BSN_1	893.83	893.05	19.65	31.27	0%	2%	0.88	5.90	0.52	0.65	572%	9%	1017.59	151.37	0.091	85%	0.06%
BSN_2	688.55	661.10	11.63	12.20	4%	2%	5.00	7.25	0.37	0.39	45%	5%	137.60	91.18	0.054	34%	0.06%
BSN_3	499.92	480.48	6.63	6.96	4%	1%	11.94	12.23	0.95	1.00	2.4%	8%	41.86	39.28	0.079	6%	0.20%
BSN_4	295.04	286.87	10.97	11.51	3%	4%	19.63	17.36	0.68	0.71	12%	4%	15.03	16.52	0.055	10%	0.33%
BSH_1	893.83	897.18	33.23	34.87	0%	4%	0.88	5.34	0.70	0.74	508%	13%	1017.59	167.88	0.14	84%	0.08%
BSH_2	688.55	658.11	10.43	10.94	4%	2%	5.00	7.94	1.31	1.38	59%	17%	137.60	82.88	0.17	40%	0.20%
BSH_3	499.92	486.24	7.18	7.53	3%	1%	11.94	12.20	0.57	0.59	2.2%	5%	41.86	39.84	0.049	5%	0.12%
BSH_4	295.04	284.65	6.83	7.16	4%	2%	19.63	17.77	1.12	1.18	9%	6%	15.03	16.02	0.068	7%	0.42%

Conclusions

Biomarker analysis for diagnostic and treatment tracking has been moving to the forefront of the medical field. Many important biomarker analytes existent in various biological matrices exist in very low levels, complicating their analysis through traditional methodologies like external calibration or internal standard calibration. Without accurate and precise methodologies for quantifying such analytes, medical professional struggle to make sound, data-based decisions for a patient's care. Thor's Hammer Metaspiking technology is an interesting and novel analytical tool for boosting instrumental signal of low-level analytes in an analytical sample for improved detection and quantification of target species.

Through the addition of known natural analyte standard to the isotopically enriched spike typically utilized for IDMS and SIDMS quantification of glutathione, low level concentrations of GSSG are boosted to levels above the LOQ, enabling more accurate and precise quantification. Improved quantification of GSSG subsequently improves the calculation of the important GSH/GSSG ratio biomarker.

Several Metaspikes combinations of $^{612}\text{GSSG}$ and $^{616}\text{GSSG}$ have been produced and tested in both IDMS and SIDMS systems of quantification. Unsurprisingly, different Metaspikes perform better at different levels of analyte present in the analytical sample. In IDMS applications, TH-D and TH-E demonstrated the lowest associated average error (1.6% and 1.7%, respectively) while demonstrating the greatest reduction in error across all analyte levels from 3-50 $\mu\text{g/g}$. (**Figure 2.4**) In SIDMS systems, TH-D, with a 10% natural and 90% isotope composition, demonstrated best performance at the mid-range levels of GSSG from 7-13 $\mu\text{g/g}$ (**Tables 2.8-2.10**) while TH-A, with a 30% natural and

70% isotope composition, demonstrated best performance at the high range concentrations between 15-30 $\mu\text{g/g}$. (**Table 2.7**) TH-B, with a 50% natural and 50% isotope composition, is the only Metaspikes utilized in SIDMS systems of quantification to enable improved quantification of low level GSSG concentrations between 0-3 $\mu\text{g/g}$ beyond what the standard spiking technique could provide. (**Table 2.7**)

This initial work demonstrates the proof of concept for the application of Thor's Hammer Metaspiking and reveals the improvement in accuracy and precision enabled by the new technology.

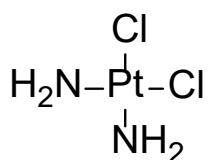
References

1. Dalle-Donne, I.; Rossi, R.; Colombo, R.; Giustarini, D.; Milzani, A., Biomarkers of oxidative damage in human disease. *Clin Chem* **2006**, *52* (4), 601-23.
2. Fahrenholz, T.; Wolle, M. M.; Kingston, H. M.; Faber, S.; Kern, J. C., 2nd; Pamuku, M.; Miller, L.; Chatragadda, H.; Kogelnik, A., Molecular speciated isotope dilution mass spectrometric methods for accurate, reproducible and direct quantification of reduced, oxidized and total glutathione in biological samples. *Anal Chem* **2015**, *87* (2), 1232-40.
3. Currie, L. A., Limits for Qualitative Detection and Quantitative Determination: Application to Radiochemistry. *Analytical Chemistry* **1968**, *40* (3), 586-592.
4. Matuszewski, B. K.; Constanzer, M. L.; Chavez-Eng, C. M., Matrix effect in quantitative LC/MS/MS analyses of biological fluids: a method for determination of finasteride in human plasma at picogram per milliliter concentrations. *Anal Chem* **1998**, *70* (5), 882-9.
5. Bukowski, M. R.; Picklo, M. J., Sr., Quantitation of Glutathione, Glutathione Disulphide, and Protein-Glutathione Mixed Disulphides by High-Performance Liquid Chromatography-Tandem Mass Spectrometry. *Methods Mol Biol* **2019**, *1967*, 197-210.
6. Forman, H. J.; Zhang, H.; Rinna, A., Glutathione: overview of its protective roles, measurement, and biosynthesis. *Mol Aspects Med* **2009**, *30* (1-2), 1-12.
7. Howard M. Kingston, M. P. Accurate Measurement for Disease Diagnosis and Drug Metabolite Screening. January 16, 2018.

8. Mehmet Pumucku, H. M. K. QUANTIFICATION OF PREVIOUSLY UNDETECTABLE QUANTITIES. 2021.
9. Patterson, K. Y., Veillon, C., O'Haver, T.C., Error Propagation in Isotope Dilution Analysis as Determined by Monte Carlo Simulation. *Analytical Chemistry* **1994**, *66* (18), 2829-2834.
10. Previs, S. F.; Herath, K.; Castro-Perez, J.; Mahsut, A.; Zhou, H.; McLaren, D. G.; Shah, V.; Rohm, R. J.; Stout, S. J.; Zhong, W.; Wang, S. P.; Johns, D. G.; Hubbard, B. K.; Cleary, M. A.; Roddy, T. P., Effect of Error Propagation in Stable Isotope Tracer Studies: An Approach for Estimating Impact on Apparent Biochemical Flux. *Methods Enzymol* **2015**, *561*, 331-58.
11. Allegrini, F.; Olivieri, A. C., IUPAC-consistent approach to the limit of detection in partial least-squares calibration. *Anal Chem* **2014**, *86* (15), 7858-66.

Chapter 3: Glutathione and Cancer: Treatment Tracking for Platinating Agents in Chemotherapy

Cisplatin is a square planar metallic coordination compound with a platinum center. (Figure 3.1) The compound was first synthesized by M. Peyrone in 1844, but its biological potential was not discovered until 1965 when researchers, Rosenberg et al, discovered the compound's ability to hinder cell division.¹ The compound was promptly sent off for oncological research testing and by 1978, the FDA had approved cisplatin for use in cancer treatment in the United States.¹



Molecular Weight: 298.03

cisplatin

Figure 3. 1. The molecular structure of cisplatin.

Cisplatin's mechanism of action involves its transport into the cellular membrane. Outside of the cellular membrane, the chlorine ion concentration is much higher stabilizing the original square planar cisplatin structure. Some researchers propose the drug enters the cell via passive diffusion and while this may play a small role, literature shows much of the drug is more likely to be transported into the cell via the copper transporter 1.² Given the platinum metal centers +2 charge state, mimicking that of the favorable Cu^{2+} , it has been observed the transporter brings the cisplatin drug into the cellular membrane at much faster rates than that of passive diffusion.¹ Once inside the cell, the chlorine ion concentration drops significantly, and the now labile chlorine ligands are more easily replaced with water ligands which can then be further oxidized to hydroxyl groups.^{2,3} This

series of ligand exchange and oxidation yields five additional structures related to the original cisplatin compound.³ (**Figure 3.2**) Likewise, this ligand interchange is important, as the “aquated” version of cisplatin is believed to be the bioactive form of the drug.²

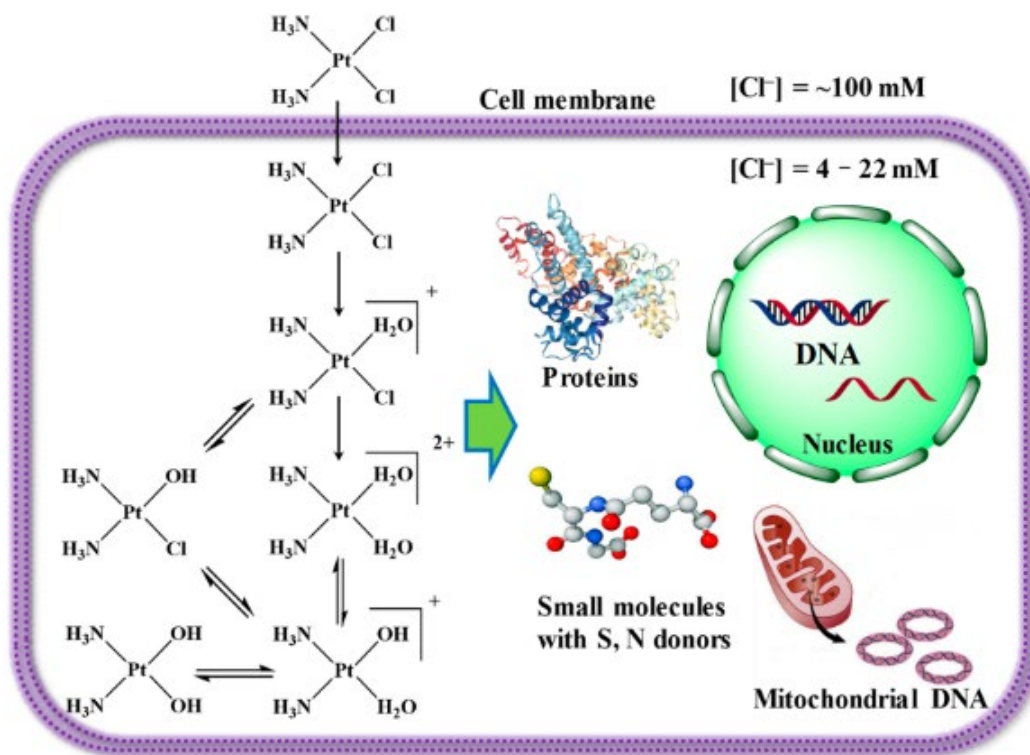


Figure 3. 2. Biotransformation of cisplatin following entrance within the cellular membrane.³

Once aquated, the electron rich oxygen atoms work to bind to electron acceptors such as sulfur and nitrogen. Important for cancer cell elimination, aquated cisplatin has been proposed to bind to the N7 position of guanine bases causing the formation of lesions.^{4, 5} (**Figure 3.3**)

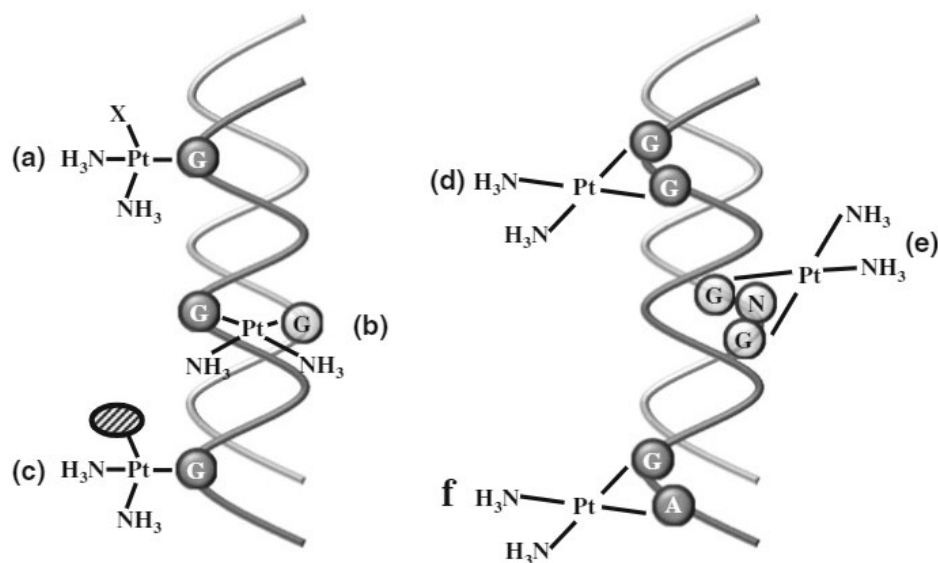
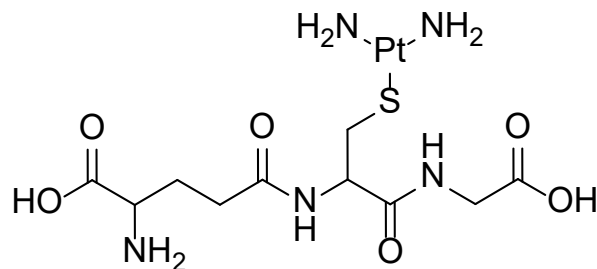


Figure 3.3. DNA binding of cisplatin to guanine bases.⁵

Cisplatin also works to obstruct several DNA repair pathways permitting the lesions to persist and induce cellular apoptosis.^{4,6} This is the preferred mechanism of action for cisplatin when utilized for cancer treatment as it ensures the death of the cancer cell. However, cisplatin suffers greatly from chemoresistance, due to the high intracellular concentration of various nucleophilic species like glutathione, cysteine, and metallothionine.^{2,7} With highly reactive thiol groups, cisplatin is targeted, bound, and eliminated from the body via Phase II Detoxification through the urine at a very fast rate.⁷

(Figure 3.4)

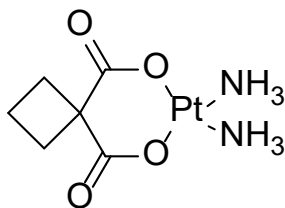


Molecular Weight: 533.44

Figure 3.4. The molecular structure of cisplatin conjugated to one molecule of reduced glutathione, GSH.

Though an immunologically appropriate response, a depletion of antioxidant levels within the cell results in increased oxidative stress, a known contributor to cancer progression.^{2,8} Likewise, the elimination of the antitumor agent via the urine prohibits the interaction of said agent with the cancer DNA and therefore renders the drug treatment inefficient or useless.⁷

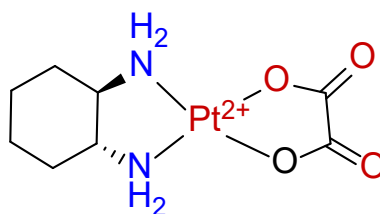
Combatting chemoresistance has been an ongoing exploration for many clinicians. Disguising the platinating drug from the body has been the first endeavor of many synthetic chemists, which led to the production of two cisplatin derivatives: carboplatin and oxaliplatin.⁹ (**Figures 3.5** and **3.6**) The higher organic content surrounding the platinum center hides the platinating agent from the body's immune system more effectively allowing for a longer half-life duration and increasing the potential for DNA damage and cancer elimination.² Though seemingly more beneficial for avoiding detoxification, carboplatin and oxaliplatin suffer from decreased cancer killing efficacy usually requiring much higher doses and longer durations of treatment.¹⁰ The disguise from the immune system also promotes a later issue resulting in the drug sequestering in the body potentially causing undue harm later to healthy tissue and cells. Researchers are still currently unsure as to what all bio-transformations carboplatin and oxaliplatin may undergo.⁹



Molecular Weight: 371.26

carboplatin

Figure 3. 5. The molecular structure of carboplatin.



Molecular Weight: 397.29
oxaliplatin

Figure 3. 6. The molecular structure of oxaliplatin.

Current clinicians and medical researchers who analyze and quantify patient samples following platinum-based cancer treatments traditionally utilize inductively coupled plasma mass spectrometry (ICP-MS) to obtain total platinum concentrations within a blood or urine sample over the course of time following treatment administration.⁹ The current standard operating procedure in these labs is to use an iridium internal standard calibration curve quantification. Not only has our lab shown that calibration curves do not always perform the best, but use of iridium instead of a more favorable platinum isotope introduces potential for error with the quantification. Likewise, this method only provides the analyst with a total platinum concentration and gives no indication of biotransformations that may have occurred.⁹

This researcher has sought to improve the quantitative analysis of patient samples following platinum-based chemotherapy treatments. The use of a more appropriate isotopically enriched platinum internal standard will not only more accurately normalize calibration curves but also enable IDMS and SIDMS mathematics to be used for a simplified quantitative protocol. Similarly, the synthesis of all three main platinating agents currently approved for use in the oncology field with an isotopically enriched form of platinum will enable speciated analysis of cisplatin to provide a more inclusive and

encompassing view of the biological transformation that the drug undergoes during a patient's treatment.

Materials & Methods

Reagents and Standards:

Standard reference material for cisplatin, carboplatin, and oxaliplatin were purchased from Sigma Aldrich: carboplatin (P/N: PHR1528, Lot#: LRAB3831, MW: 397.29 g/mol, certified purity: 99.4%); oxaliplatin (P/N: C2538, Lot#: MKCK1243, MW: 371.25 g/mol, assay purity: 99.6%). Negative synthetic blood was purchased from Immunoanalysis Corp (p/n: SB-0050). Naturally abundant reference standard for reduced glutathione (99%+ pure, p/n: 70-18-8) was purchased from Sigma-Aldrich. Isotopically enriched platinum-194 (96.54% purity) was purchased from Applied Isotope Technologies. Trace metal analysis grade nitric (p/n: 7697372) and hydrochloric (p/n: 7647010) acids were purchased from Fisher Scientific and reagent grade hydrogen peroxide was purchased from VWR.

Equipment & Instrumentation:

The column used for LC-MS/MS analysis of platinated drug compounds was a Phenomenex SynergiTM 4 μ m Hydro-RP 80 Å LC column C18, 150 x 4.6 mm (p/n: 5375-0097). The Agilent 7700 ICP-MS was utilized for total platinum analyses. The Agilent 1200 series HPLC in tandem with the Agilent 6460 QQQ-MS (s/n: US92170174, NSF MRI: 0821401) with an Agilent Jetstream electrospray ionization source (Model: G1958-65138; s/n: US91500324) was utilized for speciated analyses. All data was collected and processed using Agilent's MassHunter Acquisition and Qualitative Analysis programs (Version 10.0 SR1; Build: 10.0.142).

Method Development – LC-MS/MS Analysis

A standard binary gradient system was utilized for the separation of target analytes. Sample injection volume was 5 μ L with a 20 second needle wash. Mobile phase A was water with 0.1% formic acid while mobile phase B was acetonitrile with 0.1% formic acid. The gradient was designed to begin with 5.0% B and hold for 0.5 minutes, then ramp to 95% B over the course of 9.5 minutes, then decrease to 5.0% B over 1 minute and hold for 2 minutes for column post-run cleanup, leading to a total run time of 12 minutes. The column was maintained at a temperature of 30 °C. The triple quadrupole was set to the following parameters: gas temperature at 300 °C, gas flow at 8 L/min, nebulizer pressure at 45 psi, sheath gas temperature 250 °C, sheath gas flow at 11 L/min, capillary voltage at 5,000 V for both positive and negative modes, nozzle voltage at 500 V for both positive and negative modes, and a delta EMV at 250 V. The instrument was operated in various modes including MS2 scan, selected ion monitoring (SIM), multiple reaction monitoring (MRM), precursor ion, and product ion modes. In scan mode, a broad m/z range from 50-1000 was utilized with a 500 ms scan time in the positive polarity mode. The fragmentor was maintained at 135 V while the cell accelerator voltage was at 7 kV. For SIM mode, designated ions were tracked (see later tables) and the dwell time was set for 200 ms. Product ion scans utilized a fragment m/z range of 80-1,000 with a scan time of 500 ms and a range of collision energies including 10, 25, 30, and 45 kV.

Platinated Drug Detection – LC-MS/MS Analysis

Carboplatin

A neat solution of carboplatin SRM was prepared around 100 μ g/g in water. An aliquot of the prepared solution was filtered through a 0.45 μ m syringe filter into an LC-

MS vial and analyzed in MS2 scan mode for the detection of all possible m/z ions. (**Figure 3.7**)

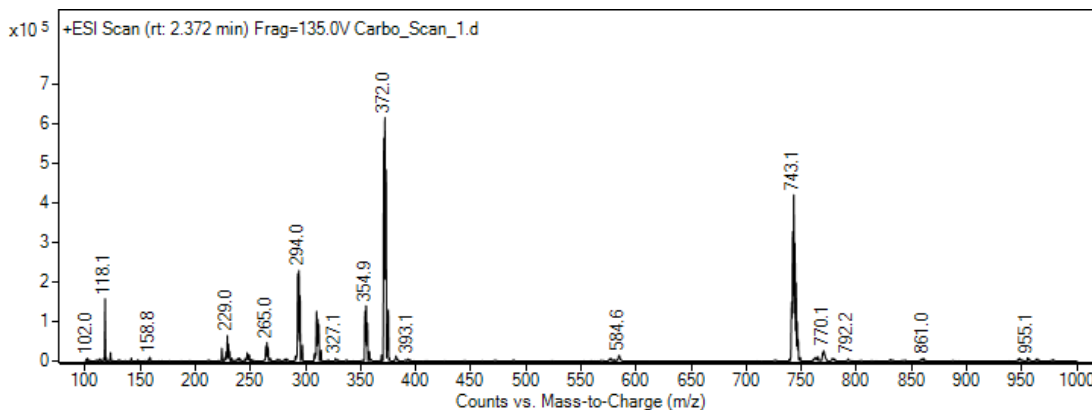


Figure 3. 7. Positive mode ESI scan result of carboplatin neat solution in water.

With a molecular weight of 371.25 g/mol, the expected $[M+1]^+$ ion is 372.0 m/z, which was clearly observed to be the highest abundant ion following the MS2 scan of the sample. Due to the isotopic breakdown of platinum (**Figure 3.8**) with major isotopes of ^{194}Pt , ^{196}Pt , and ^{198}Pt , the 371, 373, and 374 m/z ions are also observed.

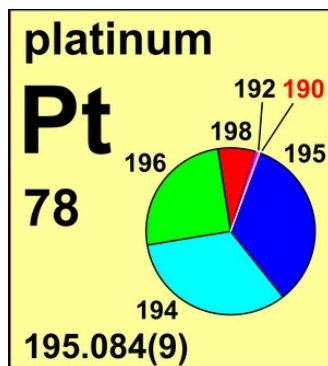


Figure 3. 8. Isotopic abundances for platinum's six isotopic species.

Interestingly, the next most abundant m/z ion detected is 743.1 m/z, which upon literature research is determined to be the dimer form of carboplatin.¹¹ (**Figure 3.9**)

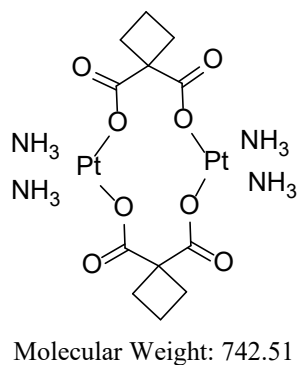


Figure 3. 9. Dimerized structure of two carboplatin molecules.

As suggested by literature, and confirmed by experimental results, a single compound of carboplatin can lose one or both ammonia groups. (**Figure 3.10**) This is the weakest link in the compounds natural structure lending the easy fragmentation of the molecule.

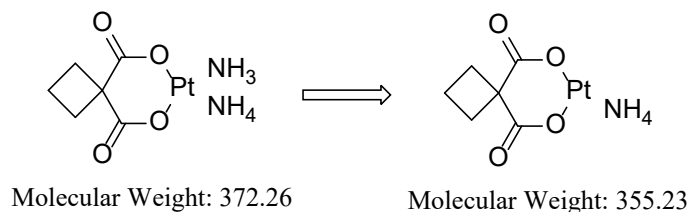
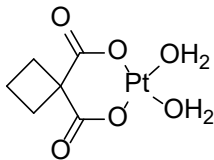


Figure 3. 10. Fragmentation pattern from 372 parent ion to the 355 m/z product ion.

Given the fragile nature of the ammonia groups connection to the platinum center, it is also possible for the platinum center to pick one or two water ligands, much like its cisplatin counterpart. This results in the formation of the ion at 373 m/z, the third most abundant m/z detected from analysis of the SRM. (**Figure 3.11**) In a similar fashion, the loss of one water ligand also brings the product ion mass to 355 m/z.



Molecular Weight: 373.22

Figure 3. 11. Aquated structure of carboplatin.

To further delineate fragmentation patterns of carboplatin for the development of an MRM detection method, product ion scans were conducted using the 372 and 373 m/z ions as the precursor ion choices with a broad product ion scan range from 100-1,000 using a 25 kV collision energy. (**Figure 3.12** and **3.13**)

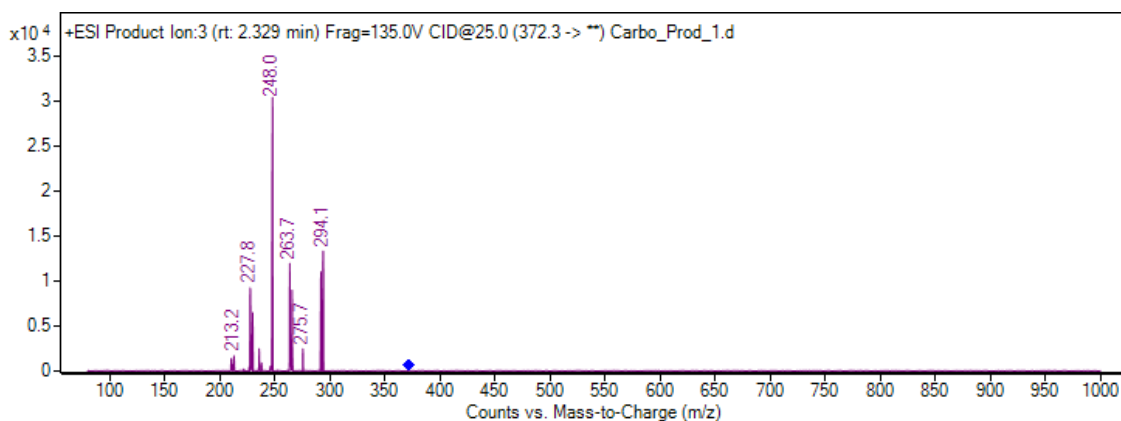


Figure 3. 12. Resulting product ion scan of carboplatin using the 372 m/z precursor ion and 25 kV collision energy.

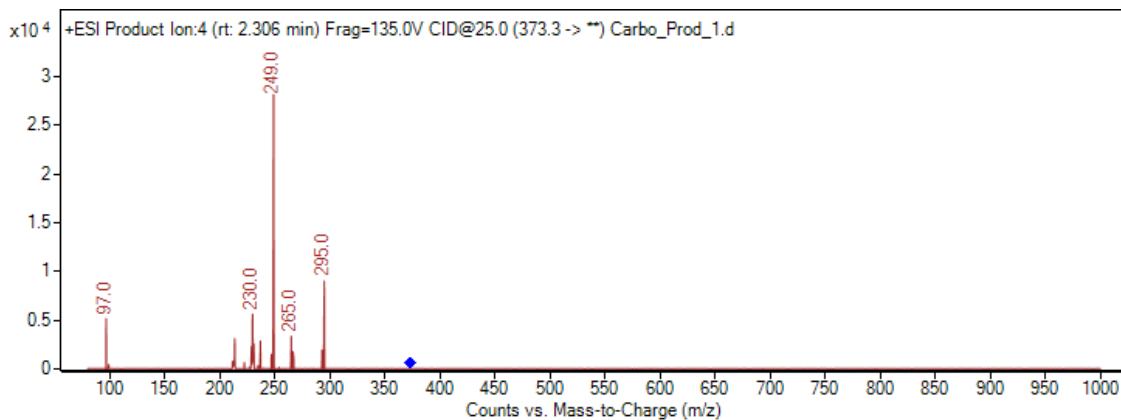


Figure 3. 13. Resulting product ion scan of carboplatin using the 373 m/z precursor ion and 25 kV collision energy.

The loss of the cyclobutene dicarbaldehyde adduct with subsequent aquation of the platinum center yields the low abundant 265 m/z ion seen in the 373 m/z scan. Subsequent loss of water ligands or hydrogen atoms can yield the more abundant 249 and 230 product ions. (**Figure 3.14**) This same trend can be noted for the 372 m/z product ion scan, though the m/z is shifted one unit down.

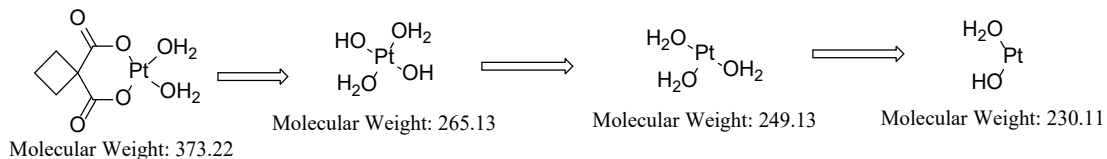


Figure 3. 14. Proposed fragmentation pattern for carboplatin molecule at a collision energy of 25 kV.

Oxaliplatin

A neat solution of oxaliplatin SRM was prepared around 100 $\mu\text{g/g}$ in water. An aliquot of the prepared solution was filtered through a 0.45 μm syringe filter into an LC-MS vial and analyzed with MS2 scan mode for the detection of all possible m/z ions. (**Figure 3.15**)

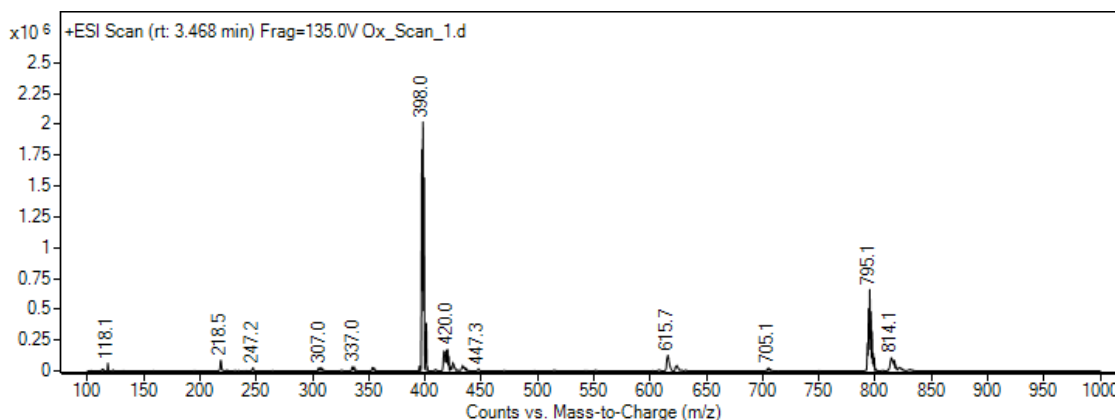


Figure 3. 15. Positive mode ESI scan result of oxaliplatin neat solution in water.

With a molecular weight of 397.29 g/mol, the expected $[M+1]^+$ ion is 398 m/z which was clearly observed following the MS2 scan of the sample. Due to the isotopic

breakdown of platinum with major isotopes of ^{194}Pt , ^{196}Pt , and ^{198}Pt , the 397, 399, and 401 ions are also observed with the 399 ion being the next most abundant.

Interestingly, the third most abundant m/z ion detected is 795.1 which based upon the similar trend observed with carboplatin was determined to be the dimer form of oxaliplatin. (**Figure 3.16**)

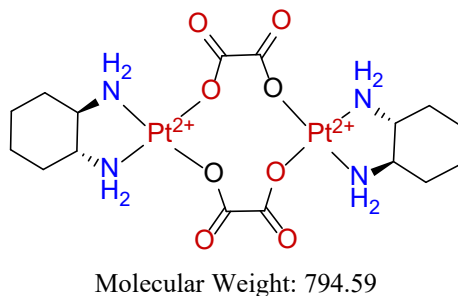


Figure 3. 16. Dimerized structure of two oxaliplatin molecules.

To further delineate fragmentation patterns of oxaliplatin for the development of an MRM detection method, a product ion scan was conducted using the 398 and 399 m/z ions as the precursor ion choice with a broad product ion scan range from 100-1,000 using a 25 kV collision energy. (**Figure 3.17** and **3.18**)

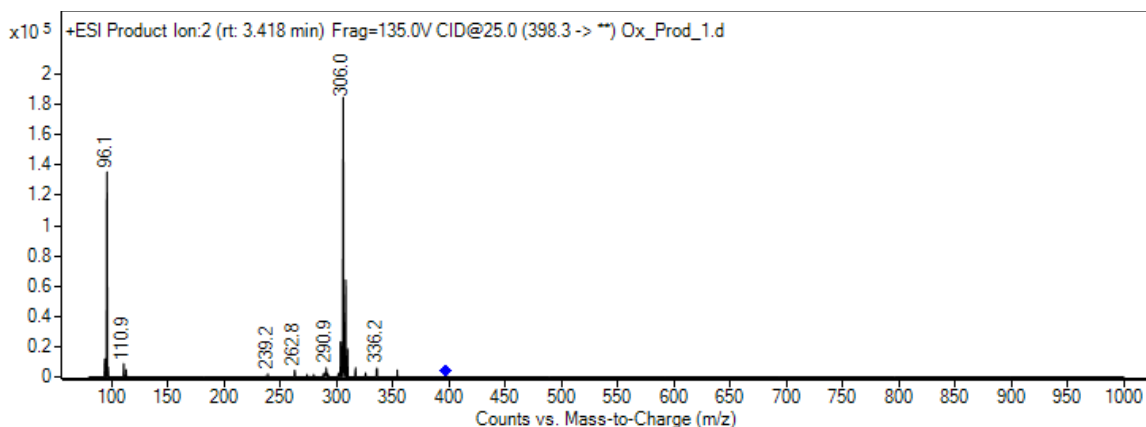


Figure 3. 17. Resulting product ion scan of oxaliplatin using the 398 m/z precursor ion and 25 kV collision energy.

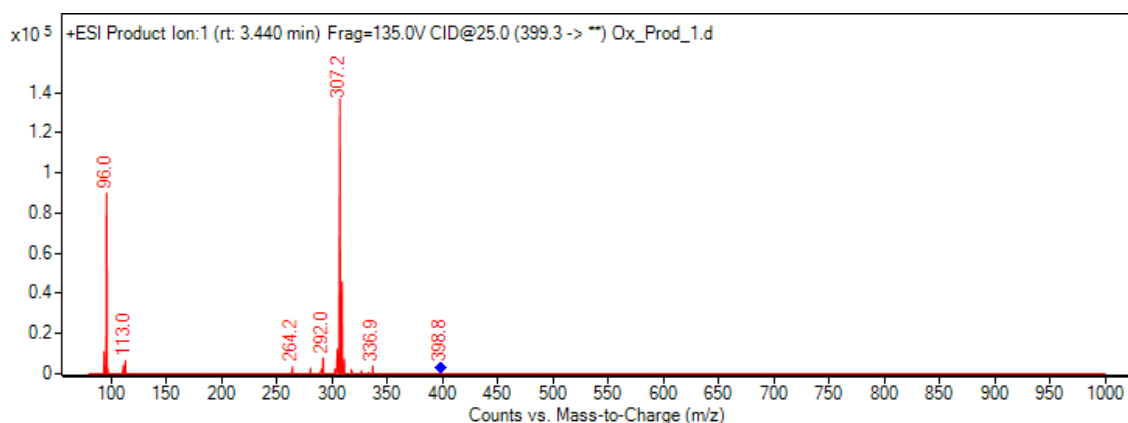


Figure 3. 18. Resulting product ion scan of oxaliplatin using the 399 m/z precursor ion and 25 kV of collision energy.

Similar to results reported by Gao et al, when fragmented, the most abundant precursor ion of 398 m/z yields the prominent product ions of 306 m/z and 96 m/z. In the published literature by Gao et al, it is indicated that the loss of -2HCOOH molecules from the precursor ion and subsequent formation of a Schiff base forms the 306 m/z product ion.⁹ (Figure 3.19)

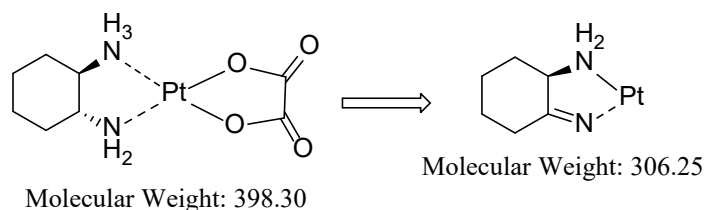


Figure 3. 19. Fragmentation pattern of oxaliplatin to the formation of a Schiff base product ion.

Cisplatin

A neat solution of cisplatin SRM was prepared at a concentration of ~80 µg/g in water. An aliquot of the prepared solution was filtered through a 0.45 µm syringe filter into an LC-MS vial for analysis in MS2 scan mode for the detection of all possible m/z ions.

As seen in **Figure 3.20**, several potential ions are observed, lending cisplatin as the most complicated platinated drug analyte in solution to develop an LC-MS/MS method for.

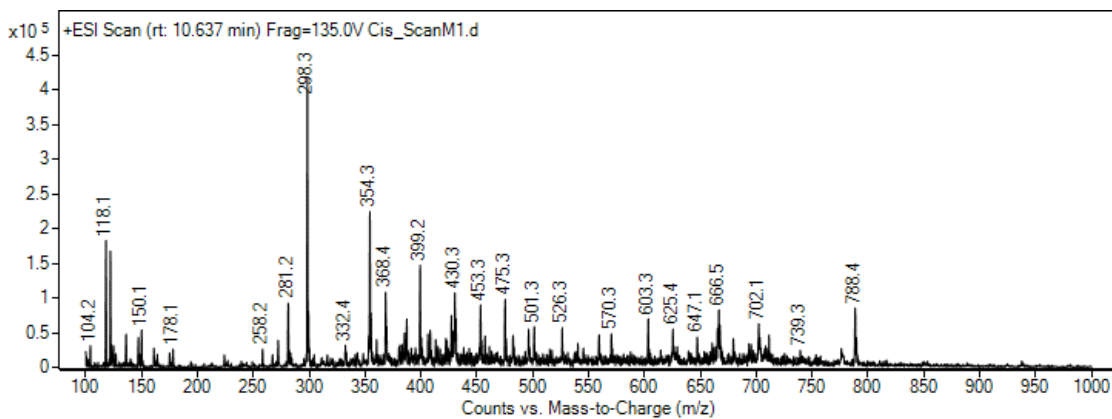


Figure 3. 20. Positive mode ESI scan result of cisplatin neat solution in water.

With an exact mass of 298.96 g/mol, the expected $[M+1]^+$ ion is 299 m/z. Due to the isotopic breakdown of platinum with major isotopes of ^{194}Pt , ^{196}Pt , and ^{198}Pt , additional precursor ions include 298, 300, and 301 m/z. The most abundant ion upon immediate analysis of the cisplatin solution shows the 298 ion is most abundant, eluting from the column around 10.6 minutes.

As described by several literature resources, however, cisplatin non-enzymatically exchanges chlorine ligands for water ligands.^{1-3, 6} These water ligands can then subsequently oxidize to form a hydroxyl group, leading to an array of potential structures for the detection of cisplatin species. (**Figure 3.21**)

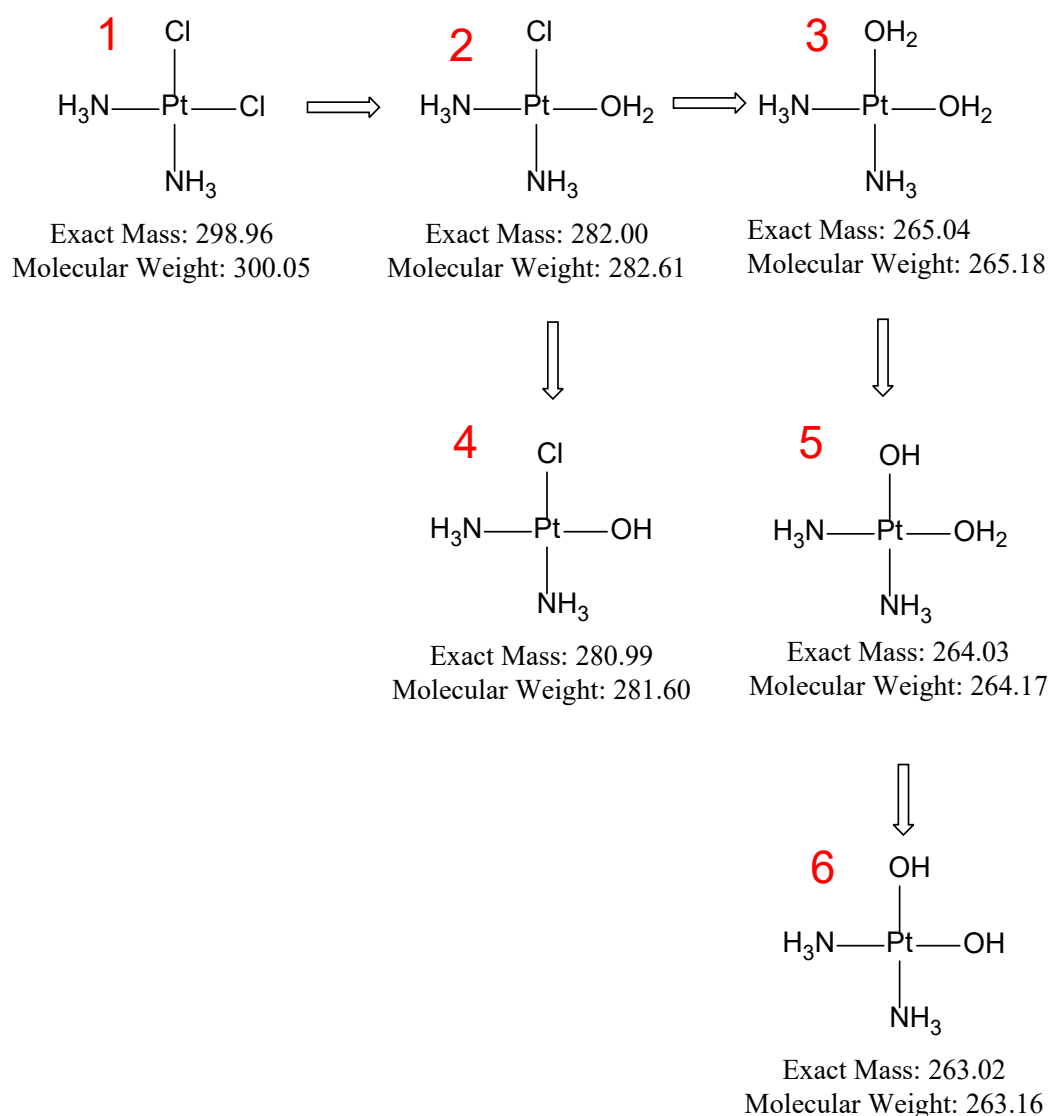


Figure 3. 21. Aquation and subsequent oxidation of cisplatin in water solution.

After the solution was permitted two days of resting at room temperature, another broad MS2 scan was performed, yielding very different results. Instead of a single peak at ~10.6 minutes, prominent signal was observed at 1.4 minutes as well. Mass spectrum results were extracted from the signal produced at these retention times. (**Figures 3.22 and 3.23**)

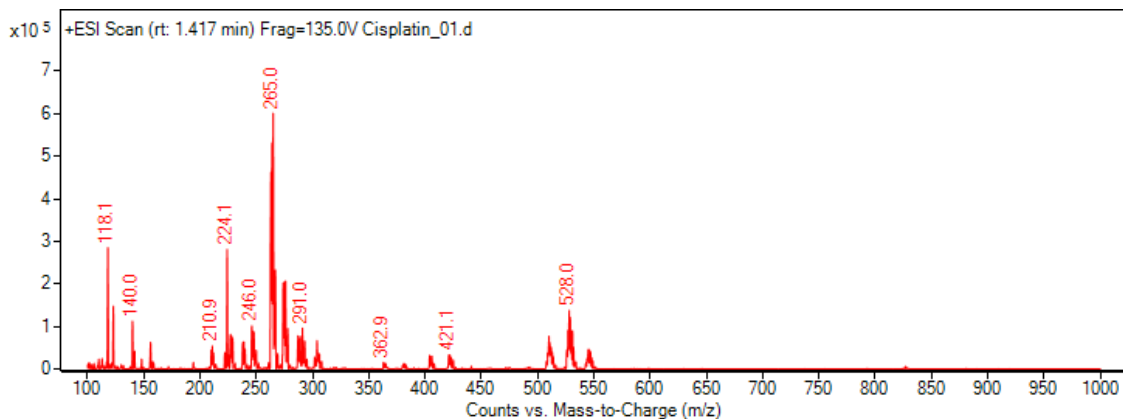


Figure 3. 22. Extracted mass spectrum of the signal observed upon MS2 scan analysis of cisplatin SRM in water at 1.4 minutes.

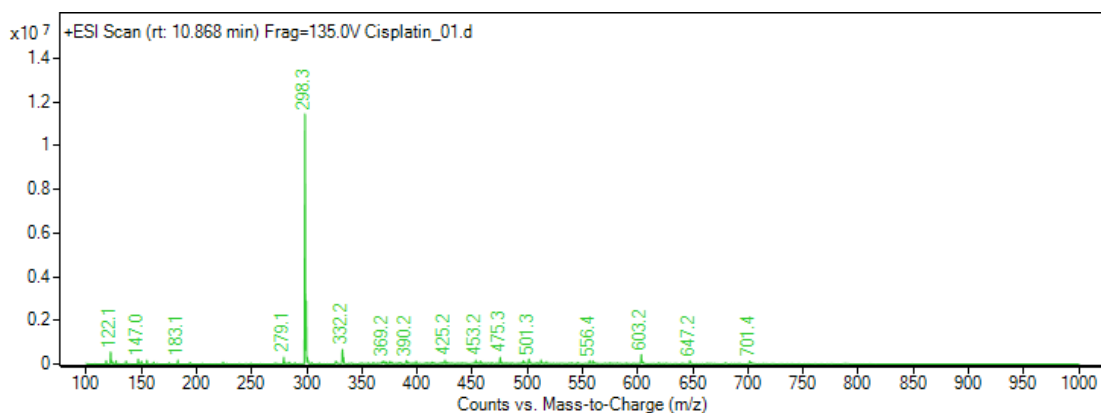


Figure 3. 23. Extracted mass spectrum of the signal observed upon MS2 scan analysis of cisplatin SRM in water at 10.8 minutes.

The proposed aquated structures of cisplatin shown in **Figure 3.21** show the progression of cisplatin's reaction in a solution of water given time and dependent on the concentration of chlorine ions in solution. When chlorine ion presence is very low and time has been allowed for the exchange of chloro and water ligands, literature and experimental results indicate that structure 3 becomes more and more predominant, with a m/z of 265. Until full conversion to the aquated form has occurred, presence of the original cisplatin compound is still observed. Given the increased polarity of the aquated structure, the earlier

elution for structure 3.21.3 and later elution for structure 3.21.1 experimental results matches theoretical expectations.

The development of an MRM method for detection of cisplatin was more involved than that of carboplatin and oxaliplatin given the lack of literature resources developing an MRM technique. Product ion scans were conducted for the precursor ions 298 and 299 at varying collision energies to determine an optimal fragmentation pattern for the compound.

(Table 3.1)

Table 3. 1. Product ion scan results for the two primary precursor ions of cisplatin.

Precursor Ion (m/z)	Collision Energy (kV)	Retention Time (min)	Peak Area (counts)	Abundant Product Ions (m/z)
298	10	2.360	502509	288.1, 252.2, 180.9, 130.2
	15	2.368	256477	288.3, 177.2, 130.2
	25	2.360	152083	288.0, 200.0, 180.6, 155.9, 130.0
	30	2.338	194554	256.1, 180.8, 154.1, 109.2
	45	2.331	117054	135.3, 108.8
299	10	2.375	487727	290.8, 257.1, 211.0, 180.9, 130.2
	15	2.353	291031	287.8, 257.0, 211.2, 130.0
	25	2.375	106863	256.7, 211.1, 131.2, 108.9
	30	2.383	112813	211.2, 185.0, 154.2, 109.3
	45	2.345	43242	156.0, 108.1

Through the piece-wise fragmentation of each individual ligand on the cisplatin compound, several potential product ions include: 281.93, 264.90, 263.99, 246.96, 229.93, 229.02, 211.99, and 194.96 m/z. **(Figure 3.24)** The most consistently observed product ions from the experimental results was the fragmentation of 299 m/z to 211 m/z or 257 m/z, with 257 m/z being the most abundant of the two at lower collision energies and 211 m/z more abundant at higher collision energies.

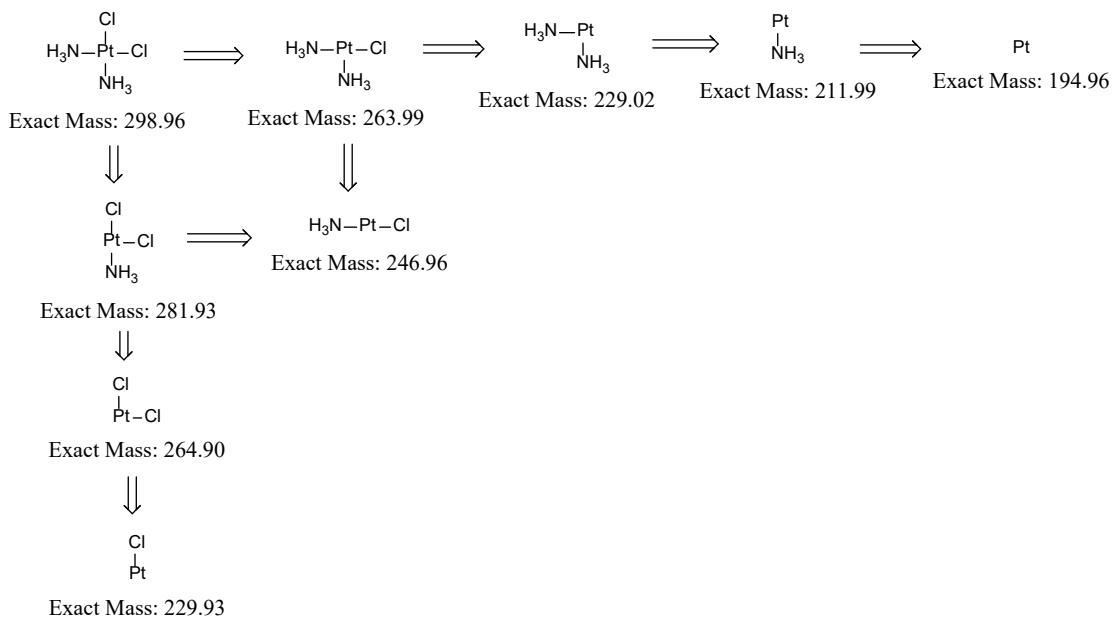


Figure 3. 24. Fragmentation pattern of cisplatin.

An initial MRM method was designed for the detection of all platinated drug compounds simultaneously, which tracked for cisplatin using $298 \rightarrow 130.2$ (180.9) and $299 \rightarrow 257.0$ (109.0) fragmentation patterns. However, these MRM transitions did not yield observable signal. Using other product ion choices for cisplatin, a second MRM method was designed, which was able to achieve signal for the cisplatin compound. (**Table 3.2**)

Table 3. 2. Proposed MRM detection method for all platinated drug compounds simultaneously.

Compound	Precursor Ion (m/z)	Product Ion(s) (m/z)	Collision Energy
Cisplatin	301.1	240.2, 109.1	25
	299.6	187.1, 159.2	
	266.2	210.0, 193.9	
Carboplatin	372.3	263.7	
	373.3	230, 249, 295	
Oxaliplatin	398.3	96.1, 306	
	399.3	96, 264.2, 292, 307.2	

An important aspect of an analytical method for the detection of a target analytes is determining the LOD and LOQ of said method, which is determined through the use of a calibration curve and subsequent calculations, as described in Chapters 1 and 2. A series of standards containing decreasing concentrations of carboplatin, oxaliplatin, and cisplatin were generated and analyzed using the above method to determine LOD and LOQ, which were all well below the levels expected from an analytical sample derived from a patient's blood or urine, according to literature. (**Table 3.3**)

Table 3. 3. LOD and LOQ for platinated drug compounds analyzed on the LC-QQQ-MS.

Compound	R²	LOD (µg/g)	LOQ (µg/g)
Cisplatin	0.9985	0.122 +/- 0.068	0.369 +/- 0.205
Carboplatin	0.9500	0.327 +/- 0.012	0.991 +/- 0.037
Oxaliplatin	0.9318	0.268 +/- 0.001	0.812 +/- 0.002

Conjugation Studies

Although carboplatin and oxaliplatin have been synthesized to conceal themselves from bodily detection, decreasing the rate of elimination greatly to promote anticancer activity, these two platinated compounds act more slowly and require longer treatment cycles.¹⁰ Likewise, because each compound can evade the immune systems detection, the downstream bodily impact regarding sequestration is not well understood. For this reason, cisplatin is still the preferred platinated drug used in oncological treatment.¹² Therefore it is important to understand the chemistry taking place in the body when cisplatin is introduced, mainly the formation of conjugated species.

Researchers who currently study cisplatin treatment in oncological patients typically assess biological fluids for total platinum concentrations, while avoiding

speciated quantification of conjugate forms.^{13, 14} Glutathione is one of the main biological nucleophiles that works to conjugate platinum metal in the body, seeing it as a foreign substance.¹⁵

Solutions of cisplatin in water and reduced glutathione in water were prepared at 10 and 100 ug/g, respectively. These solutions were mixed at 1:1 volumetric proportion and incubated in a water bath at 32 °C for an hour. Samples were retrieved from the water bath and filtered through a 0.45 um syringe filter into an LC-MS vial for analysis on the LC-QQQ-MS using a broad MS2 scan mode. Several peaks with major signal were observed at 1.171, 2.024, and 2.359 minutes while minor peaks were observed at 1.339, 1.439, and 1.573 minutes. **(Figure 3.25)**

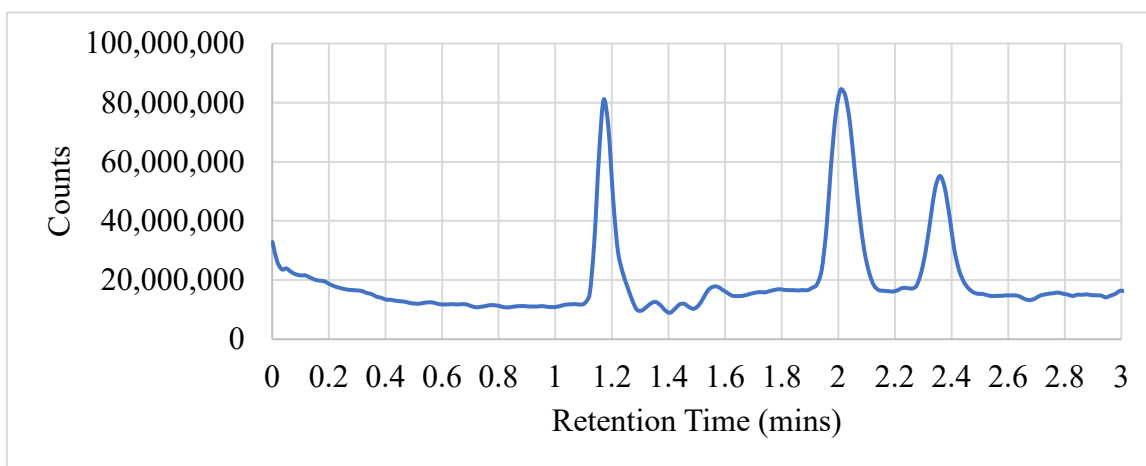


Figure 3. 25. Chromatographic results of broad MS2 scan for incubated cisplatin+GSH sample on the LC-MS/MS.

Mass spectrum results were extracted from each peak signal. **(Figures 3.26 to 3.31)**

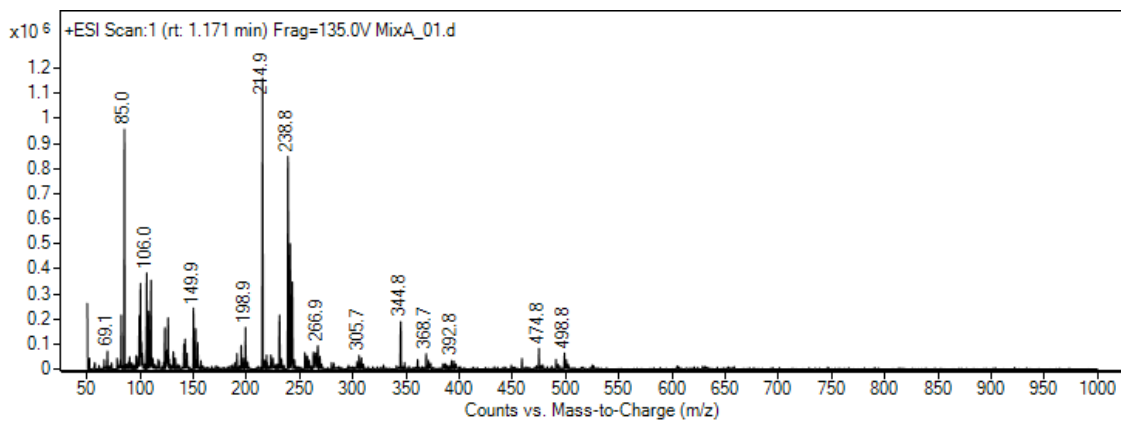


Figure 3. 26. Mass spectrum extracted from the peak signal at 1.171 minutes.

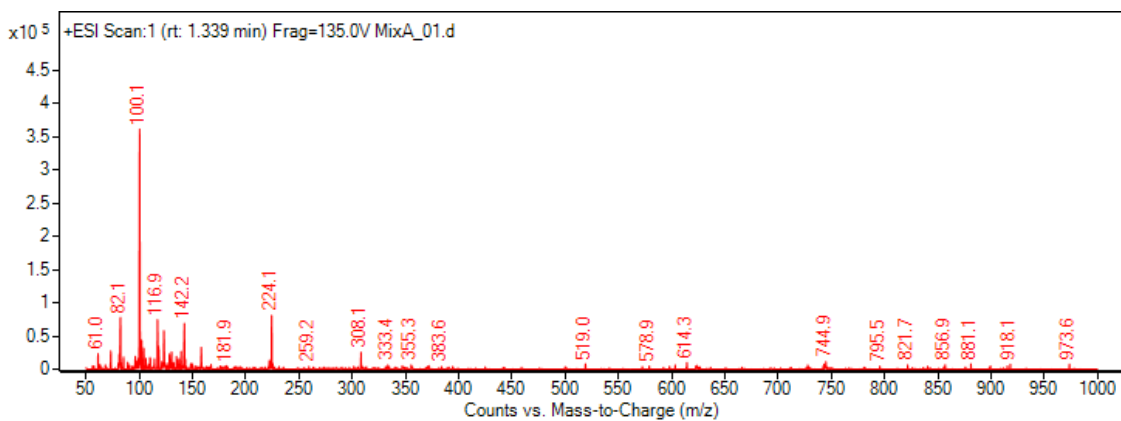


Figure 3. 27. Mass spectrum extracted from the peak signal at 1.339 minutes.

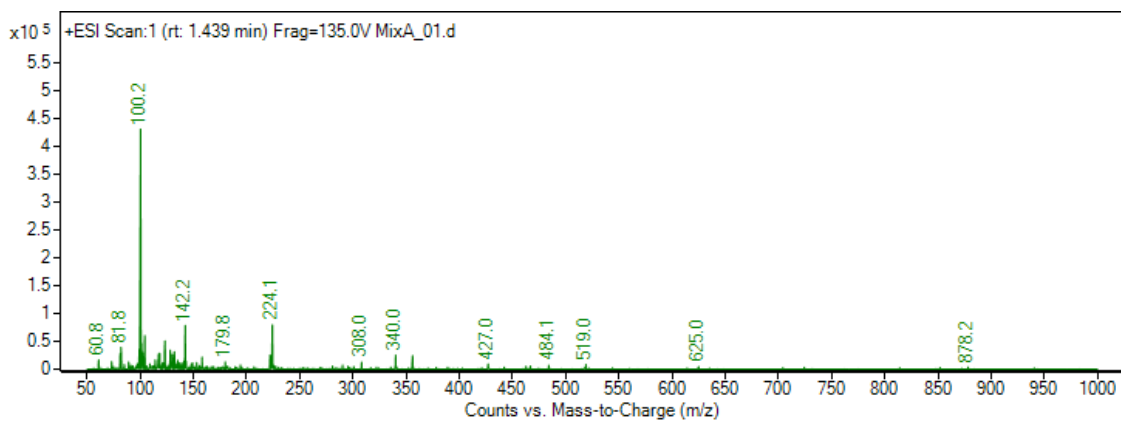


Figure 3. 28. Mass spectrum extracted from the peak signal at 1.439 minutes.

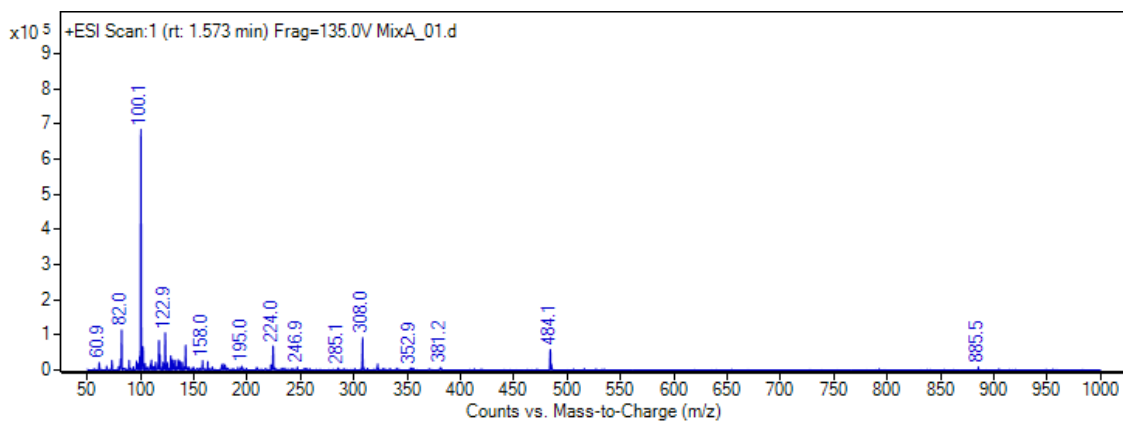


Figure 3. 29. Mass spectrum extracted from the peak signal at 1.573 minutes.

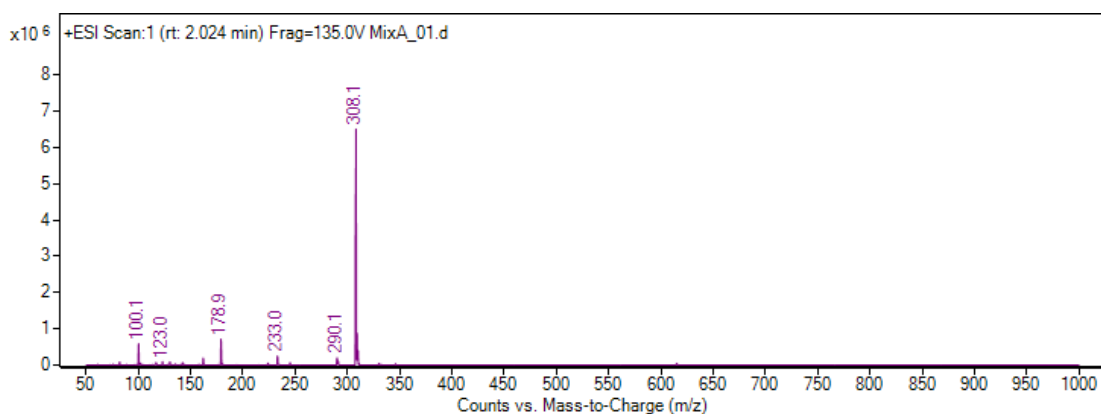


Figure 3. 30. Mass spectrum extracted from the peak signal at 2.024 minutes.

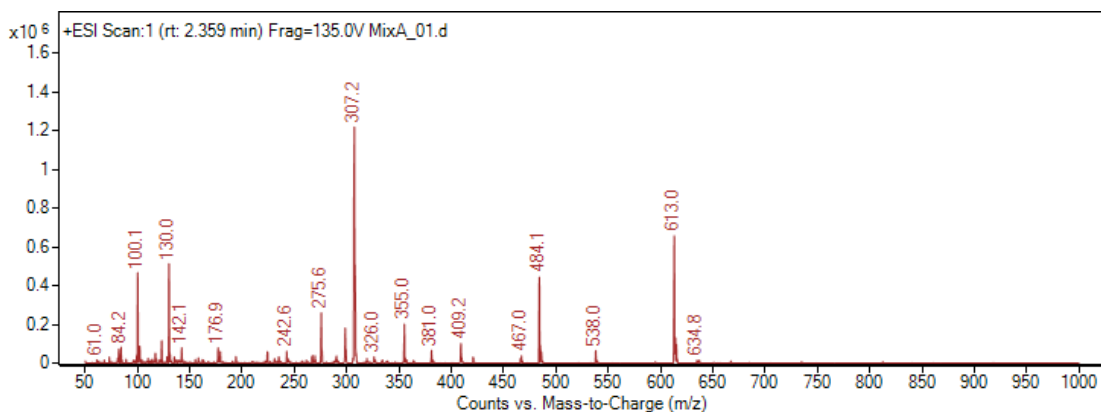


Figure 3. 31. Mass spectrum extracted from the peak signal at 2.359 minutes.

The first potential conjugate species is the singly conjugated Pt ion with one reduced glutathione molecule. Given the tripeptide nature of glutathione, the weakest bonds are the peptide bonds, likely to fragment first, followed by loss of amine groups, and further breakdown of the structure. **(Figure 3.32)** The loss of each amino acid group should demonstrate an ion corresponding to the amino acids m/z along with the ion associated to the platinum bound portion. Platinum can also be doubly conjugated by two glutathione molecules which will follow a similar trend in the fragmentation pattern. **(Figure 3.33)**

The peaks observed at retention times of 2.024 and 2.359 minutes are indicative of glutathione in its reduced and oxidized form, respectively, confirmed by the mass spectrum signature extracted at each time. **(Figures 3.30 and 3.31)** The large presence of these peaks was expected, given reduced glutathione was added in excess concentration to that of the cisplatin, and with time glutathione will auto-oxidize to its dimer form. This leaves the final large peak at 1.171 minutes as the only highly abundant signal not clearly or explicitly assigned to a given structure based on previous knowledge.

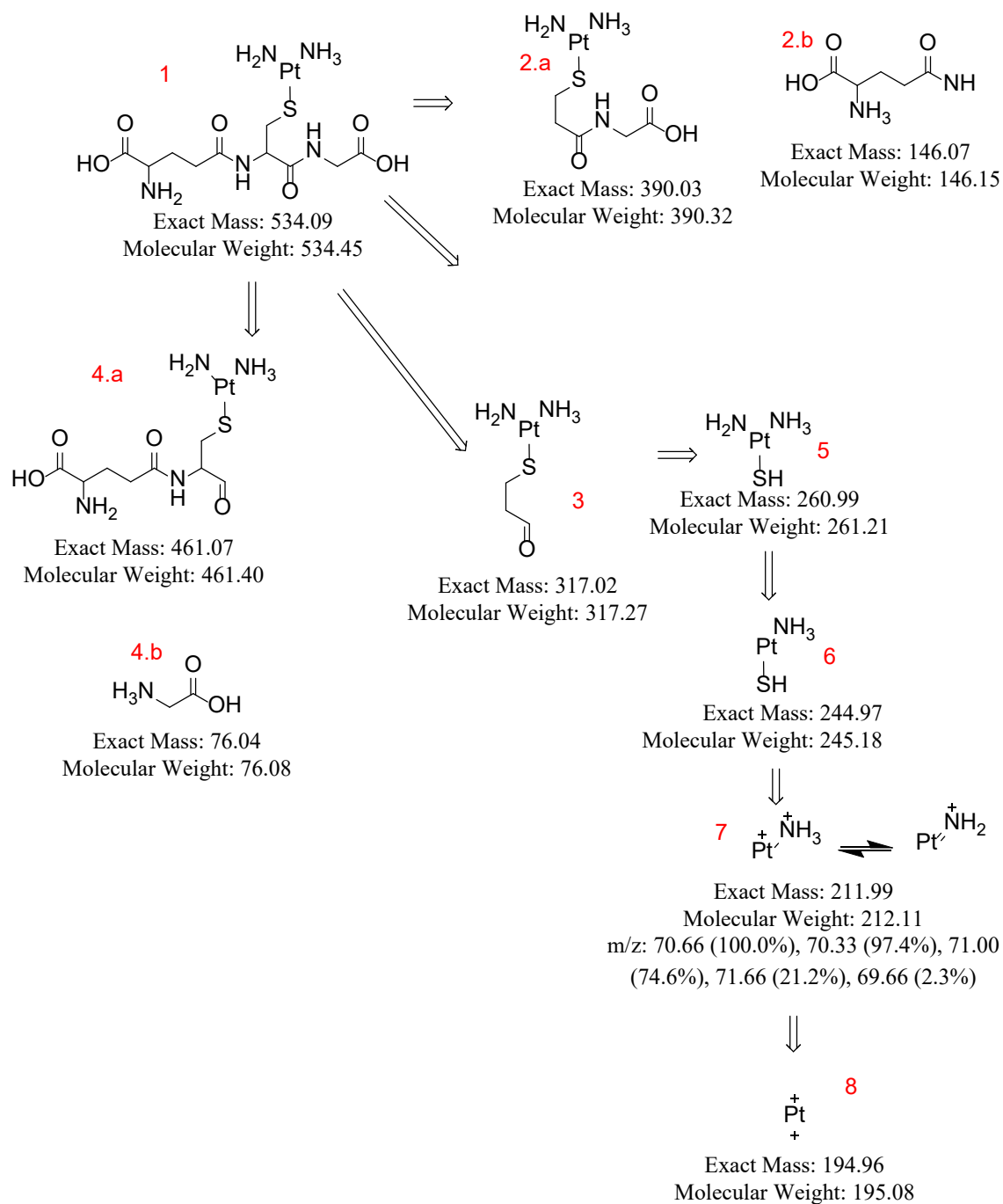


Figure 3. 32. Potential fragmentation pattern of singly conjugated platinum to glutathione.

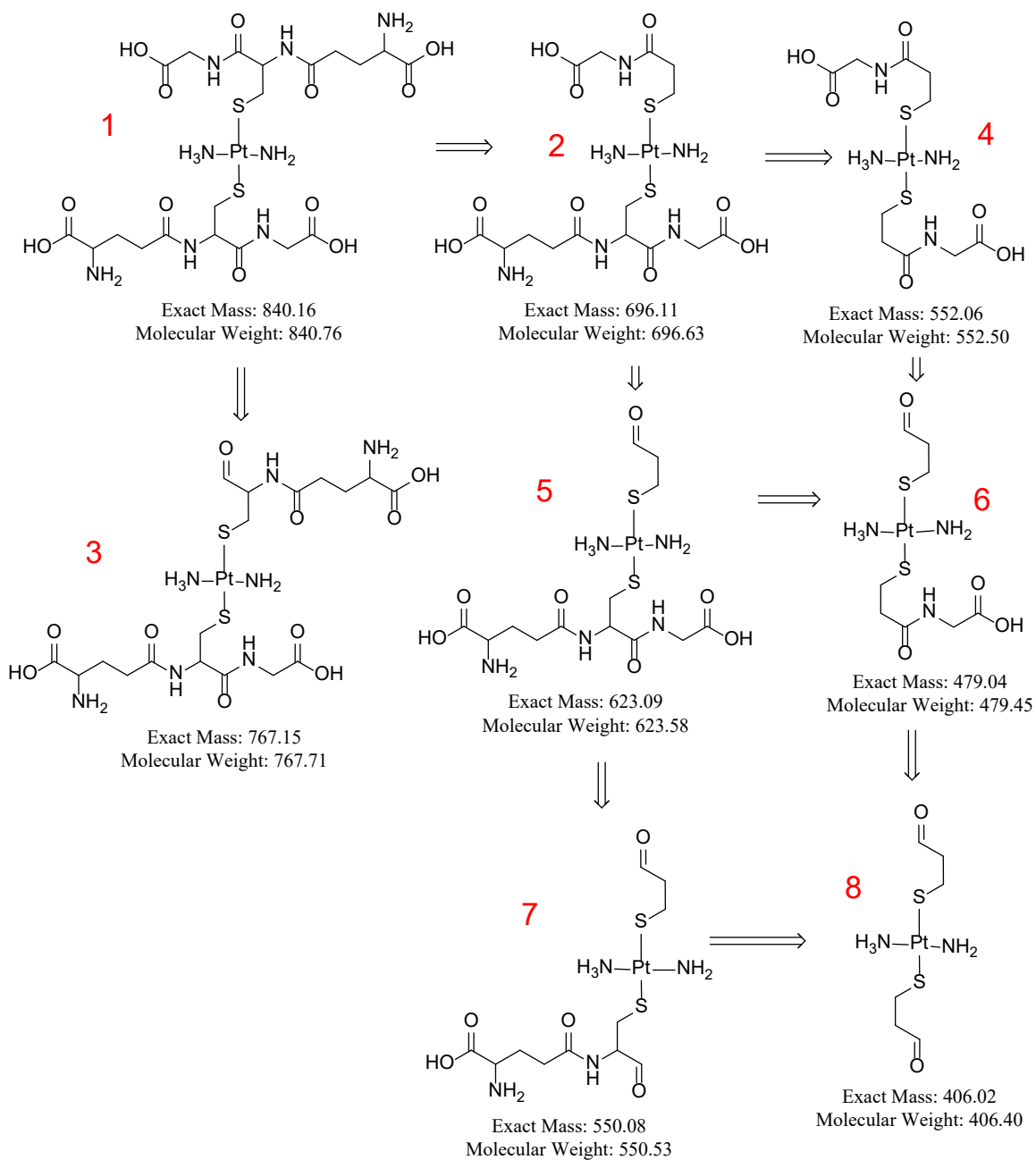


Figure 3.33. Potential fragmentation pattern for doubly conjugated platinum with glutathione.

Because platinum has six isotopes, identification of m/z ions corresponding to each proposed structure can be identified confidently through the presence of all six respective m/z ions. (Table 3.4) The most abundant platinum isotopes are 194, 195, and 196 at 34%, 33%, and 28% abundant. Therefore the $[M-1]^+$, $[M]^+$, and $[M-1]^+$ ions should be most

abundant with small abundance of the $[M-5]^+$, $[M-3]^+$, and $[M+3]^+$ ions. It should also be noted that carbon's C-13 isotope as well as nitrogen's N-15 isotope can potentially shift the mass by 1 per every carbon or nitrogen with a C-13 or N-15 signature present in the molecular structure. However, the abundance of C-13 is 1% naturally and N-15 is even less abundant at 0.37% naturally occurring and therefore both should be a very minor representation for any shifts in mass. The presence of several amine functional groups also lends the way for different sites of protonation, potentially leading to doubly or triply positively charged species.

All ion abundance data for extracted mass spectrum at each retention time was exported to a CSV file to view all low and high abundant ions. This data was used to match up potential structures of the fragmentation patterns of different conjugated species. (**Table 3.5**)

Table 3. 4.Fragmentation ions for each proposed structure of singly and doubly conjugated platinum with glutathione. (F=Figure, C=structure assignment number)

Compound	Precursor Ion – Natural 195Pt	Isotopic Ions for Platinum Isotopes
F3.32_C1	534.1	529, 531, 533, 535, 537
F3.32_C2.a	390.0	385, 387, 389, 391, 393
F3.32_C2.b	146.1	141, 143, 145, 147, 149
F3.32_C3	317.0	312, 314, 316, 318, 320
F3.32_C4.a	461.1	456, 458, 460, 462, 464
F3.32_C4.b	76.0	71, 73, 75, 77, 79
F3.32_C5	260.9	255, 257, 259, 261, 263
F3.32_C6	244.9	239, 241, 243, 245, 247
F3.32_C7	211.9	206, 208, 210, 212, 214
F3.32_C8	194.9 (singly charged)	189, 191, 193, 195, 197
	97.4 (doubly charged)	92, 94, 96, 98, 100
F3.33_C1	840.2	835, 837, 839, 841, 843
F3.33_C2	696.1	691, 693, 695, 697, 699
F3.33_C3	767.2	762, 764, 765, 768, 770
F3.33_C4	552.1	547, 549, 551, 553, 555
F3.33_C5	623.1	618, 620, 622, 624, 626
F3.33_C6	479.0	474, 476, 478, 480, 482
F3.33_C7	550.1	545, 547, 549, 551, 553
F3.33_C8	406.0	401, 403, 405, 407, 409

Table 3. 5. Extracted mass spectral data for the signal observed at 1.171 minutes.

Retention Time for Extracted Mass Spectral Data = 1.171 minutes		
Compound	Identified Ions (m/z)	Counts
F3.32_C1	529.6	628
	531.0	4,885
	533.3	4,651
	534.9	1,796
	535.1	702
	537.2	2,166
F3.32_C2.a	385.0	9,907
	387.7	15,369
	389.9	3,546
	390.7	13,257
	391.0	4,425
	393.0	18,321
F3.32_C2.b	141.9	102,298
	143.2	14,719
	145.0	11,392
	146.1	9,613
	147.0	4,346
	149.9	244,563
F3.32_C3	312.9	2,961
	314.5	10,644
	316.3	1,324
	317.0	396
	318.6	10,165
	320.6	3,377
F3.32_C4.a	456.7	1,729
	458.8	43,368
	460.8	6,292
	461.7	1,088
	462.9	9,029
	464.9	7,276
F3.32_C4.b	71.9	1,331
	73.0	22,297
	75.0	123
	76.9	407
	77.9	31,251
	79.8	15,038
F3.32_C5	255.9	12,349
	257.0	51,705
	259.0	23,756
	260.7	13,449
	261.0	2,816

	263.0	56,151
F3.32_C6	239.0	723,666
	241.9	98,978
	243.9	8,805
	244.9	38,844
	245.6	5,468
	247.7	5,984
F3.32_C7 (singly charged)	206.9	1,141
	208.9	6,459
	210.6	11,829
	211.0	6,995
	212.9	9,822
	214.9	1,162,277
F3.32_C7 (doubly charged)	103.0	6,141
	104.0	22,549
	105.7	270,940
	106.0	384,590
	107.9	232,486
F3.32_C8 (singly charged)	189.0	18,419
	191.0	52,826
	193.1	14,258
	194.8	95,655
	195.0	78,745
	197.0	44,522
F3.32_C8 (doubly charged)	92.2	24,384
	94.0	16,709
	96.8	11,405
	97.9	49,923
	98.0	50,796
	100.1	342,873
F3.33_C1	834.4*	3,337
	838.3*	3,950
	839.6	1,585
	840.5	588
	841.2	2,037
	842.8*	155
F3.33_C2	690.7	582
	692.8*	4,983
	694.6*	7,257
	696.4	1,646
	697	n/a
	699.5	2,223
F3.33_C3	762.3	3,957
	764.5	3,188
	766.3	5,987

	767.2	1,945
	768.6	458
	770.7	2,424
F3.33_C4	547.8	1,127
	549.0	2,457
	551.0	158
	552.4	3,359
	553.0	535
	555.0	349
F3.33_C5	618.9	4,637
	620.9	10,021
	622.1	1,761
	623.3	1,716
	624.2	8,448
	626.5	871
F3.33_C6	474.8	83,682
	476.7	16,352
	478.6	17,541
	479.0	4,145
	480.4	3,865
	482.7	10,610
F3.33_C7	545.9	265
	547.8	1,127
	549.0	2,457
	550.5	3,284
	551.0	158
	554.9	565
F3.33_C8	400.8*	10,139
	404.8*	6,858
	405.0	4,149
	406.0	891
	407.5	763
	409.0	2,035

-
- The proposed parent ion displayed no observable signal from baseline, but mass shifted -1 or +1 showed significant signal.

All six proposed ions for each structure in the suggested fragmentation pattern were observed except for one ion (697 m/z) for F3.33_C2. This denotes the likely presence of each suggested compound in the fragmentation pattern. Unsurprisingly, structure F3.32_C2.b and F3.32_C4.b (the structures of glutamate and glycine ions) are observed in

higher abundance, likely due to the fact they can be derived from any conjugated species as well as reduced or oxidized glutathione structures. The ions with the highest observed counts at 1,162,277 counts was derived from the 214.9 m/z ion of F3.32_C7. Regarding the isotopic breakdown of Pt, the 214.9 m/z ion corresponds to the Pt-198 isotope with an abundance of only 7.4%. Counts in the millions for this isotope, while the other five isotope ions are much lower does not align with the expected outcome, inducing doubt of the ions presence.

Using the ChemDraw software library of spectral interpretation, suggested m/z values for F3.32_C7 were calculated to be 104, 105, 106, and 107 m/z. For the molecular weight of the natural compound at 212 g/mol with a double charge, the expected ion of highest abundance is 106 m/z, which is confirmed by the mass spectral data.

For the singly conjugated species, the platinum center can also form an additional bond with a chlorine ligand, aqua ligand, or hydroxyl ligand. This bond formation would shift the mass of the compound by 35.4, 18, or 17 amu, respectively. This phenomenon is observed for each ligand listed, with respective ions of up shifted mass observed in the spectral data.

Examining the mass spectral data for the smaller peaks at 1.3, 1.4, and 1.5 minutes shows decreased abundance of ions corresponding to the singly conjugated platinum-glutathione species, while the abundance of fragment ions for the doubly conjugated species intensifies. The spectral data for the peak at 1.5 minutes shows the highest abundance for the in-tact doubly conjugated species, F3.33_C1, while showing little fragment ions.

Given the outcome of the spectral results, it is likely that bare unconjugated aquated cisplatin and its singly conjugated species to glutathione, elute around 1.1-1.3 minutes and are more abundant than the doubly conjugated species, which is proposed to elute around 1.4-1.5 minutes. These species are separated via chromatography from the two species of glutathione, reduced and oxidized, which elute at 2 and 2.3 minutes, respectively.

Method Development – ICP-MS Analysis

Instrument parameters were set as the following: RF power at 1550 W, RF matching at 1.80 V, sample depth at 8.0 mm, nebulizer gas flow at 0.82 L/min, nebulizer pump at 0.10 rps, makeup gas flow at 0.40 L/min, and octupole RF at 200 V. Platinum isotopes tracked during analysis included 190, 192, 194, 195, 196, and 198.

Instrumental Performance of ICP-MS Analysis for Platinum

Initial assessment of instrument capability for detecting platinum isotopes included the preparation of several cisplatin standards from the SRM at decreasing concentrations in water solution as well as natural platinum metal CRM at decreasing concentrations in a 0.1% HNO₃ solution. Samples were analyzed using the previously discussed method to generate calibration curves, **Figure 3.34** and **3.35**, and determine LOD and LOQ. (**Table 3.6**)

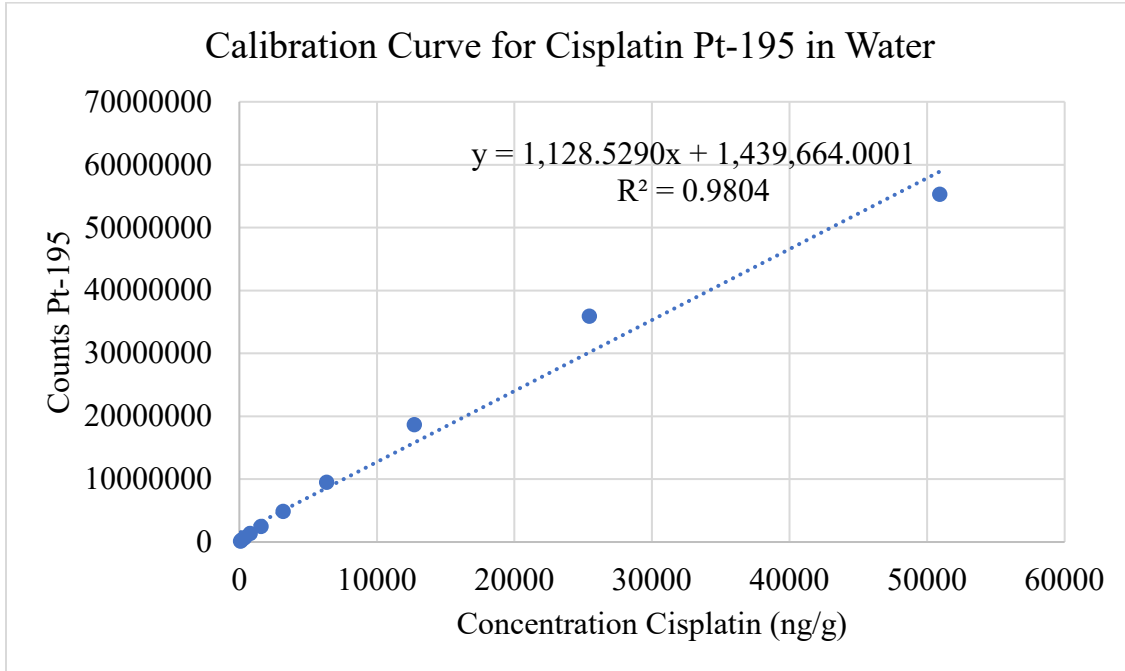


Figure 3. 34. Calibration curve for analysis of ¹⁹⁵Cisplatin standard solutions in water on the ICP-MS.

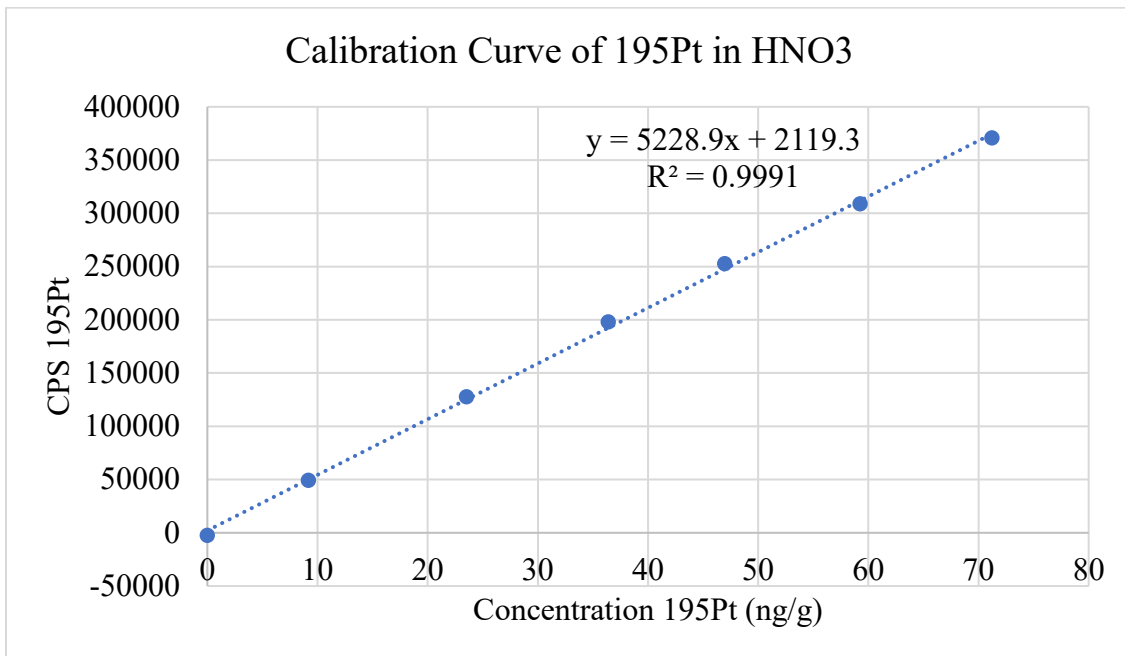


Figure 3. 35. Calibration curve for the analysis of ¹⁹⁵Pt standard solutions in HNO₃ on the ICP-MS.

Table 3. 6. LOD and LOQ determinations for total platinum content from cisplatin and platinum metal analysis on the ICP-MS

Analyte	R ²	LOD (ng/g)	LOQ (ng/g)
Cisplatin	0.9804	0.1642 +/- 0.002	0.4974 +/- 0.006
195-Pt	0.9991	2.863 +/- 0.125	8.676 +/- 0.378

From these results, isotopic abundances for all six platinum isotopes were able to be calculated and compared to reported IUPAC known isotopic abundances. (Table 3.7)

Table 3. 7. Abundance determinations for the six platinum isotopes following ICP-MS analysis of cisplatin and 195-Pt metal in solution.

Isotope	Known Abundance	Abundance for Cisplatin	%Error from Known	Abundance for 195-Pt	%Error from Known
Pt-190	0.014	0.0126	10.1%	0.0130	7.0%
Pt-192	0.782	0.794	1.5%	0.7887	0.9%
Pt-194	32.97	33.08	0.3%	34.81	5.6%
Pt-195	33.83	34.02	0.6%	33.09	2.2%
Pt-196	25.24	25.00	0.9%	24.37	3.5%
Pt-198	7.163	7.090	1.0%	6.928	3.3%

With an instrumental method capable of detecting the target analyte, the next focus was to recertify the isotopically enriched standard purchased by the laboratory over a decade prior. CRM of enriched 194-Pt metal was purchased and prepared in a solution of 0.5% HNO₃ (aqueous) by previous lab members of the Kingston research group. (194-Pt at 96.54% isotopic purity, Company: AIT, Batch#: 186243, Lot#: PT12162008A) This prepared solution was originally certified at 1,246.9024 +/- 5.9754 µg/g, but the certification expired in 2012. To recertify the solutions concentration of enriched 194-Pt, RIDMS was used utilizing a naturally pure 195-Pt solution. An aliquot of the isotopically enriched solution was diluted and analyzed in replicates of six for the determination of

isotopic abundance. (Table 3.8) Results of this analysis indicate isotopic purity has not changed with the abundance of 194-Pt at 96.54%.

Table 3. 8. Abundance determination for isotopically enriched 194-Pt solution following ICP-MS analysis.

Isotopically Enriched Solution Abundances						
	190 Pt	192 Pt	194 Pt	195 Pt	196 Pt	198 Pt
Avg	0.0000026	0.0002321	0.9654	0.0249	0.0080	0.0015
SD	0.0000001	0.0000017	0.0000437	0.0000522	0.0000758	0.0000139
95% CI	0.0000001	0.0000017	0.0000458	0.0000547	0.0000795	0.0000146

An aliquot of the stock isotopic solution was diluted by a factor of 100 to yield a final concentration of ~10 ug/g. Natural platinum CRM was diluted to yield a final concentration of 12.021 ug/g, and this was used to prepare four separate RIDMS samples which were analyzed in quadruplicate for determination of 194-Pt concentration with N=16. The determined concentration of concentrated stock 194-Pt solution was 1,136.5040 +/- 3.1030 ug/g and a coefficient of variance of 0.5%. The recertification of isotopic concentration was only 9.18% different from that of the original certification, which is within the acceptable +/-15% difference. The recertification of the isotopic spike solution permits the employment of IDMS quantification with the isotope.

Extraction of Platinum Content from Urine and Blood for Totals Quantification via ICP-MS Analysis

In preparation for future patient samples, extraction protocols for recovering platinum from blood and urine were researched and tested on a series of QC samples in respective matrices. Negative synthetic urine and negative synthetic blood were used to prepare three QC samples containing cisplatin at high, mid, and low range concentrations based on reported literatures values for expected concentration in blood or urine:

QC1_Blood @ 29.317 $\mu\text{g/g}$, QC2_Blood @ 23.578 $\mu\text{g/g}$, QC3_Blood @ 10.023 $\mu\text{g/g}$,
QC1_Urine @ 19.966 $\mu\text{g/g}$, QC2_Urine @ 16.862 $\mu\text{g/g}$, and QC3_Urine at 7.544 $\mu\text{g/g}$.

Microwave assisted acid digestion of the biological sample matrices was utilized to extract platinum for ICP-MS analysis. Approximately 0.500 g of analytical sample was weighed into a microwave vessel and spiked with 0.010 g of concentrated isotopically enriched solution at 1,136.5040 $\mu\text{g/g}$. To each vessel, 9 mL of concentrated HNO_3 , 1 mL concentrated HCl , and 1 mL concentrated H_2O_2 were added. The vessels were inverted several times to thoroughly mix before being placed in the Ethos UP high-performance microwave digestion system by Milestone. The microwave was set to ramp from 22 °C to 180 °C over 5.5 minutes time, then hold for 9.5 mins with a constant power of 1800 MW. Following digestion, samples were allowed to cool before placing transferring the contents of the vessel to centrifuge tubes and centrifuging the samples for 30 minutes at 3,300 rpm. Approximately 2 mL of the supernatant was filtered into a clean centrifuge tube through a 0.45 μm syringe filter and diluted to a final volume of 20 mL with water before instrumental analysis.

IDMS quantification was achieved by first applying the mass bias correction factor to the collected counts of each isotope of platinum. The mass bias sample provides correction for fluctuation from normal regarding isotopic abundances and is prepared by applying the designated extraction protocol to 0.5 g of natural ^{195}Pt solution. The error of calculated abundance from known isotopic abundance were used in decimal form, multiplied to each of the counts for the respective isotope. Mass bias corrections factors for ^{194}Pt and ^{195}Pt were determined to be 0.01805 and 0.02204, respectively. The

corrected data is then processed with IDMS mathematics, **Equation 3.1**, to determine the concentration of total ¹⁹⁵Pt in the sample. (**Table 3.9**)

$$C_x = \frac{C_s W_s}{W_x} \left(\frac{{}^{194}A_s - R_{194} \frac{{}^{195}A_s}{195}}{R_{194} \frac{{}^{195}A_x}{195} - {}^{194}A_x} \right)$$

Equation 3. 1. IDMS equation for quantification of cisplatin.

Table 3. 9. IDMS results of extracted biological samples.

IDMS Quantification Error Analysis			
Sample	Theoretical Cisplatin Conc (µg/g)	Calculated Cisplatin Conc (µg/g)	%Error
Urine_1	19.966	16.437	17.7%
Urine_2	16.862	11.244	33.3%
Urine_3	7.544	3.179	57.9%
Blood_1	29.317	34.031	16.1%
Blood_2	23.578	28.371	20.3%
Blood_3	10.023	8.915	11.1%

IDMS quantification of cisplatin from blood and urine was done precisely with %CV between 0.4% and 1.0%, but the accuracy lacked with only QC3_Blood meeting acceptance of +/-15% error. Error for the blood extraction was lower than that associated with the urine extraction. This is likely due to the difference in biological matrix utilized. Urine is composed of around 95% water, and the remaining 5% is composed of salts, creatine, and acids. Whole blood is composed of 45% plasma and 55% red blood cells where the plasma contains 90% water, 7% protein, and 3% ions, salts, and small molecules. Extraction protocols for the microwave acid digestion of biological fluids vary the amount and type of acids utilized to properly digest the sample. It could be the case that the current

protocol employed is better suited for digestion of blood while another protocol may work better for the urine.

Calibration curve quantification of the 195-Pt concentration was also employed to compare to IDMS results. Nine standard solutions of cisplatin in water with concentration ranging from 0.1 to 25 ug/g were utilized to generate the calibration curve ($y=1,540,413.88x - 2,256.3383$; $R^2 = 0.9997$) then employed for quantification. (**Table 3.10**) The original set of ten standards included the highest concentration at 50 ug/g, but upon a Grubb's Test assessment of Standard #1's data results, it was determined to be an outlier at the 95% CI ($G_{\text{calc}} = 2.62 > G_{\text{table}} = 2.228$) and was therefore discarded from the curve.

Table 3. 10. Calibration curve results of extracted biological samples.

Calibration Curve Quantification Error Analysis				
Sample	Avg Conc 195-Pt (µg/g)	95%CI	%CV	%Error
Urine_1	23.983	0.955	4%	20%
Urine_2	19.200	0.362	2%	14%
Urine_3	10.093	0.304	3%	34%
Blood_1	25.443	2.198	9%	13%
Blood_2	22.180	0.329	1%	6%
Blood_3	12.437	1.050	8%	24%

Calibration curve quantification of cisplatin from extracted biological samples demonstrated acceptable precision with %CV between 1-8% for both matrix types. Acceptable accuracy was achieved for the higher QC samples in either matrix, while the lower concentration QC3 demonstrated higher error. Blood extraction yielded more accurate results than urine extraction, which correlates with the results seen in IDMS quantification.

IDMS quantification of cisplatin demonstrated very precise results with narrow uncertainty even at the 99% CI but lacked accuracy. (Figure 3.36) Calibration curve quantification showed improved accuracy while sacrificing some precision. Either of the methods of quantification would likely improve greatly with a more optimized extraction protocol for the biological matrices.

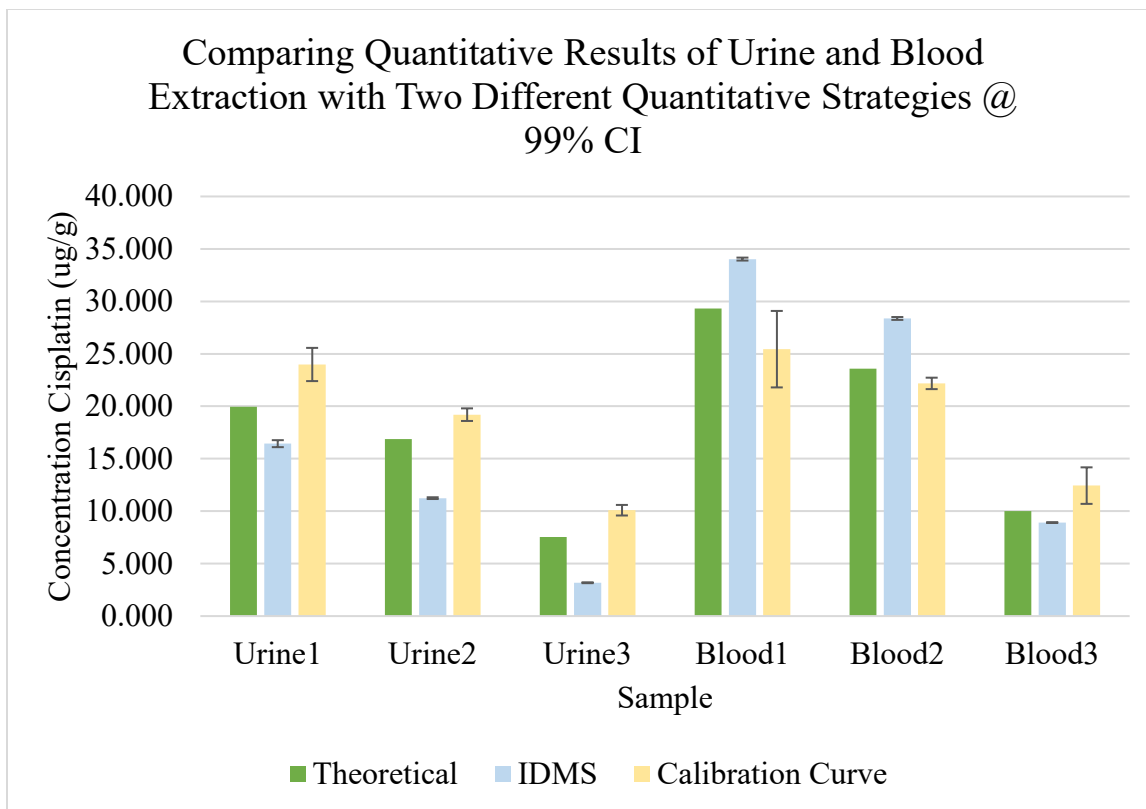


Figure 3. 36. Graphical comparison of the quantification of cisplatin following microwave assisted acid digestion of biological matrices and ICP-MS analysis.

Conclusions

Instrumental methods for the detection of cisplatin, oxaliplatin, and carboplatin have been developed for the LC-MS/MS. Fragmentation patterns for each analyte match reported data in the current literature, and structural assignments have been proposed for the various species of cisplatin. Estimations of LOD and LOQ of each analyte have been estimated in the ug/g concentration range providing guidance on the instrument's analytical

capability. Conjugation studies performed to mimic the body's binding of platinum compounds by reduced glutathione were performed, and the presence of singly and doubly conjugated forms of platinum were confirmed by mass spectral data.

An instrumental method for total platinum analysis on the ICP-MS has been developed to detect for all six isotopes of platinum metal. Abundances of natural Pt-195 correlate well with the expected isotopic pattern reported by IUPAC. Solution of isotopically enriched Pt-194 was recertified with a high level of certainty with a measured abundance of Pt-194 at 96.54%, matching the reported isotopic purity on the label. The certification of the isotopic spike enables IDMS quantification of natural Pt-195 concentration alongside external calibration quantification. LOD and LOQ estimations for the ICP-MS analysis indicate the ability to detect and quantify platinum in the ng/g concentration range. Extraction protocols for the microwave assisted acid digestion of biological matrices, urine and blood, have been tested and were moderately successful in quantifying analyte species. Optimization of both extraction protocols would be required for best extraction efficiency and improved accuracy in the quantification of total platinum content.

References

1. Dasari, S.; Tchounwou, P. B., Cisplatin in cancer therapy: molecular mechanisms of action. *Eur J Pharmacol* **2014**, *740*, 364-78.
2. Galluzzi, L.; Senovilla, L.; Vitale, I.; Michels, J.; Martins, I.; Kepp, O.; Castedo, M.; Kroemer, G., Molecular mechanisms of cisplatin resistance. *Oncogene* **2012**, *31* (15), 1869-83.
3. Qi, L.; Luo, Q.; Zhang, Y.; Jia, F.; Zhao, Y.; Wang, F., Advances in Toxicological Research of the Anticancer Drug Cisplatin. *Chem Res Toxicol* **2019**, *32* (8), 1469-1486.
4. Riddell, I. A., Cisplatin and Oxaliplatin: Our Current Understanding of Their Actions. *Met Ions Life Sci* **2018**, *18*.
5. Nejdil, L.; Kudr, J.; Blazkova, I.; Chudobova, D.; Skalickova, S.; Ruttkay-Nedecky, B.; Adam, V.; Kizek, R., Mechanisms of Uptake and Interaction of Platinum Based Drugs in Eukaryotic Cells. In *Platinum Metals in the Environment*, 2015; pp 401-415.
6. Shen, D. W.; Pouliot, L. M.; Hall, M. D.; Gottesman, M. M., Cisplatin resistance: a cellular self-defense mechanism resulting from multiple epigenetic and genetic changes. *Pharmacol Rev* **2012**, *64* (3), 706-21.
7. Holditch, S. J.; Brown, C. N.; Lombardi, A. M.; Nguyen, K. N.; Edelstein, C. L., Recent Advances in Models, Mechanisms, Biomarkers, and Interventions in Cisplatin-Induced Acute Kidney Injury. *Int J Mol Sci* **2019**, *20* (12).

8. Klaunig, J. E., Oxidative Stress and Cancer. *Curr Pharm Des* **2018**, *24* (40), 4771-4778.
9. Gao, X.; Tsai, R. Y. L.; Ma, J.; Wang, Y.; Liu, X.; Liang, D.; Xie, H., Determination of Oxaliplatin by a UHPLC-MS/MS Method: Application to Pharmacokinetics and Tongue Tissue Distribution Studies in Rats. *Pharmaceuticals (Basel)* **2021**, *15* (1).
10. Collins, I. M.; Roberts-Thomson, R.; Faulkner, D.; Rischin, D.; Friedlander, M.; Mileskin, L., Carboplatin dosing in ovarian cancer: problems and pitfalls. *Int J Gynecol Cancer* **2011**, *21* (7), 1213-8.
11. Xie, M.; Liu, W.; Lou, L.; Chen, X.; Ye, Q.; Yu, Y.; Chang, Q.; Hou, S., Unusual dimeric chemical structure for a carboplatin analogue as a potential anticancer complex. *Inorg Chem* **2010**, *49* (13), 5792-4.
12. Moncharmont, C.; Auberdiac, P.; Melis, A.; Afqir, S.; Pacaut, C.; Chargari, C.; Merrouche, Y.; Magne, N., [Cisplatin or carboplatin, that is the question]. *Bull Cancer* **2011**, *98* (2), 164-75.
13. Heudi, O.; Brisset, H.; Cailleux, A.; Allain, P., Chemical instability and methods for measurement of cisplatin adducts formed by interactions with cysteine and glutathione. *Int J Clin Pharmacol Ther* **2001**, *39* (8), 344-9.
14. Perry, B. J.; Balazs, R. E., ICP-MS method for the determination of platinum in suspensions of cells exposed to cisplatin. *Analytical Proceedings including Analytical Communications* **1994**, *31* (9).

15. Chen, H. H.; Kuo, M. T., Role of glutathione in the regulation of Cisplatin resistance in cancer chemotherapy. *Met Based Drugs* **2010**, 2010.

Concluding Remarks: Glutathione

The work presented in this dissertation encompasses the investigation of the important biological compound, glutathione. Glutathione plays several key roles in maintaining redox homeostasis and protecting the body from xenobiotic material. The compound exists in several speciated forms within the body, species that can interconvert during sample collection, preparation, and analysis, which has complicated the quantification of the analyte for many researchers. Previous researchers in the Kingston research laboratory developed a methodology for quantifying this conversion of species to enable the correction of GSH to GSSG oxidation, permitting accurate and precise determination of both glutathione species. This methodology was then applied to patient and healthy control samples in the field of autism spectrum disorder, proving the GSH/GSSG ratio to be a valuable biomarker for disease status.

Measurement of glutathione levels in blood were employed using whole blood extraction after retrieval via venipuncture draw, which presents several drawbacks. Recent research has endeavored to minimize blood analysis protocols onto a new clinical tool known as dried blood spot cards. The major issue with dried blood spot analysis is the lack of quantitative validation where the cards have been traditionally employed for purely qualitative purposes. This work has developed a validated, minimized protocol for glutathione quantification derived from the manual extraction of dried blood spot samples. This method was put under various stressors such as varying storage conditions and storage for different lengths of time to assess the dried blood spot cards robustness for sample preservation. This development enables the potential future collection of patient samples from a simple finger stick performed in the comfort of the patient's home which can then

be mailed using simple postal services. Not only will medical professionals be able to reach vast ranging patient populations, but more frequent assessment of patient condition will be enabled permitting treatment tracking for a more personalized system of medicine.

This work also endeavored to develop a fully automated system of extraction of dried blood spot samples using a dried blood spot autosampler connected in tandem with the high-pressure liquid chromatography tandem mass spectrometry instrumentation. This system would eliminate human error from the extraction protocol, streamline the workflow, and increase laboratory throughput of sample analysis. The fully automated system of extraction and analysis enabled detection of both glutathione species and could permit accurate and precise quantification of reduced glutathione bound to N-ethylmaleimide, but failed validation parameters regarding the analysis of oxidized glutathione.

A remaining hang-up of glutathione analysis is the low-level concentration of oxidized glutathione and the struggles faced with its ionization efficiency in instrumental analysis. Difficulty confidently detecting analyte presence also complicates quantitative endeavors often leading to higher levels of imprecision and inaccuracy. This imprecision also further affects subsequent calculations, like that of the GSH/GSSG ratio. To mitigate this issue, a new analytical instrument signal boosting technology termed Thor's Hammer Metaspiking has been developed. By manipulating the isotopic abundances of the traditional spike used in IDMS and SIDMS quantification, low-level analyte signal can be raised above the threshold of the LOQ, permitting more accurate and precise quantification of low level analyte species.

This biomarker ratio has been a highly sought-after measurement in the medical field, not only for autism spectrum disorder, but for various neurological disorders such as

Alzheimer's and Parkinson's as well as other states of dysfunction like cancer. Glutathione plays a major role in the detoxification processes responsible for platinumated drug treatment resistance in the field of oncology. Cisplatin, carboplatin, and oxaliplatin are the only platinumated drugs currently FDA approved for use in the United States of America, and understanding the body's immunological response to their use is important for optimizing cancer treatment and limiting patient harm. Current clinical practice assesses total platinum concentration in patient blood and urine samples through ICP-MS analysis to determine drug elimination rates. While valuable in some regard, total analysis does not provide information regarding the various biotransformation occurring when platinumated drug compounds are introduced into the body. Analysis using LC-MS/MS instrumentation can provide this information, enabling a more accurate representation of biochemical processing during the patient's treatment. Current oncological research also does not utilize an internal standard of chemically indistinguishable nature, instead employing other metals. The use of isotopically enriched platinum enables a better representation of analyte's instrumental response, improving quantitative analysis as well as eliminating the need for traditional calibration curve quantification through the employment of IDMS.

Future Work

Full validation of the automated system of extraction and analysis of dried blood spot samples utilizing the dried blood spot autosampler will require optimization of the interplay between the solid phase extraction and chromatographic separation of glutathione. Levels of oxidized glutathione are very low and require the highest possible extraction efficiency to enable adequate detection of analyte signal to enable quantification, which at present the automated system cannot accomplish.

Further optimization of Thor's Hammer Metaspiking will also aid the quantification of glutathione from dried blood spot samples. Given the results of this work, different Metaspikes perform better at different analyte concentration levels. With additional experimental data and advanced mathematical representation, the goal would be to develop an algorithm for determining which Metaspike would enable the best quantification of an unknown sample.

The work reported for LC-MS/MS and ICP-MS analysis of platinated drug compounds is preliminary, demonstrating instrumental capabilities and providing the groundwork for what could be a very robust and important project for another researcher's dissertation work.